

**ENVIRONMENTAL INFECTION
TRANSMISSION: ASSESSING ROUTES OF
TRANSMISSION FOR INFLUENZA AND
OTHER AGENTS**

by
Ian H. Spicknall

A dissertation submitted in partial fulfillment
of the requirements for the degree of
Doctor of Philosophy
(Epidemiological Science)
in The University of Michigan
2011

Doctoral Committee:

Professor James S. Koopman, Co-Chair
Associate Professor Joseph N. S. Eisenberg, Co-Chair
Professor Ana V. Diez-Roux
Associate Professor Allison E. Aiello
Associate Research Scientist Rick L. Riolo

© Ian H. Spicknall 2011
All Rights Reserved

For my parents

ACKNOWLEDGEMENTS

I am immensely indebted to my entire doctoral committee. In particular I thank Jim for introducing me to transmission modeling many years ago; I am inspired by his ever-present enthusiasm and engagement with this work. I thank Joe for more recently extensively mentoring me through my initial navigation through the social ecosystem of the scientific community. I thank Rick for his immense patience, and expertise in all things agent-based. I would also like to thank Hal Morgenstern, Ana, and Jim for providing multiple perspectives on epidemiologic methods and theory; my thinking has been considerably shaped by each of you in complementary ways. I would additionally like to thank Betsy Foxman for also providing valuable mentoring during my master's program and early doctoral program. I would like to thank Mark Wilson for unwittingly inspiring me to study science for the benefit of public health during my undergraduate experience. I thank my peers in my lab group, including Josep, Jijun, Sheng, Nottasorn, and Bryan. I thank other fellow doctoral students who have provided such an intellectually stimulating environment to be a part of including Ethan, Stina, Jong-Hoon, Megan, Vanessa, Emily and Marta. This would not have been possible without everyone I have met and learned from along my journey.

TABLE OF CONTENTS

DEDICATION	ii
ACKNOWLEDGEMENTS	iii
LIST OF FIGURES	vi
LIST OF TABLES	vii
LIST OF APPENDICES	viii
CHAPTER	
I. Introduction	1
1.1 Specific Aims	1
1.2 Background and Research Setting	3
1.2.1 What is a contact?	3
1.2.2 Types of Influenza Contacts: Influenza Routes of Exposure	4
1.2.3 Consequences of opening Pandora's box	5
1.3 Model Forms	6
1.3.1 Individual Based Modeling	6
1.3.2 Equation Based Modeling	6
1.3.3 Choice of Model Form	6
II. Informing Optimal Environmental Influenza Interventions: How the Host, Agent, and Environment Alter Dominant Routes of Transmission	8
2.1 Abstract	8
2.2 Introduction	9
2.3 Materials and Methods	12
2.3.1 The model	12
2.3.2 Sampling and simulation	15
2.3.3 Statistical analyses	17
2.4 Results	17
2.4.1 Transmission mode dominance	17
2.4.2 Transmission mode intensity	19
2.5 Discussion	23
III. Surface Touching Patterns Alter Hand Hygiene and Surface Decontamination Efficacy	28
3.1 Abstract	28
3.2 Introduction	29
3.3 Materials and Methods	33

3.3.1	Important Assumptions	39
3.4	Results	40
3.4.1	Touch Specificity and Intervention Efficacy	41
3.4.2	Touch Specificity and Sub-Routes of Contact-Mediated Transmission	42
3.4.3	Comparison of HH implementation	46
3.5	Discussion	49
IV. Comparing Contact Mediated Transmission		53
4.1	Abstract	53
4.2	Introduction	55
4.3	Results	60
4.3.1	Parameterization	60
4.3.2	Contact mediated infection potential via each pathogen	64
4.3.3	Intervention efficacies by pathogen	66
V. Conclusions and Future Directions		71
5.1	Summary	71
5.1.1	Conclusions from Chapter II	71
5.1.2	Conclusions from Chapter III	73
5.1.3	Conclusions from Chapter IV	74
5.2	Suggestions for future research	75
5.3	Implications	76
APPENDICES		79
BIBLIOGRAPHY		120

LIST OF FIGURES

Figure

2.1	The epidemiologic triad for environmentally mediated influenza transmission. . . .	11
2.2	Schematic of pathogen flow through the environment with specific events in bold resulting in respiratory, inspiratory, contact or droplet exposure.	14
2.3	Venn diagram of influenza transmission mode dominance.	18
2.4	Distribution of the A) host density, B) self inoculation rate, and C) shedding magnitude parameters for different categories of transmission mode dominance.	20
2.5	The contact-route CART diagram.	22
3.1	Routes of contamination and intervention of contact mediated influenza transmission.	31
3.2	Venues with random versus increasingly less random touching patterns.	34
3.3	Ordinary differential equation based model schematic of contact mediated influenza transmission through two fomites.	36
3.4	Cumulative incidence and intervention efficacy as a function of surface touching specificity, using unfixed and fixed pre-intervention incidence models	43
3.5	Cumulative incidence and intervention efficacy of sub-routes of contact transmission as a function of surface touching specificity, using unfixed and fixed pre-intervention total incidence models.	44
3.6	Hand hygiene intervention efficacy when targeted to separate infection categories of people as a function of touching specificity using fixed incidence models.	47
4.1	Hand hygiene and surface decontamination efficacy in norovirus, S. aureus, rhinovirus and influenza as a function of rate of intervention application.	67
A.1	Distribution of the airborne viral inactivation rate parameter for different categories of transmission mode dominance.	95
A.2	Distribution of the surface viral inactivation rate parameter for different categories of transmission mode dominance.	96
A.3	Distribution of the skin viral inactivation rate parameter for different categories of transmission mode dominance.	97
A.4	Distribution of the finger-surface transfer efficiency parameter for different categories of transmission mode dominance.	98
A.5	Distribution of the lower respiratory infectivity parameter for different categories of transmission mode dominance.	99
A.6	Distribution of the upper respiratory infectivity parameter for different categories of transmission mode dominance.	100
A.7	Distribution of the lung deposition parameter for different categories of transmission mode dominance.	101
A.8	Distribution of the host movement rate parameter for different categories of transmission mode dominance.	102
A.9	Distribution of the viral proportion respirable parameter for different categories of transmission mode dominance.	103
A.10	Distribution of the surface touching rate parameter for different categories of transmission mode dominance.	104
A.11	Distribution of the transfer proportion from self inoculation site to target site parameter for different categories of transmission mode dominance.	105

A.12	The respiratory-route CART diagram.	106
A.13	The droplet-route CART diagram.	107
B.1	Pulsed intervention efficacy against contact transmission as a function of surface touching specificity, using fixed pre-intervention total incidence models.	117

LIST OF TABLES

Table

2.1	Parameter sampling constraints used to generate a 10,000 unit Latin hypercube sample.	16
2.2	Terminal node description of the contact CART figure.	23
3.1	Parameter Description and Values Used	39
4.1	Comparison of Contact Mediated Transmission Parameters.	61
4.2	Comparison of total shedding during infection ($\frac{\alpha}{\gamma}$) required to attain 50% final fraction infected.	64
4.3	Shared parameter values between pathogens	65
A.1	Parametric means in different transmission mode dominance categories.	94
A.2	Terminal node description of respiratory CART figure.	96
A.3	Terminal node description of droplet CART figure.	104
A.4	Univariate correlations of respiratory infection.	112
A.5	Univariate correlations of inspiratory infection.	112
A.6	Univariate correlations of droplet-spray infection.	113
A.7	Univariate correlations of contact mediated infection.	113
C.1	Rough estimate of total shedding over course of infection among pathogens.	119

LIST OF APPENDICES

Appendix

A.	Preamble and Chapter II Supporting Materials	80
A.1	Preamble	80
A.2	Chapter II Supporting Materials	80
A.2.1	Model structure	80
A.2.2	Model Parameterization	87
A.2.3	Description of Figure 2.3's Venn Diagram Categories	93
A.2.4	Description of CART figures	95
A.2.5	Comparison to Previous Models	108
A.2.6	Correlation Analysis	111
B.	Chapter III Supporting Materials	114
B.1	Sub Route Equations	114
B.2	Pulsed intervention application	116
C.	Chapter IV Supporting Materials	118
C.1	Calculation of β_H for S. Aureus	118
C.2	Calculation of $\frac{\alpha}{\gamma}$ for all pathogens	118

CHAPTER I

Introduction

1.1 Specific Aims

Traditional transmission models use an abstract and usually poorly defined concept of *contact* to transmit infection. For vector-borne diseases and for sexually transmitted infections discrete *contacts* may occur, transmit infection, and be easily measurable. This allows for models of STI and vector-borne infection to easily relate to data and vice versa. However, a disconnect between empiricism and theory development may arise as a modeled abstract *contact* becomes less relate-able to real world processes which transmit infection. This dissertation models more detailed processes that lead to transmission. Thereby, these processes that lead to infection more closely resemble the processes that do so in reality. By doing so we may investigate issues that conventional transmission models are unable to address. Specifically we are able to model explicit routes of transmission that operate through the environment. Additionally we can investigate phenomena that alter strengths of specific transmission routes such as features of the host, pathogen, and environment, as well as interventions which attenuate transmission by altering these features. We do so first using influenza as the model-pathogen, and in chapterIV we compare across influenza, rhinovirus, staphylococcus aureus, and norovirus.

Aim 1

To examine how variation of parameters of influenza transmission related to either features of the host, pathogen, environment, or their interaction, affect transmission mode dominance and intensity.

Sub Aim A. Other assume that transmission mode dominance is universal and invariant under different scenarios defined by parameters related to either the host, agent, environment or the interaction of these entities. We examine how transmission mode dominance changes as a function of these characteristics.

Sub Aim B. We examine and summarize the dominant causal mechanisms which give rise to the different categories of transmission modes operating.

Aim 2

To examine how population level surface touching heterogeneity alters influenza transmission and influenza intervention efficacy.

Sub Aim A. We examine how random touching without preference versus more preferential touching affects contact mediated transmission.

Sub Aim B. We examine how hand hygiene efficacy varies with surface touching specificity.

Sub Aim C. We examine how surface decontamination efficacy varies with surface touching specificity.

Aim 3

To compare contact mediated transmission parameters, transmissibility, and intervention efficacy across multiple pathogens that are at least partially transmitted

via the contact route.

Sub Aim A. Norovirus is considered the most infectious, and potentially has the high transmission potential of any agent studied. We examine how norovirus transmissibility compares to other pathogens in a transmission system which includes environmental transmission parameters specific to each pathogen.

Sub Aim B. We examine how effective hand hygiene is for each pathogen when applied at different rates.

Sub Aim C. We examine how effective surface decontamination is for each pathogen when applied at different rates.

1.2 Background and Research Setting

1.2.1 What is a contact?

To model a potentially infection transmitting contact, there is implicit pathogen transfer from a contagious person, animal, or other entity, to a susceptible person. For vector-borne infections, clearly a bite of a competent and *infected* vector may initiate an infection process at some probability. Similarly, sexually transmitted infections also have clearly defined *contacts* in the form of different sexual acts. However, most other infections that are assumed to be *directly* transmitted, have some environmental component between excretion and exposure. That is, following excretion, the pathogen exists in the environment for some period of time, before causing exposure and potentially initiating infection in a susceptible.

For all pathogen transmission that falls under this category, it becomes difficult to operationalize a meaningful measurement of a contact. For influenza, the rule of thumb has been, if a person comes within some number of feet of another, then a *contact* has occurred. However, this is imperfect, as the duration of such a contact

ought to alter the intensity (and therefore likelihood of infection transmission) of the contact. Rather than modeling influenza *contacts* like this, we are taking a different approach, in which we are no longer concerned with a *contact* or *contact rate* in the conventional transmission modeling sense of these words. Rather, in this dissertation, in order to transmit infection, we explicitly keep track of actual numbers of pathogens being excreted, existing intermediately in the environment, and eventually being inoculated to potentially initiate infection. We are not the first to do so, as this kind of modeling has been performed for water-borne pathogens [19], airborne pathogens [53], as well as for influenza which is transmitted via multiple routes including both aerosol-mediated and contact-mediated transmission routes [6, 51].

1.2.2 Types of Influenza Contacts: Influenza Routes of Exposure

To define an influenza *contact* that can potentially cause infection, the CDC has defined the following routes of transmission. Direct contact transmission occurs when the virus is transferred by contact from an infected person to another person without a contaminated intermediate object. Indirect contact transmission involves the transfer of influenza by contact with a contaminated intermediate object. Droplet spray transmission is person-to-person transmission of influenza through the air by droplet sprays. A key feature is deposition by impaction on exposed mucous membranes. Finally, aerosol transmission is person-to-person transmission of influenza through the air by aerosols in the inspirable size range or smaller. Particles are small enough to be inhaled into the oropharynx and distally into the trachea and lung. These definitions for contact transmission are still inadequate because they do not explicitly define the self inoculation process which must occur; that is that when direct contact transmission occurs from skin to skin transfer of virus, not transmission has happened yet, only transfer. In our work we consider droplet-spray exactly

as defined by the CDC. We divide the CDC’s definition of aerosol transmission into two. The virus on the respirable size range of particles we assume are still respired to the deep lung alveoli, while virus on the medium sized inspiratory range particles we assume are too large to disperse rapidly; so these particles are more localized around the shedder, and additionally these particles are assumed to be unable to penetrate as deep as the smaller respiratory particles; thus they deposit in the upper airways rather than the lower airways and use a different HID_{50} . For contact transmission, we ignore the CDC’s definition of *direct contact transmission*, as we do not allow skin to skin contact; all of our contact-mediated transmission is assumed to be *indirect*, as virus on large particles is shed, settles rapidly to the local fomite environment, may be picked up when people touch the surface, and finally self-inoculated to potentially cause infection.

1.2.3 Consequences of opening Pandora’s box

Explicitly modeling how features of pathogen fate and transport affect transmission opens a potential Pandora’s box of complexity. There are positives and negatives associated with doing so. Benefits of doing so include being able to entertain research questions of an entirely different nature. These include issues related to specific environmental modes of transmission, as well as phenomena related to intervening upon these routes of transmission. However, detriments include being forced to describe very detailed processes, for which very little or very weak data exist. Additionally, it is likely that with increasingly detailed model specification, inferences become decreasingly generalizable. Because we are interested in making general inferences, we attempt to model as general and abstract of a scenario possible, while also incorporating detailed complexities inherent to environmental infection transmission.

1.3 Model Forms

In this dissertation we use two primary model forms. In chapter II we employ individual based modeling while in chapters III and IV we use equation based deterministic compartmental modeling.

1.3.1 Individual Based Modeling

Individual based modeling works by having a discrete number of entities (in our case people and pathogens in the environment) which perform specific actions based on a set of rules. In our model, people excrete pathogens to the environment, where the pathogens may inactivate, or cause exposure and potentially initiate infection in another person. Model behavior is built from the bottom up, as a collection of interconnected pieces that obey and perform a given set of rules.

1.3.2 Equation Based Modeling

Equation based modeling by contrast uses a top down approach, whereby a set of governing equations determine all behavior. Here, key underlying assumptions we make when using this model form include infinite population size and continuous population distributions. Analysis of models of this form is generally considered to be cleaner and more straightforward compared to their individual based model counterparts.

1.3.3 Choice of Model Form

Our guiding principle in choice of model form was to use the simplest, most general model form possible while we examine the effects of complexities introduced. In chapter II we are interested in examining the effects of parameter variability on influenza modes of transmission. Each route of transmission is different from other

routes with regard to the spatio-temporal requirements of the shedder and susceptibles. The respiratory route did not require collocation in space over any temporal window since aerosolized pathogens in this model were assumed to instantaneously disperse throughout the entire venue at excretion. The contact route required a susceptible to be in a cell recently occupied by a shedder, since shedding to fomites only occurs in a localized fashion around the shedder at excretion. The droplet-spray route had the most strict spatio-temporal requirements as it required a susceptible and infectious person to be collocated at excretion. Because of these different requirements, and to easily vary host density as well as the other 17 parameters, we chose to use the individual based modeling model form. This was the easiest way to introduce this spatio-temporal heterogeneity as well as be able to vary the size of the venue while maintaining the spatio-temporal model structure.

In chapter III we are interested in examining the effect of non-random versus random surface touching behavior solely on the contact route of transmission as well as resulting intervention efficacies against this route. While this could certainly be done in an individual based modeling framework, it could also be easily done in a deterministic compartmental equation based model. Both model analyses would yield similar inferences, but we chose the latter for quicker model development and analysis.

In chapter IV we are interested in comparing the strength of the contact route for four different pathogens. Again, we chose to make the simplest possible comparison in a deterministic compartmental equation based model. Future work could include greater complexity such as how more complicated touching patterns affect inferences drawn from chapters III and IV using an individual based modeling framework.

CHAPTER II

Informing Optimal Environmental Influenza Interventions: How the Host, Agent, and Environment Alter Dominant Routes of Transmission

2.1 Abstract

Influenza can be transmitted through respirable (small airborne particles), inspirable (intermediate size), direct-droplet-spray, and contact modes. How these modes are affected by features of the virus strain (infectivity, survivability, transferability, or shedding profiles), host population (behavior, susceptibility, or shedding profiles), and environment (host density, surface area to volume ratios, or host movement patterns) have only recently come under investigation. A discrete-event, continuous-time, stochastic transmission model was constructed to analyze the environmental processes through which a virus passes from one person to another via different transmission modes, and explore which factors increase or decrease different modes of transmission. With the exception of the inspiratory route, each route on its own can cause high transmission in isolation of other modes. Mode-specific transmission was highly sensitive to parameter values. For example, droplet and respirable transmission usually required high host density, while the contact route had no such requirement. Depending on the specific context, one or more modes may be sufficient to cause high transmission, while in other contexts no transmission may

result. Because of this, when making intervention decisions that involve blocking environmental pathways, generic recommendations applied indiscriminately may be ineffective; instead intervention choice should be contextualized, depending on the specific features of people, virus strain, or venue in question.

2.2 Introduction

On June 11, 2009 the WHO declared the H₁N₁ influenza virus a pandemic. Health organizations worldwide were prompted to escalate their efforts to minimize transmission within their jurisdictions. Airports began to monitor incoming passengers while schools increased their already intensive surveillance activities. Recommendations were established with regard to masks, hygiene, decontamination, and isolation of suspected cases. This interest in intervention and control of person-to-person transmitted illnesses with multiple potential routes of transmission began to intensify during the emergence of SARS and later the H₅N₁ (avian influenza) virus. Heightened awareness of the potential for another pandemic influenza led to increased funding to study non-pharmaceutical interventions by the CDC as well as increased efforts in modeling influenza transmission. These studies were funded in order to better understand optimal intervention and control strategies. Much insight was gained into influenza mitigation strategies such as border closure, social distancing, antiviral prophylaxis, restriction of public transportation, and school closure [22, 23, 20, 25, 27, 28, 6, 68]. To date, however, little is known about the relative contributions of the different influenza transmission modes and how these might vary due to heterogeneity in viral strain, host, and environment.

This manuscript explores potential effects of these unknown factors by presenting: 1) a transmission model structure that explicitly describes the environmental

processes through which viruses pass from one person to another, thereby distinguishing the different modes of transmission; and 2) an analytical approach that explores which factors increase or decrease different modes of transmission under the given model structure. The model analyzed is an environmental infection transmission system model that elaborates the approach to such models by Li et al. [42] by formulating the model in a discrete event framework and greatly expanding on the details of the various processes involved. It does not define contact events with transmission probabilities for each event as most transmission models do [36]. A problem with that approach is defining what constitutes a contact. Instead we define events related to virus excretion, environmental survival, uptake, and causation of infection. This allows us to address events at a level that is more relevant to possible interventions and the construction of more meaningful causal theory.

To inform relevant intervention options for influenza, we consider four potential modes of transmission: respirable, inspirable, direct-droplet-spray, and contact mediated transmission [37, 67, 10]. In this manuscript we consider each mode as follows. Respirable transmission occurs when viruses on small particles ($<10 \mu\text{m}$ diameter) are inhaled and deposit in the alveolar region of the lower respiratory tract. Inspirable transmission occurs when viruses on medium size particles (>10 and $<100 \mu\text{m}$ diameter) are inhaled and deposit in the upper respiratory tract. Direct-droplet-spray transmission (hereafter referred to as droplet transmission) occurs when viruses on large particles ($>100 \mu\text{m}$ diameter) from the cough or sneeze of an infected individual deposit directly on a susceptible individual's mucous membranes. Contact transmission occurs when an infected person contaminates their own hands or contaminates surfaces via their hands or via droplets with virus laden large particles. Transfer of pathogens may then result in contamination of the hands of others who

then may touch their eyes, nose or mouth to self-inoculate, potentially infecting the upper respiratory tract. We assess how different feasible model parameters influence how much transmission follows these different routes.

For example, different viruses may have different infectivity, survivability, transferability, or shedding profiles. Similarly, among different populations who have different behaviors, susceptibility profiles, or shedding profiles, the same virus may have different effects depending on the type of population present. Finally, even with identical viral strains and human populations, environmental venues may have variable host densities, surface area to volume ratios, or host movement patterns that can generate different population level infection outcomes. These diverse sources of heterogeneity that we address form the corners of the epidemiologic triad (Figure 2.1).

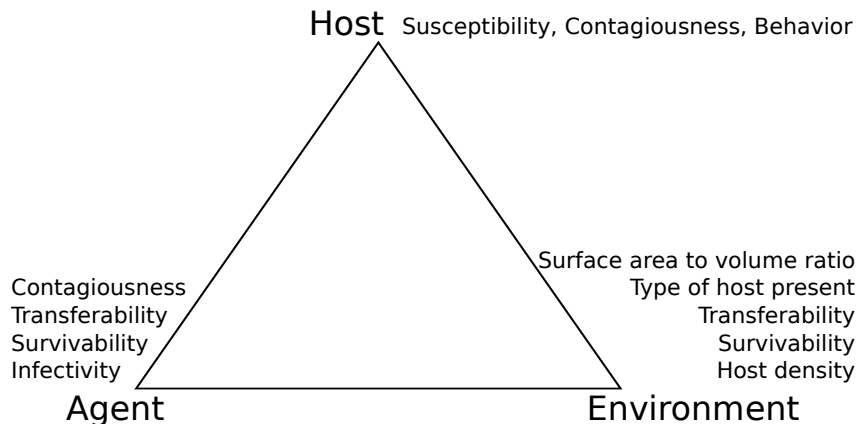


Figure 2.1: The epidemiologic triad for environmentally mediated influenza transmission. Specific features are listed in each corner that are relevant to either the agent (specific virus strain), host, and environmental venue.

We assess the effects of these sources of heterogeneity on relative magnitude of influenza transmission modes in a scenario where all individuals move randomly in an identical fashion. We construct a detailed stochastic individual based model of

environmental influenza transmission. We use values from empirical literature as well as expert judgment to parameterize this model. We apply upper and lower parameter constraints to 18 parameters, and obtain a Latin hypercube sample of this constrained parameter space. We analyze the resulting outcome space with respect to how different transmission modes are more or less important in specific contexts.

With this work we contribute to the body of literature discussing the dominant mode of influenza transmission [67, 63, 8, 40, 62, 41]. Additionally, this work takes an incremental step forward from previous environmental infection transmission models [6, 42, 53, 19, 51] as: 1) we model all four modes of influenza transmission simultaneously; 2) we do so in an agent based framework rather than with ordinary differential equation based framework; and 3) this model is solely informed parametrically by empirical workno model fitting or optimization procedures were used to parameterize this model. We explicitly point out where the holes in the empirical literature exist. We show that depending on the scenario, one mode may be more or less important than another. Therefore, when intervening, generic recommendations applied indiscriminately may be ineffective; instead intervention choice should be contextualized depending on the specific features of people, virus, or venue in question. We consider how features related to pathology, behavior, and microbiology in the host, pathogen, and environment (Figure 2.1) alter the magnitude of transmission via each mode.

2.3 Materials and Methods

2.3.1 The model

We model environmental influenza transmission in a venue by considering infections resulting from contact-mediated, respirable, inspirable, and droplet exposures. We model a single uniform abstract venue with no variation in space with regard to

fomites or behavior in order to seek simple general insights. This venue homogeneity helps us identify sources of heterogeneity in transmission attributable to the factors we study in the epidemiological triad (Figure 2.1). The venue is described as a lattice grid with discrete cell locations which people visit. Each cell in the lattice has a surface area, given by its length and width (2 meters by 2 meters), and local air volume, resulting in a surface area to volume ratio.

Figure 2.2 provides a schematic of all processes resulting from each shedding event that lead to exposure. We use continuous time to model discrete spatial units, humans, pathogens, and transmission-related events. Transmission-related events are described in the caption of figure 2 and in greater detail in the online material. An infectious individual sheds virus as a function of a shedding rate (a cough rate), shedding magnitude (how much mucous volume is put out), and viral concentration of material being excreted. Together, this determines the number of virus particles excreted. Next, particles are categorized by the relative weights of cough particles: $<10\mu\text{m}$; between $>10\mu\text{m}$ and $<100\mu\text{m}$; and $>100\mu\text{m}$. Note that we assume the same viral concentration regardless of particle size. We assume that only virus on particles $>100\mu\text{m}$ may cause droplet exposure if there are individuals collocated with the shedder. We assume that all viruses on particles $<10\mu\text{m}$ are instantly and thoroughly mixed throughout the venue by invoking the well mixed room assumption for these small particles. We assume these remain aerosolized until either the virus inactivates, leaves the venue due to air exchanges, or is utilized in respiratory exposure in the lung alveoli.

We assume virus on particles $>10\mu\text{m}$ and $<100\mu\text{m}$ remain in the local environment of the shedder because these particles would be too large to invoke the well mixed room assumption. These may inactivate, settle to the local surface environment, or

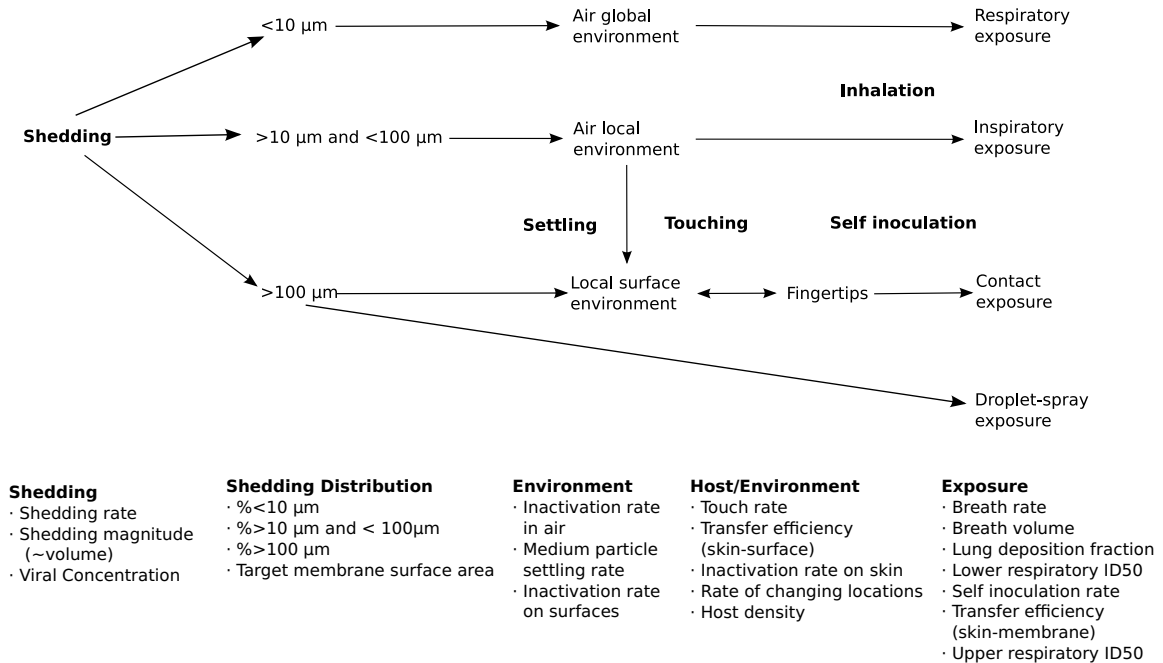


Figure 2.2: Schematic of pathogen flow through the environment with specific events in bold resulting in respiratory, inspiratory, contact or droplet exposure.

Relevant governing parameters of transmission are listed below each phase. Viral inactivation occurs in the air, on surfaces, and on fingertips (not explicitly shown). Moving from the left to the right of the diagram, viral excretion magnitude is determined by the shedding rate, volume, and concentration. Where these viruses go is determined by the size of the particle they adhere to during excretion. Based on cough particle size distribution data, these are divided proportionally. Viruses on small particles are well mixed, and are assumed to either inactivate or be inhaled (respiratory exposure) before settling would occur. Viruses on medium particles may either inactivate, settle to the local surfaces, or be inhaled (inspiratory exposure). Some viruses on large particles may be utilized initially in droplet exposure, proportional to the target facial membrane surface area multiplied by the number of susceptible collocated with the shedder. Viruses on larger particles not utilized in droplet exposure is assumed to settle immediately to the local surface environment. Here it may inactivate, or be picked up on fingertips. Once on fingertips, the virus may inactivate, be deposited back to a surface environment, or be used in contact exposure via self-inoculation. Respiratory exposure assumes lower respiratory penetration and uses an ID₅₀ specific to this region. Inspiratory, droplet, and contact exposure assumes the potential for infection only occurs in the upper respiratory tract and all use the same ID₅₀ specific to this region. For simplicity, we assume exponential dose-response relationship.

result in inspiratory exposure in the upper respiratory tract. These particles are too large to penetrate to the lung alveoli.

We assume particles $>100\mu\text{m}$ that are not involved in droplet exposure settle immediately to the shedder’s local surface environment evenly spread. Here, the virus may inactivate, be picked up as people touch this surface, and then generate contact exposure via self-inoculation. For the sake of simplicity, we assume that no excreted virus adheres to the shedder’s hands (as might happen if a cough or sneeze were covered with a hand). For greater model detail refer to the supporting material.

2.3.2 Sampling and simulation

We vary 18 parameters relevant to influenza transmission related to the host, pathogen, and venue (Table 2.1). We define a median value, either taken from the literature or from expert judgment, and either apply symmetric constraints or constraints that are symmetric when observed after a log transform, so that half of the sampled values are below the defined median and half above. We sample from the constrained parameter space using Latin hypercube sampling with uniform probability distributions for each parameter. In our full Latin hypercube sample, there are 10,000 unique parameter sets defined by the values of the 18 varied parameters. For each parameter set, 500 independent simulation trials are conducted and averaged.

For each trial, we use a special simulation design: when each new infection takes place, that individual is immediately replaced with a new susceptible in their place. This allows us to observe directly the number of new infections transmitted from one infected person over the course of their infection in the presence of a completely susceptible population of constant size which is one definition of the basic reproductive number, R_0 [4, 15]. Additionally, we are able to differentiate whether infection takes place from one mode or another, allowing us to directly observe mode-specific R_0 ’s.

<i>Parameter</i>	<i>Description</i>	<i>Unit</i>	<i>Lower Constraint¹</i>	<i>Upper Constraint¹</i>	<i>Resulting Median²</i>	<i>Reference</i>
μ_A	Inactivation rate-air	Min^{-1}	0.001	0.036	0.0060	[31]
μ_S	Inactivation rate-surfaces	Min^{-1}	0.0005	0.20	0.010	[7]
μ_H	Inactivation rate-hands	Min^{-1}	0.62	1.22	0.92	[7]
τ_{S-H-S}	Transfer efficiency (surface to hand to surface)		0.017	0.60	0.10	[58, 65]
τ_{F-T}	Transfer proportion		0.05	0.25	0.15	
	(eyes/nose/mouth to target mucous)					
τ_L	Lung deposition fraction		0.083	0.75	0.42	[34]
π_L	Lower respiratory HID_{50}	$TCID_{50}$	0.067	6.7	0.67	[3]
π_U	Upper respiratory HID_{50}	$TCID_{50}$	50	5000	500	[11, 12]
α_{mag}	Shedding magnitude		0.0050	0.075	0.019	
α_{resp}	Viral proportion to respirable air		1.4E-7	1.4E-5	1.4E-6	[46, 52]
α_{insp}	Viral proportion to respirable air		0.00353	0.016	0.0095	[46, 52]
ρ_{inoc}	Rate of self inoculation	Min^{-1}	0.02	0.32	0.080	[32, 50]
ρ_{touch}	Rate of surface touching	Min^{-1}	0.19	3.0	0.75	
ρ_{move}	Rate of changing location	Min^{-1}	0.00083	3.0	0.050	
ρ_{breath}	Rate of breathing	Min^{-1}	10	22	16	[24]
ϵ_{settle}	Medium particle settling rate	Min^{-1}	4.6	11	7.6	
$\epsilon_{SA:V}$	Surface area to volume ratio	$m^2 : m^3$	1	5	3	[66, 54, 33]
$\epsilon_{density}$	Host density	$people/m^2$	0.056	5.6	0.2	

Table 2.1: Parameter sampling constraints used to generate a 10,000 unit Latin hypercube sample.

NOTE: HID_{50} = quantity of viruses required to cause infection in 50% of humans.

¹Either symmetric constraints or constraints which were symmetric when observed after a log transform were applied, so that half of the sampled values would be below the defined median and half above.

²Median values were defined from either the literature or from expert judgement. We sampled the constrained parameter space using Latin Hypercube sampling.

2.3.3 Statistical analyses

To examine transmission mode dominance we categorize regions of the full 10,000 unit space into regions where one or more transmission modes have a mode-specific R_0 above 1.7 (a plausible value of the 1918 influenza pandemic R_0 [22]). We also considered using a cut-point of 1.2, but all results were similar and for simplicity not shown. We visualize this with a Venn diagram, and use box-plots to compare the parameter distributions of each category to one another. To examine parameters which affected each transmission mode intensity, we perform a simple correlation analysis (presented in the supporting material) and use the classification and regression tree (CART) algorithm [9, 18]. The CART approach classifies parameter sets as those which lead to a mode-specific R_0 greater than 1.7, versus those less than 1.7. A tree structure is produced in which classification criteria are specified by subdivisions of parameter values.

2.4 Results

Aggregated over all 10,000 parameter sets, the contact mode has the highest average mode-specific R_0 , 1.7. The droplet, respiratory, and inspiratory routes followed with mode-specific R_0 's 0.27, 0.05, and 0.006 respectively. While this aggregate measure is often all that is reported in the literature, it ignores the heterogeneous effects of different contexts in inducing shifts in transmission mode dominance and intensity; that is to say, contact transmission is not necessarily dominant in all settings.

2.4.1 Transmission mode dominance

We divide the entire 10,000 unit space into mutually exclusive categories based on whether one or more transmission modes individually have a mode-specific $R_0 > 1.7$. The contact, respiratory, and droplet transmission routes all have parameter

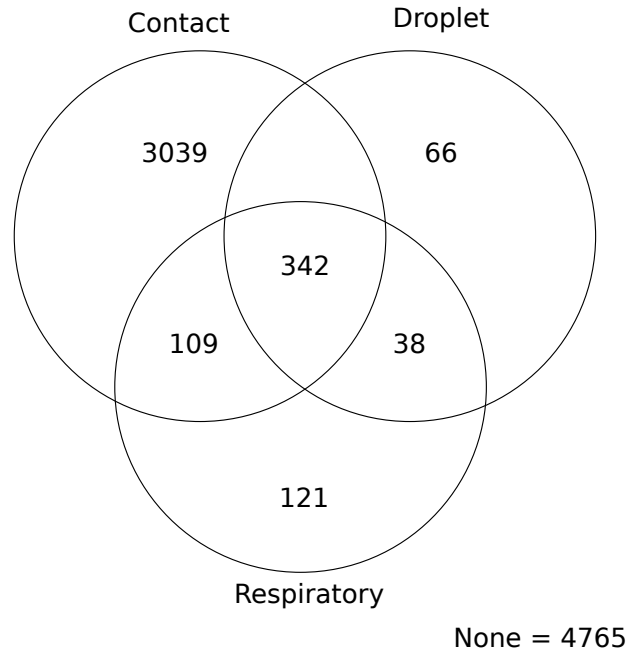


Figure 2.3: Venn diagram of influenza transmission mode dominance.

Numbers in different regions reflect the number of parameter sets which yield mode-specific $R_0 > 1.7$. Overlap indicates that more than one transmission mode has a mode-specific $R_0 > 1.7$. The 4765 parameter sets outside these three categories indicate that none of these three modes had high mode-specific transmission in these parameter sets. Note, that of these 4765 parameter sets with no single dominant mode, 577 parameter sets still yielded a total- $R_0 > 1.7$ when summed across all modes. The inspiratory transmission mode did not yield any parameter sets in which it alone dominated, and only 26 parameter sets in which it ever had mode-specific $R_0 > 1.7$.

sets which yield high transmission (mode-specific $R_0 > 1.7$) via each mode in isolation of all other modes. There are 3079 sets where contact was high with nothing else, 121 for the respiratory mode, and 66 for droplet (figure 2.3). There is no parameter set in which the inspiratory mode alone was above 1.7. Each of these domains is determined by features of the host, virus, and environment, in which any of these three modes would dominate over the others.

Additionally, there was considerable overlap, where multiple modes each have a mode-specific $R_0 > 1.7$. In these 1969 parameter sets no single mode dominates over the other modes; rather multiple modes transmit at a high intensity simultaneously. Our analysis henceforth ignores the inspiratory route as it only caused high trans-

mission in 26 parameter sets, never occurring alone. The extent of overlap differs by transmission mode (figure 2.3). The droplet route has the most overlap as 96% of parameter sets that yield high droplet transmission also yield high transmission by at least one other route. 80% of parameter sets which yield high respiratory transmission also yield high transmission by at least one other mode. The contact mode is the most isolated, as only 40% of its high transmission parameter sets also yield high transmission by other modes. In 4765 parameter sets, no individual mode has a mode-specific $R_0 > 1.7$. Of these, there are 577 parameter sets which, when summed across all modes, yields a total- $R_0 > 1.7$.

Host density ($\epsilon_{density}$) shows the most striking difference in parametric distributions between the different dominant transmission mode categories (figure 2.4). The droplet-only category has the highest distribution of $density$, followed by the respiratory-only category. The contact-only category has a low $density$ distribution, similar to the category in which there is no high transmission. Note that self inoculation rate and shedding magnitude also vary considerably between categories. Thus, features of the host, pathogen, and environment all play a role in determining transmission mode dominance. For box plots of all other parameter distributions refer to the supplemental material (figures A.1, A.2, A.3, A.4, A.5, A.6, A.7, A.8, A.9, A.10, A.11).

2.4.2 Transmission mode intensity

To gain insight into how parameter combinations affect the intensity of each transmission mode separately, we performed CART analyses. For each route, we classified the full 10,000 unit space as to whether each mode had high (mode-specific $R_0 > 1.7$) or low transmission. The CART algorithm then grouped similar regions of this outcome by making parametric divisions. We show the CART figure of the contact

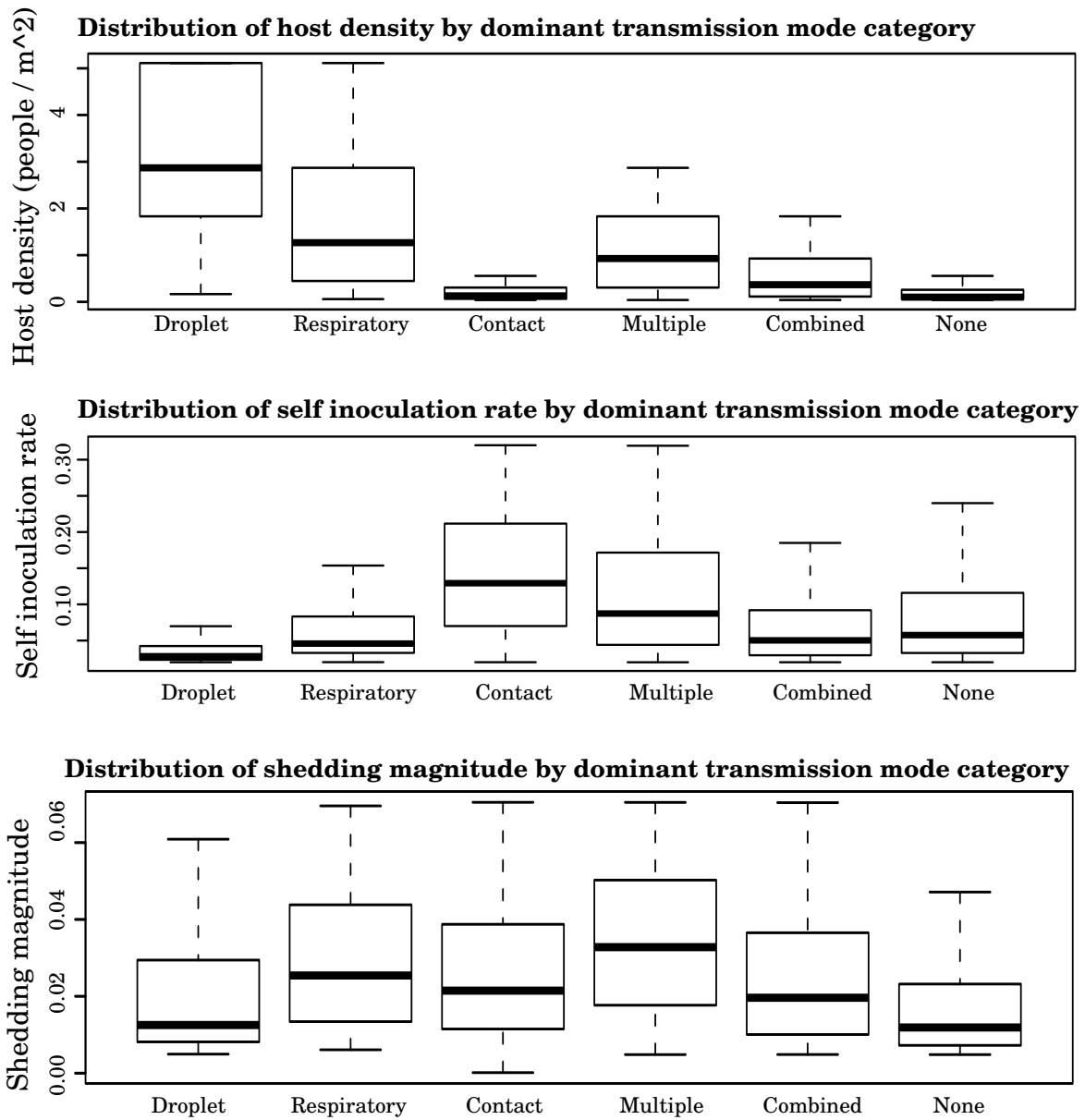


Figure 2.4: Distribution of the A) host density, B) self inoculation rate, and C) shedding magnitude parameters for different categories of transmission mode dominance.

Droplet, respiratory, and contact refer to parameter sets which only yielded high transmission by these routes alone. Multiple refers to parameter sets where more than one transmission route was causing high transmission. Combined refers to parameter sets which did not contain a single dominant transmission mode, but did cause high transmission by multiple modes combined, and none refers to parameter sets which both had no dominant modes of transmission and also did not combine to cause high transmission.

route, differentiating between high and low contact mediated transmission in figure 2.5. The numbers given in the ovals and rectangles are the proportions of all parameter sets which have a contact- R_0 greater than 1.7. Terminal nodes shown as rectangles are labeled with lower case roman numerals for ease of reference. The CART algorithm identified three parameters that differentiated between high and low contact mediated transmission (figure 2.5): upper respiratory $ID_{50}(\pi_U)$, self-inoculation rate (ρ_{inoc}), and shedding magnitude. Terminal nodes iii, v, and vi all show high contact transmission with 67%, 68%, and 86% of parameter sets that have the required parameter divisions yielding high contact transmission. We also examined the strength of all other transmission routes in these terminal nodes (table 2.2) based on the average mode-specific R_0 value. Because the contact and droplet routes share the same infectivity parameter, it is not surprising that while terminal node iii was largely contact-only, terminal nodes v and vi had high contact-and-droplet transmission combined in addition to high contact-only. In terminal node v, among the 818 parameter sets with high contact transmission, 475 of these also had high droplet transmission. In terminal node vi, among the 2912 parameter sets with high contact transmission, 1117 of these also had high droplet transmission. Thus these nodes represent scenarios where there is high contact-only transmission (node iii), as well as high combined contact-and-droplet transmission (nodes v and vi). The droplet-only transmission in these nodes is relatively small: 18 parameter sets in terminal node v and 5 parameter sets in terminal node vi. Terminal node iii by comparison is mainly composed of high contact-only transmission. The main parameter which differentiates between terminal node iii (high contact-only) and terminal nodes v and vi (high contact and droplet) is upper respiratory infectivity π_U . The latter nodes required a more infectious agent than terminal node iii.

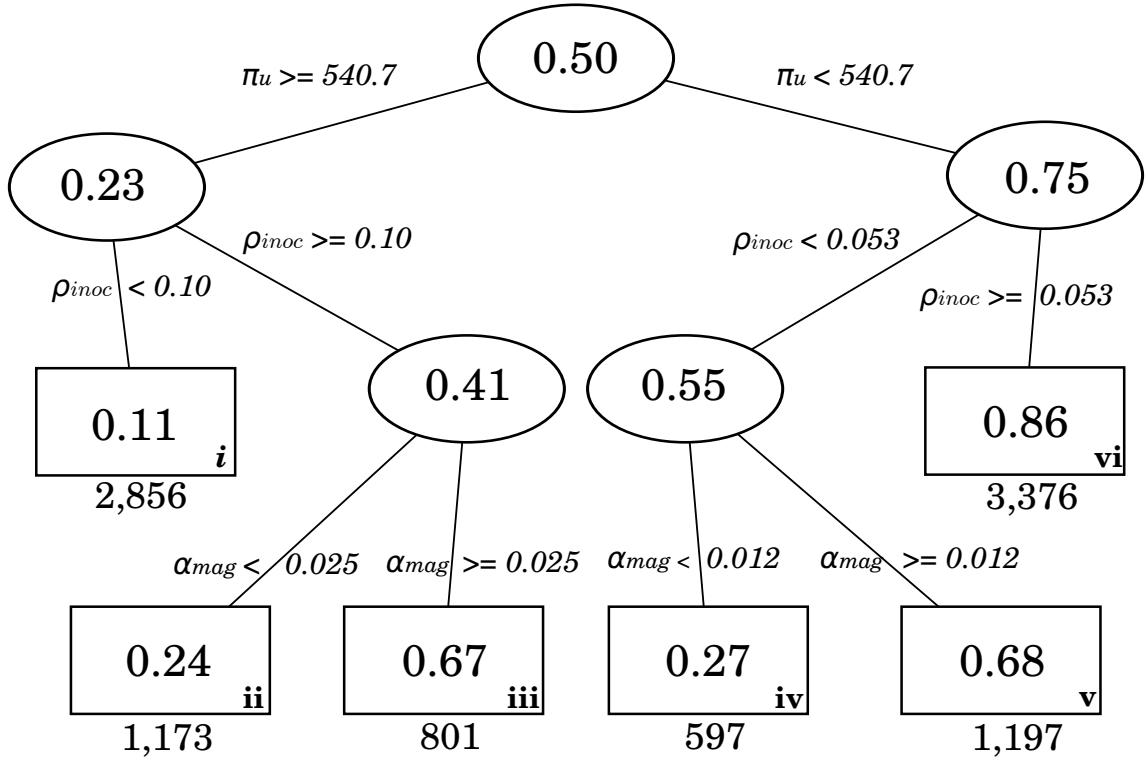


Figure 2.5: The contact-route CART diagram.

Numbers in ovals and rectangles are the proportions of parameter sets have mode-specific $R_0 > 1.7$ which meet the parameterization criteria shown on edges. Numbers at the bottom of each terminal node reflect the number of simulations which meet that classification criteria. Three parameters differentiate between areas of high versus low contact transmission: upper respiratory $ID_{50}(\pi_U)$, self inoculation rate (ρ_{inoc}), and shedding magnitude (mag). Terminal nodes are labeled with lower case roman numerals for ease of reference.

Turning to the plausibility of terminal node vi, two parameter constraints were required to yield high contact transmission in 86% of settings: first, a minimally constrained upper respiratory infectivity $\pi_U < 540.7$ (which covers 75% of the range sampled); and second, self inoculations occurring at least once every 19 minutes ($\rho_{inoc} \geq 0.053/\text{min}$). This ρ_{inoc} critical value is lower (and thus more plausible) than self inoculation rates previously observed in two published studies: 1 touch every 12 minutes [32], and 1 touch every 4 minutes [50]. Thus, this combination of constraints is certainly plausible.

From similar CART analyses, the droplet mediated transmission mode intensity

<i>Mode-specific R_0</i>	<i>Terminal node numeral</i>					
	<i>i</i>	<i>ii</i>	<i>iii</i>	<i>iv</i>	<i>v</i>	<i>vi</i>
Contact	0.72	1.34	4.84	0.60	5.87	20.76
Respiratory	0.47	0.22	0.88	0.13	0.65	0.54
Inspiratory	0.01	0.00	0.02	0.02	0.11	0.09
Droplet	0.37	0.18	0.63	1.07	4.85	3.77
Total- R_0	1.82	1.74	6.37	2.83	11.47	25.16

Table 2.2: Terminal node description of the contact CART figure.

NOTE: CART = Classification and Regression Tree Algorithm. Data represent the average values for domains in each terminal node of 2.5. The average total- R_0 may not be equal to the sum of all average mode-specific R_0 's due to skewed distributions.

is differentiated by three parameters: upper respiratory ID_{50} , host density, and shedding magnitude. Respiratory transmission mode intensity is differentiated by five parameters: host density, viral proportion respirable, shedding magnitude, lower respiratory ID_{50} , and lung deposition fraction. To test whether tree structure is sensitive to the cut point of $R_0 = 1.7$, we also construct CART figures using a cut point of 1.2. All resulting tree structures are robust, retaining similar structure, with only minor changes in the parameter values used to divide non-terminal nodes. See the supplemental material for complete discussion of the respiratory, inspiratory, and droplet CART analyses (section A.2.4). Also, correlation analyses in the supplemental material further describe how each parameter affects each mode of transmission (section A.2.6).

2.5 Discussion

This work highlights many parameters which can alter transmission mode dominance. By learning more about these transmission modes, we can better predict which modes are operating in specific scenarios. This insight can eventually help lead to definitions of 1) those factors that will enable us to predict how much transmission could take place via different modes and 2) effective interventions that can interrupt such transmissions. We have further shown that the relative importance

of different influenza transmission modes may vary based on features related to the pathogen, host, or mixing venue (figure 2.1) that may vary based on biology, behavior and environmental factors.

For example, high host density leads to conditions where either droplet, respiratory, or multiple transmission routes simultaneously operate at a high intensity (figure 2.4(a)). The infectivity parameters of the upper and lower sites of respiratory infection are also very important in determining both absolute and relative strengths of transmission modes (in figure 2.5), comparing terminal node iii which is largely contact-only to terminal nodes v and vi which also have high droplet transmission and have a higher infectivity). Additionally, the self-inoculation rate was the most important behavioral parameter influencing contact-transmission(figure 2.4(b)). Thus, we have found specific features of the environment (host density), agent (infectivity) and host (susceptibility and self inoculation rate) that are important in determining transmission mode dominance.

Our results should be interpreted with the following caveats. First, the distribution of parameter sets we used does not necessarily represent the probabilistic distribution of parameter sets in all of the real world settings. Thus it would not be appropriate to say that the contact route is most important in the vast majority of real contexts. Going further, if different parameter constraints were used, the shape of the Venn diagram in figure 2.3 could look drastically different. However, it is likely that there would still be regions where contact, respiratory, and direct-droplet-spray dominated on their own. Second, the behavioral and movement space we examined was intentionally limited. Further elaboration of these features could induce additional differences from those we observed.

With this work, we can make several recommendations for future empirical work.

The two influenza dose-response datasets study two different sites of infection using two different influenza strains. It is not clear whether all influenza strains would display a similar site-specific differential (upper versus lower respiratory tract infectivity). Empirical work examining site-specific infectivity first with one strain, and then with another would be quite valuable. This could help tease apart the relationship between innate variability of infectivity of virus strain, whether this varies by site of infection, and if this variability is similar across different strains. Another feature important to learn more about that could sway transmission dominance, is the shedding process. Specifically, examining particle size distributions and excretion rates based on type of excretion (cough, sneeze, normal breathing, speaking), examining how viral concentration varies by particle size, and quantifying how much saliva dilutes infectious nasal fluid in different types of excretions at different stages of infection would be useful.

Data uncertainty resulting from weakness of the data used for specific parameters is another motivation for future work. The surface inactivation rate, hand inactivation rate, all transfer efficiencies (as well as both infectivity parameters) are all based on datasets which contain a minimal number of data-points. If the value of these parameters lies outside of the ranges considered, these could also become quite important in altering transmission mode dominance and therefore optimal intervention choice. For this reason, more work examining these parameters would be worthwhile.

Although these results inform transmission mode dominance, this alone does not allow policy makers to make completely informed intervention decisions. Even if most transmission taking place in a given scenario is through the contact route, this does not indicate hand hygiene as the best intervention decision solely because it targets the contact route exclusively. For example, it is possible that specific

features of the scenario which relate to how hand hygiene interacts with pathogens in the environment could render a hand hygiene intervention ineffective, despite the contact route operating at a high intensity if there are substantial pathogen levels in the environment thereby allowing hands to be re-contaminated as soon as future surface touching occurs. A study similar to this could be extended to include the modeling of specific interventions, and be used to characterize a specific scenario. Doing so would be part of an overall site-specific microbial risk assessment. This would involve taking into account specific features of the environment, host, and pathogen strain as well as their dynamic interactions.

Conclusions from previous work of others may differ from our work, since we considered a broad set of parameter ranges, rather than point estimates. Previous work of Atkinson and Wein (AW) [6] and Nicas and Jones (NJ) [51] differed in their assessment of the importance of contact mediated transmission. AW found it to be negligible, NJ found it to be of varying importance under different conditions, and we found it be important in many scenarios. We argue that their inferences arose from analyses constrained to highly specified regions in multidimensional parameter space, ignoring a large number of parameterization sets reflective of the heterogeneity in the host, pathogen and environment. Advocating one transmission mode specific intervention method based on inferences from such a specified scenario may often lead to ineffective decisions, under different situations. AW used a surface area to volume ratio of 3:1m, suitable for small particles less than $6 \mu\text{m}$ [66], [54] that behave like a gas, and can possibly settle on vertical surfaces. However, larger particles will be more dominated by gravity, more likely to deposit on horizontal surfaces as indicated by table 35 of Hong [33]. Thus AW's surface area to volume ratio for settling sites for particles greater than $10 \mu\text{m}$ is not appropriate and will greatly dilute the

pathogen surface concentration compared to pathogen air volume concentration, thus artificially diminishing the contact route compared to the respiratory and inspiratory routes. See supporting materials for additional discussion of this topic.

With this work it was our goal to highlight that there may not be one and only one dominant influenza transmission route in all settings. We are no more in the aerosol camp than the contact camp. We suggest that this is influenced by features related to the host, pathogen and environment. Depending on the specific situation one or more modes may be sufficient to cause high transmission, while in others no transmission may result. It will be important to extend this work to examine the effect of realistic interventions which aim to block or attenuate the environmental pathways included here. Additionally, similar model extensions could also address the importance of different modes of transmission in a more complex setting, such as multiple venues modeled simultaneously, that can address the network-like potential of certain venues as infection disseminators to a broader population.

CHAPTER III

Surface Touching Patterns Alter Hand Hygiene and Surface Decontamination Efficacy

3.1 Abstract

Background. Hand hygiene (HH) and surface decontamination (SD) are considered effective interventions against contact mediated influenza transmission. Little is known, however, about the mechanisms behind how these interventions operate and therefore what should impact the recommendation of one intervention over another. We study how different population touching patterns alter the relative efficacies of these interventions.

Methods. We use an ordinary differential equation based environmental infection transmission system to explicitly model the contact mediated route of influenza transmission. We incorporate both HH and SD into this. We use parameter values informed by empirical studies where possible. Specifically, we model the fact that in some situations touching patterns are often preferential to certain fomites such as doorknobs, phones, and computer keyboards, while in other situations touching patterns are more random.

Results. The droplet-to-fomite contamination route deposits pathogens evenly throughout; therefore as touching is more specified to a small location, the strength of this contamination route decreases. Conversely, the strength of the hand-to-fomite

contamination route increases with higher touch specificity. Because SD is better suited to attenuating the droplet contamination route when surface touching is fairly random, and HH is better suited to attenuating the hand contamination route regardless of touching patterns, we observe changes in each intervention efficacy with touch specification; as touching of fomites becomes less random and more specified, HH efficacy increases while SD efficacy decreases. When population level touching patterns are close to random, however, SD is better at reducing transmission. HH exerts two types of effects to reduce transmission. The susceptibility effect decreases the inoculation a susceptible receives from their own hands; this effect is constant across touch specification. The contagiousness effect decreases the amount of pathogens which reach surfaces from a shedding individual; the strength of this effect increases as touch specificity does.

Conclusions. SD and HH affect different routes of contamination of contact mediated transmission. The extent that touching patterns are non-randomly specified, impacts which of these interventions are optimal.

3.2 Introduction

Influenza is transmitted by various routes: either through aerosols, direct-droplet-spray, or contact with fomites [37, 67, 10]. The contact route can be subdivided based on how pathogens initially reach fomite surfaces in the environment [70]. At excretion, through a cough or simply through talking, virus laden large particles either i) deposit directly to a shedder’s hands, or ii) settle rapidly to a fomite. We denote these two sub-routes of contact mediated transmission as the hand-to-fomite and droplet-to-fomite contamination routes respectively. For the hand-to-fomite contamination route to successfully transmit, pathogens must go from the hands of a shed-

der, to a fomite, to a susceptible individual's hands, and finally be self-inoculated. Pathogens in the droplet-to-fomite contamination route settle on surfaces localized around the individual shedding pathogens. As with the hand-to-fomite contamination route, a susceptible individual's hand must touch the contaminated fomite and then self-inoculate to cause transmission. While some is known about the efficiencies of different cleaning methods on killing different pathogens, little is known about how hand hygiene (HH) and surface decontamination (SD) interventions alter transmission in a detailed transmission system. We elucidate the distinction between these contact mediated mechanisms by examining the role of behavioral touching patterns on the efficacies of these two interventions, HH and SD.

To intervene against these contact-mediated environmental pathways, HH and SD have been suggested and implemented as non pharmaceutical interventions, both for influenza as well as other agents that are transmitted through the contact route[1, 2, 21, 35, 39, 48, 55, 14, 60, 69]. SD affects both contamination routes similarly by inactivating pathogens on the fomites, thus reducing the number reaching the hands of susceptibles and therefore the number eventually being self-inoculated. HH by comparison intervenes in both contamination routes, by not only reducing pathogen levels directly on the hands of susceptibles, but also by reducing the number of pathogens on the hands of infectious people, which then reduces the number of pathogens they transfer to fomites they touch. Figure 3.1 summarizes these intervention mechanisms.

Previous work that explicitly modeled contact mediated transmission through the environment has modeled fomites in different manners. Atkinson et al ([6]) modeled two types of fomites (porous and non-porous) each of which were homogeneous and evenly mixed and touched while each had their own specific viral inactivation and

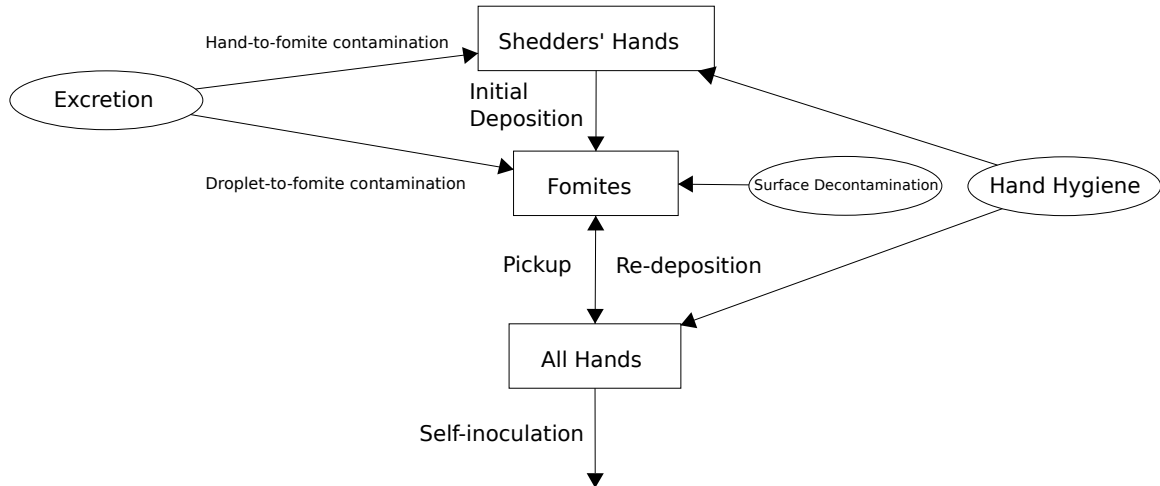


Figure 3.1: Routes of contamination and intervention of contact mediated influenza transmission. At excretion, through a cough or simply through talking, virus laden large particles either i) deposit directly to a shedder’s hands, or ii) settle rapidly to a fomite. We denote these two sub-routes of contact mediated transmission as the hand-to-fomite and droplet-to-fomite contamination routes respectively. For the hand-to-fomite contamination route to successfully transmit, pathogens must go from the hands of a shedder, to a fomite, to a susceptible individual’s hands, and finally be self-inoculated. Pathogens in the droplet-to-fomite contamination route settle on surfaces localized around the individual shedding pathogens. As with the hand-to-fomite contamination route, a susceptible individual’s hand must touch the contaminated fomite and then self-inoculate to cause transmission. Surface decontamination affects both contamination routes similarly by inactivating pathogens on the fomites, thus reducing the number reaching the hands of susceptibles and therefore the number eventually being self-inoculated. Hand hygiene by comparison intervenes in both contamination routes, by not only reducing pathogen levels directly on the hands of susceptibles, but also by reducing the number of pathogens on the hands of infectious people, which then reduces the number of pathogens they transfer to fomites they touch.

touching rates in an equation based model of household transmission. Nicas et al ([51]) modeled a single viral emission and analyzed the subsequently resulting infections from contact with the fomite environment. They simultaneously modeled two fomites (textile versus non-textile), each of which were homogeneous and evenly mixed and touched throughout using differential equations, but each compared to one another had different properties related to touching and viral inactivation rates. Li et al ([42]) modeled the fomite environment as a single homogeneous surface evenly mixed and touched throughout primarily using differential equations. They considered the importance of different types of fomites by contrasting frequently touched to infrequently touched fomites in separate scenarios. Spicknall et al ([61]) modeled the contact route by having many separate touchable fomites, but all with identical properties within a scenario, while considering numerous scenarios involving variation in touching rates and viral inactivation on the fomites in an individual based modeling framework.

The behavioral preferences for touching of different fomites vary from one setting to another. One can simplify these different population level touching preferences by considering them in one dimension (figure 3.2), varying from pure random touching, in which fomites are touched proportional to their surface area, to less random and more specified touching, where certain objects are touched more often than would be expected based on the fomite's surface area. Fomite objects such as doorknobs, computer keyboards, and telephones, are usually touched more often than would be expected due to chance alone, and often these objects are shared or touched by more than one person in a short period of time. Different patterns of fomite touching will impact the strength of contact mediated transmission as well as the relative efficacies of two contact mediated interventions, SD and HH even given similar background

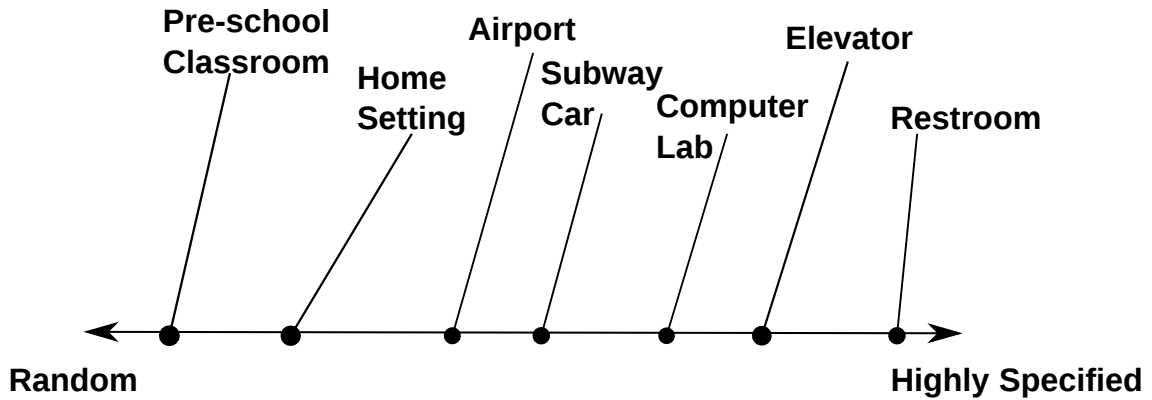


Figure 3.2: Venues with random versus increasingly less random touching patterns.

strengths of transmission.

To improve our understanding of the different effects of hand hygiene and surface decontamination, we analyze how the effects of hand hygiene and surface decontamination interventions vary as a function of different population level touching behaviors of fomites in the environment. Specifically we examine how the varying the distribution of population level touches between fomite objects affects contact mediated transmission and intervention efficacies. Figure 3.2 shows a subjective spectrum of touching distributions, from the most random touching scenarios, as in a pre-school classroom, to more specified touching scenarios such as at a home, to even more specified scenarios such as on a subway car, at a computer lab, or in a public bathroom. In this work we examine how varying the touching patterns from random to less random (more specified) situations affects transmission and intervention efficacy. We use an environmental infection transmission system (EITS) model [42] of influenza transmission which focuses solely on the contact route of transmission, ignoring the droplet-spray and aerosol mediated routes.

3.3 Materials and Methods

We use a deterministic ordinary differential equation based model of environmental influenza transmission similar to previously published models [42, 70]. The model consists of i) people and ii) pathogens in the environment: either on fomite surfaces or on hands of people. People are divided into three categories based on infection status: susceptible, infectious, and recovered, denoted by S , I , and R . People in each of these categories also have pathogen levels on the hands associated with them, denoted by E_{HS} , E_{HI} , and E_{HR} .

Rather than having a single uniform homogeneous fomite surface, we divide the fomite surface area into two. Each fomite is identical in all features, except for surface area (A_1 and A_2) and the proportion of all touches which are performed at each fomite (σ_1 and σ_2). We assume A_1 is smaller than A_2 , and that that settling of pathogens to each fomite occurs at random, proportional to the surface area each fomite represents. Under conditions of random touching, we could also assume that touching of surfaces in the environment is based on the surface area of objects. That is, if one object is ten times larger than a second object, then under the assumption of random touching, the larger object would be touched ten times more often by the population. Deviating from random touching is one example of population level heterogeneity in touch behavior. We can model this heterogeneity by dividing all touches the population performs into two proportions: i) the proportion which is performed at fomite 1, σ_1 , versus ii) the proportion performed at fomite 2, $\sigma_2 = 1 - \sigma_1$. For brevity, we refer to increased touching to fomite 1 compared to that which is defined by random touching as having a increased touch specificity; in other words higher σ_1 results in more specified touching at the population level. Figure 3.3 provides a schematic

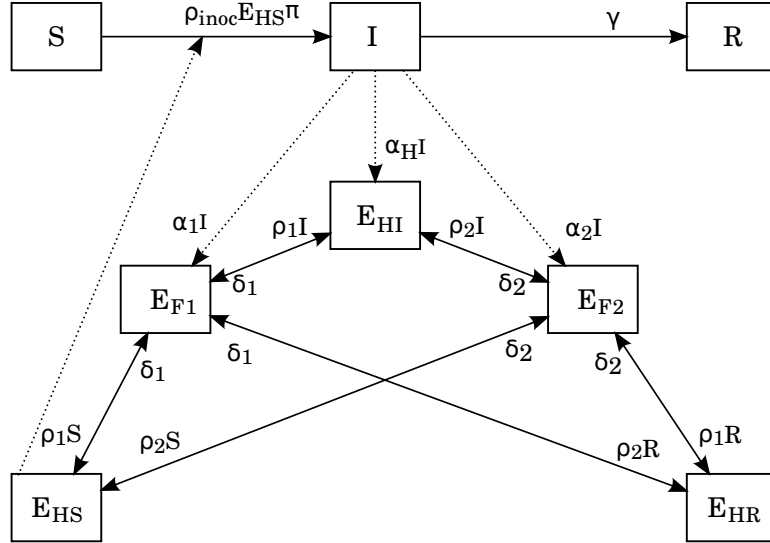


Figure 3.3: Ordinary differential equation based model schematic of contact mediated influenza transmission through two fomites.

This model consists of i) people and ii) pathogens in the environment: either on fomite surfaces or on hands of people. People are divided into three categories based on infection status: susceptible, infectious, and recovered, denoted by S , I , and R . People in each of these categories also have pathogen levels on the hands associated with them, denoted by E_{HS} , E_{HI} , and E_{HR} . We divide the total fomite surface area into two. Each fomite is identical in all features, except for surface area (A_1 and A_2) and the proportion of all touches which are performed at each fomite (σ_1 and σ_2). We assume A_1 is smaller than A_2 , and that that settling of pathogens to each fomite occurs at random, proportional to the surface area each fomite represents. We divide all touches the population performs into two proportions: i) the proportion which is performed at fomite 1, σ_1 , versus ii) the proportion performed at fomite 2, $\sigma_2 = 1 - \sigma_1$.

of this model. The following paragraph addresses the five processes modeled, one of which (surface touching) incorporates the population level heterogeneity of touch specificity .

We model the following processes. Shedding. Pathogens are shed at rate α to the environment. The proportion β_H of these go directly to the shedder's hands. The complementary proportion ($\beta_F = 1 - \beta_H$), go to the fomite surface area; however, only λ proportion of these land on touchable surfaces. Surface touching. Once on touchable surfaces, pathogens may be picked up by anyone. This is done at rate ρ , which is modeled as the product of the touch rate (ρ_{tr}), transfer efficiency of the surface (ρ_{te}), proportion of touches performed at either fomite 1 or 2 (σ_1 or σ_2),

and fingertip to surface area ratio ($\frac{A_{fingertip}}{A_{fomite}}$). Additionally, pathogens are deposited from hands to fomites at rate δ , which is modeled as the product of the touch rate (ρ_{tr}) and transfer efficiency of the surface (ρ_{te}) and proportion of touches performed at either fomite 1 or 2 (σ_1 or σ_2). Pathogen inactivation. Pathogens inactivate at rate μ_H if on hands and at rate μ_F if on fomites. Self inoculation. Touching the eyes, nose or mouth occurs at rate ρ_{Inoc} to potentially cause infection with the per pathogen probability of infection π . While self inoculation may be done by anyone providing another pathogen loss mechanism, infection may only result when a susceptible self-inoculates. Infection recovery. Infectious people recover and become immune to reinfection at rate γ .

The differential equations for this model follow where the total population is given by $N = S + I + R$. The excretion rate of viruses on large droplets to each fomite (α_1, α_2) as well as to the hands of the shedder (α_H) are given by

$$(3.1) \quad \begin{aligned} \alpha_1 &= \alpha\beta_F\lambda\frac{A_1}{A_{Total}} \\ \alpha_2 &= \alpha\beta_F\lambda\frac{A_2}{A_{Total}} \\ \alpha_H &= \alpha\beta_H \end{aligned}$$

The pathogen pickup rate from each fomite to hands is given by

$$(3.2) \quad \begin{aligned} \rho_1 &= \sigma_1\rho_{tr}\rho_{te}\frac{A_{fingertip}}{A_1} \\ \rho_2 &= \sigma_2\rho_{tr}\rho_{te}\frac{A_{fingertip}}{A_2} \end{aligned}$$

The rate of deposition from hands to each fomite is given by

$$(3.3) \quad \begin{aligned} \delta_1 &= \sigma_1\rho_{tr}\rho_{te} \\ \delta_2 &= \sigma_2\rho_{tr}\rho_{te} \end{aligned}$$

We use a standard SIR model of infection progression, where new infections are

the result of self inoculations from contaminated susceptible hands

$$(3.4) \quad \begin{aligned} \frac{dS}{dt} &= -\rho_{inoc}E_{HS}\pi \\ \frac{dI}{dt} &= \rho_{inoc}E_{HS}\pi - \gamma I \\ \frac{dR}{dt} &= \gamma I \end{aligned}$$

We model pathogens on fomites by considering fomite contamination via droplet-to-fomite contamination, pathogen loss from either pickup by people or pathogen inactivation, and pathogen gains resulting from deposition by hands to each fomite:

$$(3.5) \quad \begin{aligned} \frac{dE_{F1}}{dt} &= I\alpha_1 - E_{F1}(N\rho_1 + \mu_F) + (E_{HS} + E_{HI} + E_{HR})\delta_1 \\ \frac{dE_{F2}}{dt} &= I\alpha_2 - E_{F2}(N\rho_2 + \mu_F) + (E_{HS} + E_{HI} + E_{HR})\delta_2 \end{aligned}$$

We model pathogens on the hands of people by considering direct shedding to the hands of infectious people, pathogen pickup resulting from surface touching, and pathogen loss resulting from either inactivation, self inoculation, or deposition to fomites:

$$(3.6) \quad \begin{aligned} \frac{dE_{HS}}{dt} &= S(E_{F1}\rho_1 + E_{F2}\rho_2) - E_{HS}(\mu_H + \rho_{inoc} + \delta_1 + \delta_2) \\ \frac{dE_{HI}}{dt} &= I\alpha_H + I(E_{F1}\rho_1 + E_{F2}\rho_2) - E_{HI}(\mu_H + \rho_{inoc} + \delta_1 + \delta_2) \\ \frac{dE_{HR}}{dt} &= R(E_{F1}\rho_1 + E_{F2}\rho_2) - E_{HR}(\mu_H + \rho_{inoc} + \delta_1 + \delta_2) \end{aligned}$$

We model two types of interventions: hand hygiene (HH) and surface decontamination (SD). We model each in an abstract manner as the percent increase in the pathogen inactivation rate, either on hands (ν_H) or on surfaces (ν_F) respectively. Unless stated otherwise, we model each intervention as a 10% increase in pathogen inactivation.

Table 3.1 shows the parameter values used throughout this paper, unless otherwise explicitly stated. Except for the intervention parameters, these values all correspond to values used in Spicknall et al[61] which were informed by empirical literature where available.

<i>Parameter Symbol</i>	<i>Description</i>	<i>Value</i>
ρ_{inoc}	Self inoculation rate	0.028 per minute
π	Per pathogen infection probability	0.001386
γ	Recovery rate	0.25 per day
α	Pathogen excretion rate	1000 per minute
β_F	Fraction of pathogens shed to fomites	0.85
β_H	Fraction of pathogens shed to the hands of the shedder	0.15
λ	Fraction of pathogens shed to fomites which settle on touchable surfaces	0.7
μ_F	Pathogen inactivation rate on fomite surfaces	0.01 per minute
μ_H	Pathogen inactivation rate on hands	0.92 per minute
ρ_{tr}	Personal surface touching rate	0.75 per minute
ρ_{te}	Transfer efficiency of a surface touch	0.1
A_{F1}	Surface area of fomite1	50 cm ²
A_{F2}	Surface area of fomite2	99950 cm ²
A_{Ftotal}	Total surface area	10000 cm ²
A_{finger}	Surface area on hand doing the touching	10 cm ²
σ_1	Proportion of touches performed on fomite1	Varied throughout
σ_2	Proportion of touches performed on fomite2	(1 - σ_1)
ν_H	Percent increase in pathogen inactivation on hands resulting from hand hygiene	10%
ν_F	Percent increase in pathogen inactivation on fomites resulting from surface decontamination	10%
$\epsilon_{density}$	Host density	1.0 persons per m ²

Table 3.1: Parameter Description and Values Used

3.3.1 Important Assumptions

We make the following assumptions, which can all be relaxed in future work.

- By modeling HH and SD as a 10% increase in either μ_H or μ_F respectively, we are assuming these intervention have residual effects only. We assume no discrete pulse-like effect. We examine how modeling interventions in a pulse-like manner affects our inferences in the discussion.
- We assume that droplet-to-fomite shedding settles randomly throughout the venue modeled. Thus, we are assuming maximal pathogen dispersal via this contamination route. In reality, settling of large droplets to fomites occurs in relatively close proximity to the shedder. Maximal pathogen dispersal as-

sumes that movement of the shedder is adequate to evenly spread their localized pathogen shedding throughout the entire venue. Future work could relax this assumption.

- When we vary the proportion of pathogens being shed directly to hands (β_H), we assume that there is no additional loss of pathogens (as might happen when someone coughs into their shoulder). Thus, we assume λ is independent of β_H . Work of others [70] examines in greater detail relaxation of this assumption.

We assess the effectiveness of each intervention by comparing the cumulative incidence (CI) when the intervention is present to when it is not present, summarizing this as the intervention efficacy: $(1 - CI_{intervention}/CI_{nointervention})$. Because these interventions are applied at the population level, we only make comparisons between when the intervention is present versus absent, to summarize the total effects of each intervention.

3.4 Results

We divide the results into the following analyses. First we examine the intervention efficacies of both hand hygiene (HH) and surface decontamination (SD) across the spectrum of touch specificity, from random touching (meaning lower σ_1) to highly specified non-random touching (higher σ_1). Second we examine the strength of each contact sub-route (hand-contaminated versus droplet-settled) across the touch specification spectrum, as well as how each sub-route is affected by HH and SD. Third, we compare the effects of targeted versus non-targeted HH implementation by either implementing HH on everyone (untargeted) or to only susceptible, infectious, or recovered people (forms of targeted HH). We compare the resulting HH efficacies for each form across the spectrum of touch specificity. The first and second analyses have

two sub-analyses. In one, touch specification (σ_1) is the only parameter varied. In the other, we additionally vary the per pathogen probability of infection (π) so that the pre-intervention incidence is the same for the complete range of touch specificity scenarios considered; we refer to this as using a fixed incidence model, rather than an unfixed incidence model. We conduct this second sub-analysis to hold constant the overall background incidence in all of these scenarios, so that intervention efficacy measures are not affected by the indirect effects associated with higher or lower background transmission levels. The fixed incidence approach is appropriate when one knows the cumulative incidence and is trying to figure out what contributes to it while the unfixed reflects system dynamic effects of parameters more directly.

3.4.1 Touch Specificity and Intervention Efficacy

As more touches are preferentially performed on the smaller fomite 1 (meaning increasing σ_1) total contact transmission may either increase or decrease depending on the proportion of pathogens which initially go to the shedder's hands (β_H). Figure 3.4(a) shows that when $\beta_H = 0.15$ total contact transmission increases with increased σ_1 , while figure 3.4(b) shows that when $\beta_H = 0.04$ transmission decreases with σ_1 . The difference here is that a low β_H means more pathogens are randomly settling to fomite surfaces which dilutes the effect of high touch specificity. In both cases, each intervention reduces transmission across the spectrum of touch specificity, but we can see that each intervention efficacy ($1 - CI_{intervention}/CI_{nointervention}$) varies with the value (σ_1), and that the slope of this relationship may either be negative (given higher β_H as in 3.4(c)) or positive (given lower β_H as in 3.4(d)). However, the difference in slope direction is caused by variable background incidence levels (which is caused by β_H), rather than each intervention behaving inherently different. Thus coughing into the hand may be helpful or harmful depending on the degree of

random touching going on in the venue: if touching is highly specified transmission is increased, but if touching is fairly random transmission is reduced by coughing more into one's hand. As shown in 3.4(e) and 3.4(f), which utilize fixed incidence models, HH efficacy increases and SD efficacy decreases with increasing touch specificity regardless of the value of β_H .

Note that at nearly random touching (low σ_1) the efficacy of the SD intervention is better than the efficacy of HH, whether or not a fixed or unfixed incidence model is used. As touch specificity increases, the HH intervention becomes more efficacious than the SD intervention. The location of this transition point determining when SD is better than HH depends on the proportion of pathogens shed onto hands relative to settling to the surface fomites (β_H).

3.4.2 Touch Specificity and Sub-Routes of Contact-Mediated Transmission

To explain why SD efficacy decreases and HH efficacy increases with increased touch specificity (σ_1), we track the portion of infections which result from either the droplet-to-fomite, or hand-to-fomite contamination routes. Equations for this model can be found in the appendix. We examine the strength of each route while both routes are operating simultaneously. In all cases shown in figure 3.5, at random touching the droplet-to-fomite route of contamination is the dominant route, but as touching becomes more specified, transmission resulting from hand-to-fomite contamination becomes dominant. This transition point, for determining which route of contamination is more powerful, largely depends on β_H .

The strength of transmission resulting from hand-to-fomite contamination increases monotonically with increased σ_1 . This is true regardless of β_H , although the slope is much greater when $\beta_H = 0.15$ (figure 3.5(a)), compared to when $\beta_H = 0.04$ (figure 3.5(b)). In contrast, transmission resulting from the droplet-to-fomite con-

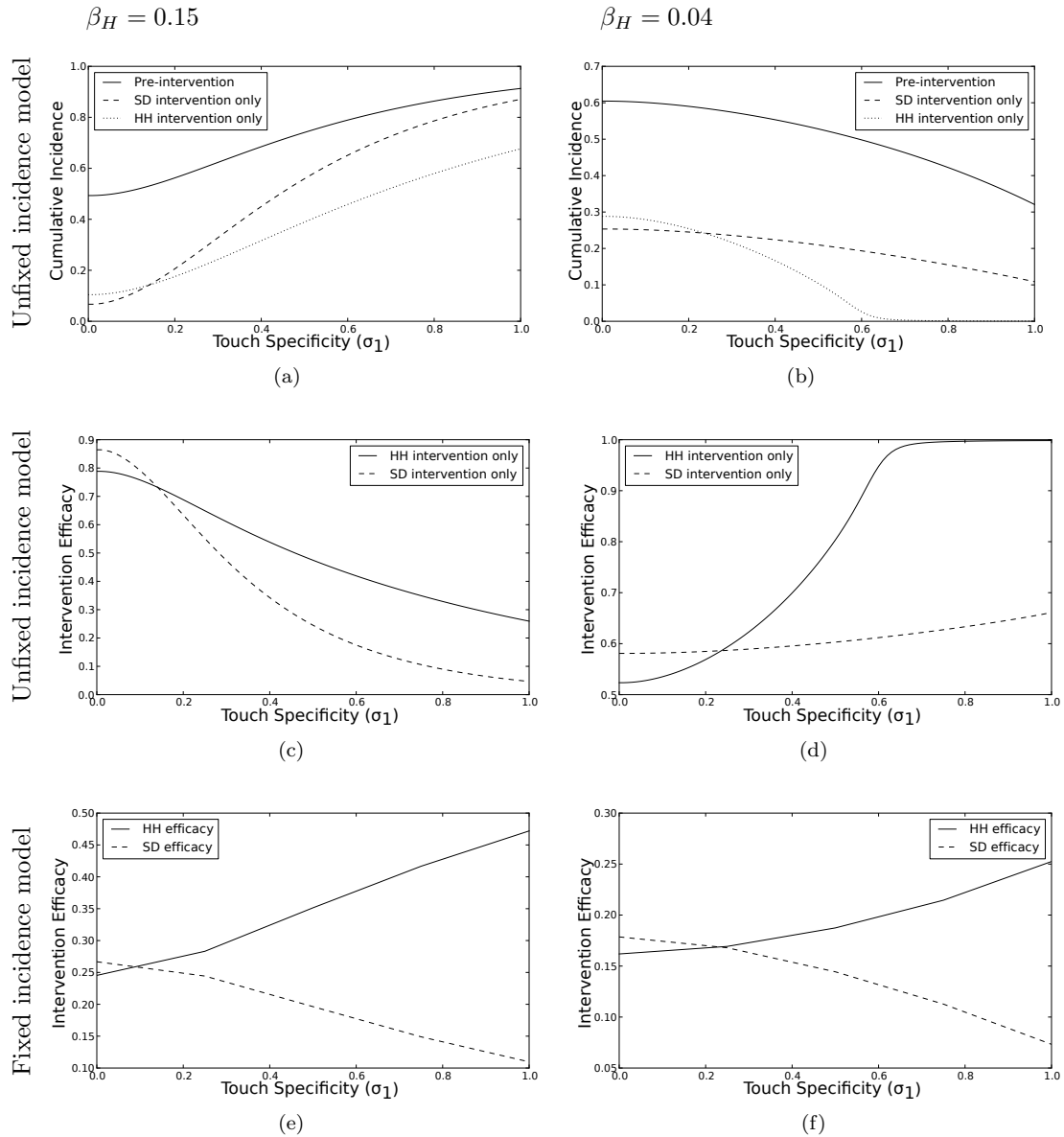


Figure 3.4: Cumulative incidence and intervention efficacy as a function of surface touching specificity, using unfixed and fixed pre-intervention incidence models

3.4(a) and 3.4(b) represent unfixed pre-intervention total incidence models, where in 3.4(a) $\beta_H = 0.15$ and in 3.4(b) $\beta_H = 0.04$. In 3.4(a) total incidence increases as touching becomes more specified and less random while in 3.4(b) it decreases. 3.4(c) shows the resulting intervention efficacies from 3.4(a), while 3.4(d) shows the resulting intervention efficacies from 3.4(b). 3.4(e) and 3.4(f) represent fixed pre-intervention total incidence models, where in 3.4(e) $\beta_H = 0.15$ and in 3.4(f) $\beta_H = 0.04$. In both 3.4(e) and 3.4(f) hand hygiene efficacy increases as touching becomes more specified while surface decontamination efficacy decreases.

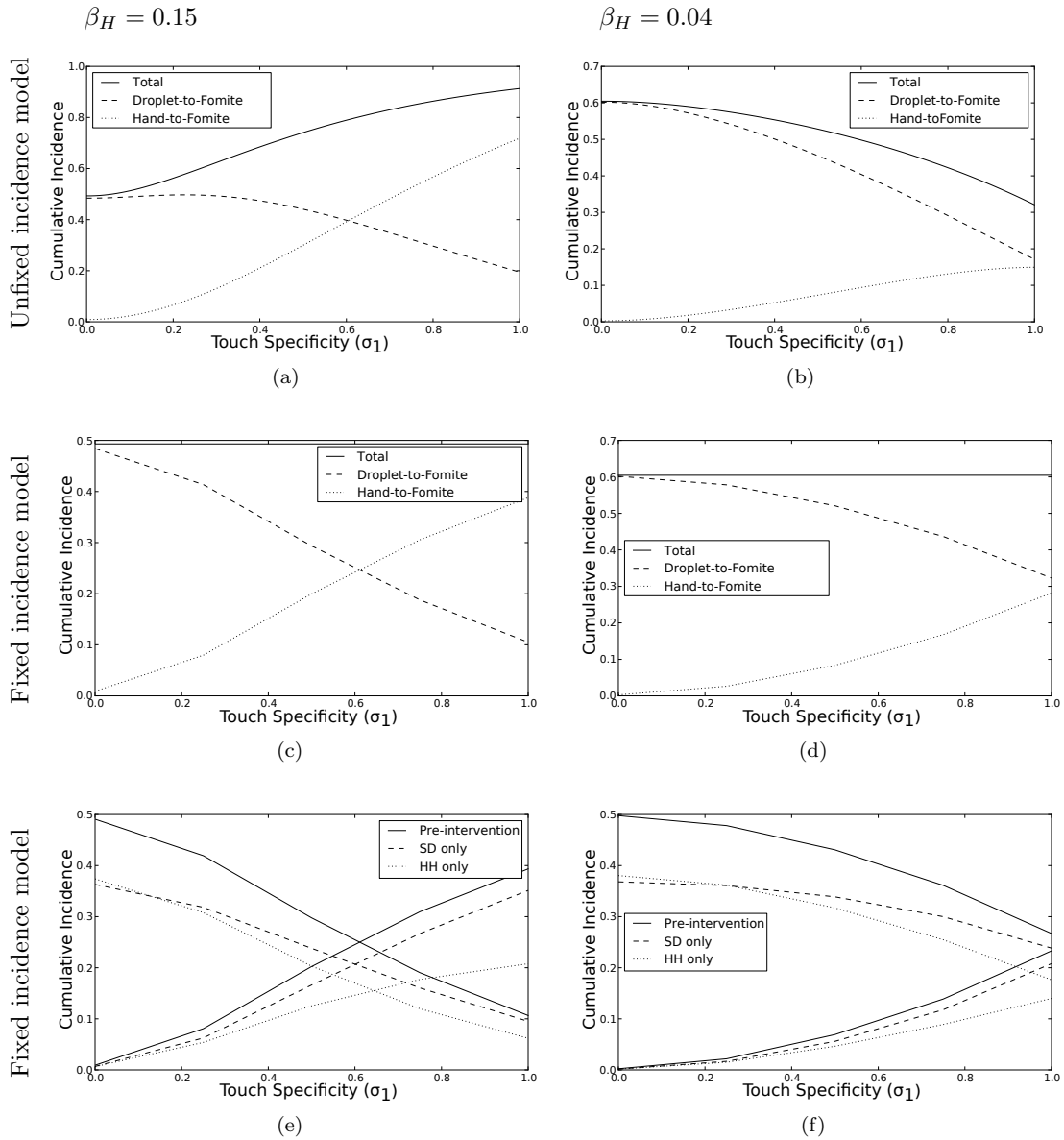


Figure 3.5: Cumulative incidence and intervention efficacy of sub-routes of contact transmission as a function of surface touching specificity, using unfixed and fixed pre-intervention total incidence models.

3.5(a) and 3.5(b) represent unfixed pre-intervention total incidence models, where in 3.5(a) $\beta_H = 0.15$ and in 3.5(b) $\beta_H = 0.04$. In 3.5(a) transmission from the hand-to-fomite route increases while transmission from the droplet-to-fomite route decreases with more specified and less random touching, and in 3.5(b) there is similar phenomena, although the hand-to-fomite slope is less severe. The remaining sub-figures examine each route of contamination using fixed incidence models. In both 3.5(c) and 3.5(d) we see monotonic increases and decreases in transmission resulting from the hand-to-fomite and droplet-to-fomite routes. In both 3.5(e) and 3.5(f) we show what happens when each intervention is applied separately to both routes. Hand hygiene (HH) reduces incidence more for the hand-to-fomite route (positive slope lines) compared to surface decontamination (SD). When touching is close to random, SD reduces transmission from the droplet-to-fomite route (negative slopes) more than HH, but as touching becomes more specified, HH eventually reduces incidence more.

tamination route at first remains fairly constant (or actually increases although not obviously apparent) in figure 3.5(a), but eventually decreases with increased σ_1 , while in figure 3.5(b) it monotonically decreases. The initial slight increase in figure 3.5(a) is due to increased background transmission causing higher transmission from the droplet-to-fomite contamination; i.e. the effect of higher β_H values leading to greater hand-to-fomite transmission and thereby greater total transmission, indirectly causes higher droplet-to-fomite transmission than if it were operating in isolation (THIS IS STILL NOT CLEAR). When we examine the strength of each contamination route using fixed incidence models (as we did in figures 3.4(e) and 3.4(f)) we see that transmission resulting from hand-to-fomite contamination monotonically increases while transmission from the droplet-to-fomite contamination route monotonically decreases for both values of β_H (figure 3.5(c) and 3.5(d)). This occurs because as σ_1 increases more pathogens which settle to fomite 2 are not being picked up, thus decreasing the strength of transmission from droplet-to-fomite contamination; conversely, as σ_1 increases, pathogens which are initially shed to the shedder's hands are deposited to fomite 1 preferentially, which are in turn more likely to be picked up, since susceptibles also are touching fomite 1 more preferentially. Thus, we observe a trade-off between these sub-routes with increased touch specificity.

Using the same fixed incidence model design, we compare how each intervention performed at attenuating transmission resulting from each contamination route. Figures 3.5(e) and 3.5(f) show both contamination routes' pre-intervention incidence values (solid lines) as well as how each intervention affects each contamination route specifically. All lines with positive slopes represent the hand-to-fomite contamination route scenarios, while all lines with negative slopes represent the droplet-to-fomite contamination route scenarios.

For transmission resulting from hand-to-fomite contamination (positive slope lines), the HH intervention was more effective across all levels of σ_1 (figures 3.5(e) and 3.5(f)). This difference is most stark at the highest levels of σ_1 . For transmission resulting from droplet-to-fomite contamination (negative slope lines), the SD intervention performs better at the lowest levels of touch specificity, when touching is very close to the definition of random touching, while when σ_1 is higher the HH intervention eventually performs better at attenuating this sub-route.

3.4.3 Comparison of HH implementation

To further explain why HH efficacy increases with increased touch specificity (σ_1), we varied how HH was implemented by applying it separately to only the hands of i) susceptible people, ii) infectious people, or iii) recovered people. Not surprisingly the third option provided very little benefit (efficacy = 0). Exclusively applying HH to susceptible hands yielded an effect that was roughly constant for all levels of touch specificity, at about 22% efficacy. When HH was applied to the hands of infectious people only, there was a monotonic increase in efficacy with increased touch specificity. This effect was never stronger than the susceptibility effect, although it should be noted that in reality implementation of this intervention could require the behavior modification of fewer people compared to getting all susceptibles to alter their behavior since only a subset of people would ever be infectious.

We also examined how HH targeting affected each route of contamination. Both routes were similarly affected, but the efficacy on the hands of infectious people of reducing transmission from the hand-to-fomite contamination route (figure 3.6(b)), was higher but with similar slope across the full spectrum of touch specificity. There was no initial efficacy by intervening on the infectious hands on the droplet-to-fomite route. The value of β_H did not affect this relationship (data not shown).

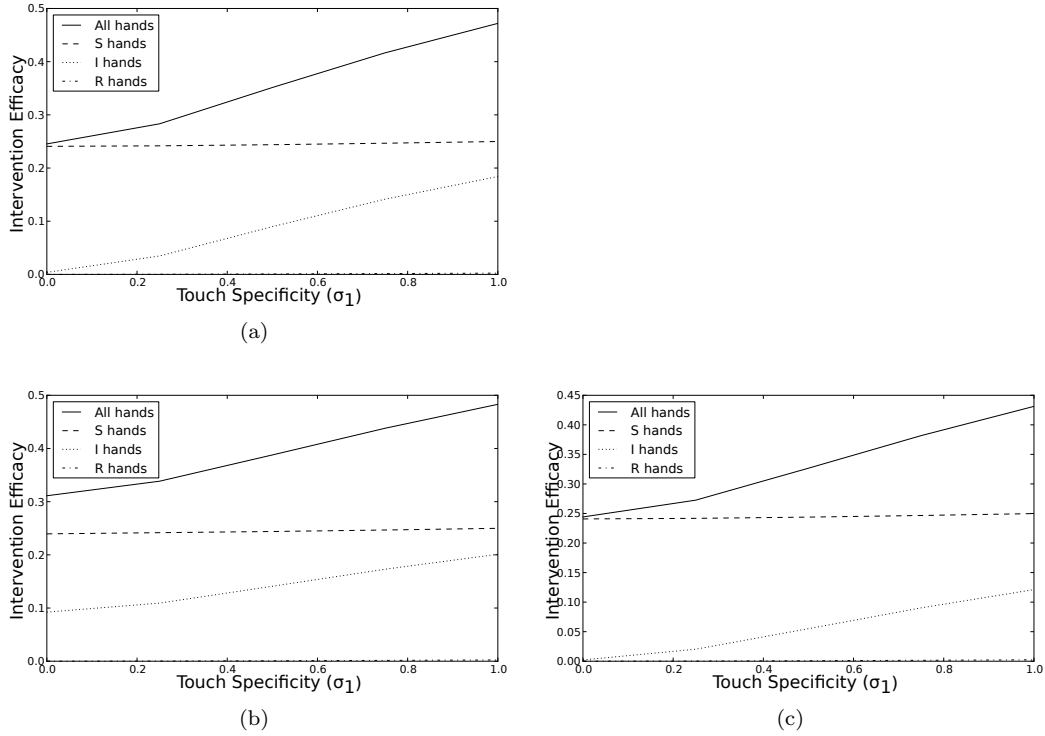


Figure 3.6: Hand hygiene intervention efficacy when targeted to separate infection categories of people as a function of touching specificity using fixed incidence models.

Figure 3.6(a) shows the effect on transmission resulting from both contamination routes combined, while 3.6(b) only shows the effect on transmission from the hand-to-fomite contamination route, and 3.6(c) only shows the effect on transmission from the droplet-to-fomite contamination route. Intervening on susceptible hands provides an effect that is roughly independent of touch specificity. Intervening on infectious hands provides greater benefit the higher the touch specificity. Intervening on hands of the recovered provides very little effect. All sub-figures use fixed pre-intervention total incidence models with $\beta_H = 0.15$.

We examined in greater detail the implementation of HH to only infectious people by further exclusively subdividing HH to either i) the pathogens that are part of the hand-to-fomite contamination route, or ii) the pathogens that are part of the droplet-to-fomite contamination route. When only applied to the pathogens that are part of the hand-to-fomite contamination route, there was nearly identical efficacy compared to when the intervention was applied to both types of pathogens on the hands of the infected people; this was true for transmission resulting from both contamination routes. When the intervention was only applied to the pathogens part of the droplet-to-fomite contamination route, there was no effect on transmission resulting from either contamination route. Thus the reduced transmission resulting from droplet-to-fomite contamination observed when applied to all pathogens on hands of infected people was due to indirect effects, due to the reduced transmission occurring from the dampened hand-to-fomite contamination route.

The increasing HH efficacy observed with increased σ_1 is a result of contagiousness-based effects, from decreasing the number of pathogens going from the a shedder's hands to preferentially touched surfaces. The susceptibility-based effects conveyed by a susceptible washing their own hands are roughly constant across values of σ_1 . HH works better with higher touch specificity because it reduces pathogen levels on the hands of those that are contagious, which thus reduces their contaminating a highly shared fomite in the environment. In contrast, SD is less efficacious with higher touch specificity because of a dilution effect; i.e. there are lots of pathogens that are being cleaned on surfaces that were not at risk of contaminating the hands of susceptible people.

3.5 Discussion

We demonstrate a trade-off between SD and HH interventions that varies by behavioral touching patterns. When touching patterns are more random SD becomes the optimal intervention. When touching patterns are less random, HH becomes the optimal intervention. Furthermore, HH effectiveness is more pronounced if targeted to contagious individuals. The modeling analysis presented here provides a solid mechanistic framework from which to conceptualize the context in which to recommend one of these contact based interventions over the other.

The mechanisms highlighted in this analysis are that the droplet-to-fomite contamination route deposits pathogens more evenly throughout; therefore as touching is more specified to a small location, the transmission strength resulting from this contamination route decreases; with only a finite amount of pathogens on the specified fomite from the droplet-to-fomite route, as consecutive people touch the object, there are less pathogens from this route present on the fomite for subsequent people to pick up. Conversely, the strength of transmission resulting from the hand-to-fomite contamination route increases with higher touch specificity. We have shown that SD is better suited to attenuating transmission from the droplet-to-fomite contamination route when touching is fairly random, but as touching gets more specified, eventually HH performs better. We have also shown that HH is better suited to attenuating the hand-to-fomite contamination route regardless of touch specificity. Thus, because of the switching of dominant contamination routes from droplet-to-fomite towards hand-to-fomite contamination, and because HH is better at attenuating hand-to-fomite transmission, SD efficacy decreases and HH efficacy increases as touching of fomites becomes less random and more specified.

HH exerts two types of effects to reduce transmission. The susceptibility effect decreases the inoculation a susceptible receives from their own hands; the effect this has on risk of infection is constant across the spectrum of touch specificity. The contagiousness effect decreases the amount of pathogens which reach surfaces from a shedding individual; the strength of this effect on risk reduction increases as touch specificity does.

Using an abstract intervention implementation when increased die-out effects are all residual and sustained through time, we have shown that SD is better at reducing transmission when population surface touching patterns are close to random. However, another way to model these interventions is to assume zero residual effect, thus all effect is exerted at regular intervals through time, in a pulse-like fashion. When we implemented this alternative intervention operation, we observed robust results: respectively SD and HH efficacy decreased and increased similarly with touch specificity. However, the transition point for when HH efficacy becomes higher than SD occurred at far higher touch specificity compared to the pure-residual effects intervention model. Additional details of this intervention design and parameterization are available in the supplemental material. In reality, these interventions probably act as a combination of both a pulse-like initial effect, as well as a residual effect of altering inactivation rates for some period afterwards. Thus, we cannot say where this transition point would be without a more detailed scenario-specific model.

Another sensitivity analysis we performed was on the proportion of pathogens excreted which go directly to the shedder's hands (β_H). We showed how more specified touching alone can lead to increased contact-mediated transmission given a higher β_H . However, with a lower β_H , more specified touching could also lead to reduced transmission. Varying β_H resulted in varied strengths of transmission resulting from

each contamination route. Because of this, when more transmission is resulting from the hand-to-fomite contamination route, HH efficacy is higher than when β_H is lower and less transmission is resulting from the hand-to-fomite contamination route. The value of β_H is another determinant of the location of the transition point in the spectrum of touch specification. The higher β_H , the less random touching must be, in order for HH to be more efficacious than SD.

Future work could relax some of the assumptions we make in this paper by using a more detailed modeling form. For example, rather than assuming complete dispersal of droplet-to-fomite pathogens, a more detailed model could have discrete individuals moving around a venue, shedding droplet-to-fomite pathogens in a localized manner, while also expressing touching specificity. Additionally, more detailed shedding behavior could be adopted, where people may either cough without covering their mouth, cough while covering their mouth, or coughing into their shoulder. Doing so, one would vary both the proportion of pathogens being shedder directly to the hands (β_H) and the proportion of remaining pathogens which settle to touchable surfaces (λ) as a function of this shedding behavior. These would both improve our understanding of these transmission pathways and how optimal intervention choice may be affected.

Incorporating a framework that accounts for touching pattern behavior provides a useful tool to analyze contact mediated transmission for not just influenza but for other pathogens that are environmentally mediated such as the enteric pathogens, rhinoviruses, *Staphylococcus aureus*, among others. In particular, if pathogens have a slower inactivation rate either on hands, touch specificity could play a much larger role in determining overall transmission strength. Another situation when increased touch specificity would result in greater gains in transmission strength would occur if

more pathogens initially are shed to the hands of the shedder. Future work could assess how pathogen features such as these alter how transmission scales with touching specificity.

Surface decontamination and hand hygiene affect different routes of contamination both for influenza, as well as all pathogens for which transmission is partially contact-mediated. Population surface touching patterns in part determine how large a part is played by these routes of contamination in the overall transmission system. These touching patterns will vary among different fomites. Quantifying how these patterns differ among fomites allows for a more nuanced approach in determining whether SD or HH is the preferred intervention. More empirical data collection and research activities are needed to advance our understanding of these transmission pathways.

CHAPTER IV

Comparing Contact Mediated Transmission

4.1 Abstract

Background. Compared to our understanding of waterborne and airborne infection transmission, contact mediated transmission remains a relatively unexplored black box. Many pathogens that cause great health and economic problems are transmitted by this route, including norovirus and *S. aureus*. In this paper we compare i) pathogen specific parameters which differ among norovirus, *S. aureus*, influenza, and rhinovirus, ii) relative shedding required to achieve specific levels of population level transmission, and iii) amenability of each pathogen to contact mediated interventions such as hand hygiene and surface decontamination.

Methods. We use an ordinary differential equation based environmental infection transmission system to model the contact mediated transmission routes of these pathogens, incorporating both hand hygiene and surface decontamination into this model. To parameterize the model, we characterize these pathogens in terms of their infectivity, survivability on human hands, survivability on fomite surfaces, and proportion of pathogens excreted which enter a contact transmission route beginning on the shedder's hands.

Results. Norovirus has the highest infectivity of these pathogens studied. *S. au-*

reus and norovirus both survive much longer in the environment on fomites and hands of people compared to influenza and rhinovirus. Norovirus requires the lowest levels of shedding over the course of an infection to cause 50% final fraction infected in the population. *S. aureus* requires 14 times more pathogen excretion, while influenza and rhinovirus requires greater than 3000 times more excretion than norovirus, when touching was performed randomly in the venue. When we examined how often a hand hygiene or surface decontamination intervention must be applied to reduce infection substantially, we observed that for hand hygiene, norovirus was most amenable, followed by *S. aureus* and rhinovirus. Influenza does not respond to hand hygiene substantially, as even with it being applied once every 10 minutes to all hands, only 20% intervention efficacy was conveyed; this is likely due to influenza's much higher inactivation rate on hands compared to these other pathogens. For surface decontamination, *S. aureus* was the most amenable, as cleaning once every 3 days conveyed nearly 100% efficacy. Norovirus was next most amenable, as cleaning once each day conveyed nearly 100% efficacy. Influenza and rhinovirus followed, but required a high frequency of venue cleaning to produce a large intervention effect.

Conclusions. If empirical estimates from the literature are accurate, it is likely that contact mediated interventions such as hand hygiene and surface decontamination provide a much smaller benefit against influenza and rhinovirus transmission, compared to *S. aureus* and norovirus transmission. These latter agents are much more easily transmissible, in part because of their greater survivability in the environment on fomites and human hands.

4.2 Introduction

For many infectious diseases, transmission may be mediated by the environment. Examples of this include transmission through the air [53], water [18, 19], surfaces via the contact mediated route [70], and combinations of these [6, 51, 42, 61]. While small particle aerosol and water-borne transmission may often appropriately use either the well mixed room or well mixed water volume assumptions, making similar assumptions regarding homogeneous pathogen distributions on surfaces is less likely to be appropriate. Because of this increased complexity, it is arguable that the contact mediated transmission route is the least understood among these environmental routes.

A simplified diagram of the contact route is shown in figure 3.1. Pathogens may enter the environment in two abstract ways: i) Direct emission from the shedder in the droplet-to-fomite contamination route: this includes both rapid settling of large particles which contain pathogens resulting from a cough as well as air dispersal and later settling of pathogens as is the case for commensal turned pathogenic agents which may reside on the skin such as *S. aureus*. ii) Transfer of pathogens from the shedder's hands to the environment: this route implies that the shedder must touch a pathogen reservoir on their body, such as the case of touch a *S. aureus* colonization site, touching the nose when mucous is being excreted (rhinovirus), covering a cough with the hand (influenza), or fecal contamination of the hand (norovirus). Once pathogens are on touchable surfaces in the environment via either route of contamination, they may get transferred to the hands of susceptibles. Once on the hands of susceptibles, the pathogens may get transferred to a target site of infection (or site of colonization for the case of agents which are often skin commensals

such as *S. aureus*).

Similar assumptions to the well mixed room assumption may be applied to surfaces. In this case the assumption is that all touchable surfaces are touched at the same rate, and that after each touching event, all surfaces are instantaneously well mixed. When surface touching is performed completely at random, this assumption is sensible, as stochastic heterogeneities would be washed out at time equals infinity. However, if there is preference for touching certain surfaces versus others in a venue (meaning touching is not performed randomly), assuming random touching becomes less valid, as these differences can alter transmission patterns greatly (chapter III).

In this manuscript we implement, analyze, and compare models of the contact mediated route of transmission for a select group of pathogens which have different features. We compare the different features of these pathogens in terms of their infectivity, survivability in the environment and on hands, and proportion of pathogens going into a transmission system which either begin first on the shedder's hands or are shed directly to the environment. We compare the relative transmissibilities of these pathogens by doing so first in a model which assumes random touching, and second in a model where surface touching is less random. We finally compare how well pulse-like hand hygiene and surface decontamination perform at reducing transmission for each of these pathogens when applied at different rates.

Materials and Methods

We use a deterministic ordinary differential equation based model of environmental influenza transmission similar to previously studied models [42, 70]. The model consists of i) people and ii) pathogens in the environment: either on fomite surfaces or on hands of people. People are divided into three categories based on infection sta-

tus: susceptible, infectious, and recovered, denoted by S , I , and R . People in each of these categories also have pathogen levels on the hands associated with them, denoted by E_{HS} , E_{HI} , and E_{HR} .

To model deviation from random surface touching, we divide the fomite surface area into two. Each fomite is identical in all features, except for surface area (A_1 and A_2) and the proportion of all touches which are performed at each fomite (σ_1 and σ_2). We assume A_1 is smaller than A_2 , and that that settling of pathogens to each fomite occurs at random, proportional to the surface area each fomite represents. We divide all touches the population performs into two proportions: i) the proportion which is performed at fomite 1, σ_1 , versus ii) the proportion performed at fomite 2, $\sigma_2 = 1 - \sigma_1$. Under conditions of random touching based on fomite surface area, the model form may be simplified to only contain a single fomite homogeneous fomite. The following paragraph addresses the five processes modeled.

We model the following processes. Shedding. Pathogens are shed at rate α to the environment. The proportion β_H of these go directly to the shedder's hands. The complementary proportion ($\beta_F = 1 - \beta_H$), go to the fomite surface area; however, only λ proportion of these land on touchable surfaces. Surface touching. Once on touchable surfaces, pathogens may be picked up by anyone. This is done at rate ρ , which is modeled as the product of the touch rate (ρ_{tr}), transfer efficiency of the surface (ρ_{te}), and proportion of touches performed at either fomite 1 or 2 (σ_1 or σ_2), and fingertip to surface area ratio ($\frac{A_{finger}}{A_{fomite}}$). Additionally pathogens may be deposited from hands to fomites at rate δ , which is modeled as the product of the touch rate (ρ_{tr}) and transfer efficiency of the surface (ρ_{te}) and proportion of touches performed at either fomite 1 or 2 (σ_1 or σ_2). Pathogen inactivation. Pathogens inactivate at rate μ_H if on hands and at rate μ_F if on fomites. Self inoculation.

Touching the eyes, nose or mouth occurs at rate ρ_{Inoc} to potentially cause infection with the per pathogen probability of infection π . While self inoculation may be done by anyone providing another pathogen loss mechanism, infection may only result when a susceptible self-inoculates. Infection recovery. Infectious people recover and become immune to reinfection at rate γ .

The differential equations for this model follow where the total population is given by $N = S + I + R$. The excretion rate of large droplets during excretion to each fomite as well as to the hands of the shedder are given by

$$(4.1) \quad \begin{aligned} \alpha_1 &= \alpha\beta_F\lambda\frac{A_1}{A_{Total}} \\ \alpha_2 &= \alpha\beta_F\lambda\frac{A_2}{A_{Total}} \\ \alpha_H &= \alpha\beta_H \end{aligned}$$

The pathogen pickup rate from each fomite to hands is given by

$$(4.2) \quad \begin{aligned} \rho_1 &= \sigma_1\rho_{tr}\rho_{te}\frac{A_{finger}}{A_1} \\ \rho_2 &= \sigma_2\rho_{tr}\rho_{te}\frac{A_{finger}}{A_2} \end{aligned}$$

The rate of deposition from hands to fomites is given by

$$(4.3) \quad \begin{aligned} \delta_1 &= \sigma_1\rho_{tr}\rho_{te} \\ \delta_2 &= \sigma_2\rho_{tr}\rho_{te} \end{aligned}$$

We use a standard SIR model of infection progression, where new infections are the result of self inoculations from contaminated susceptible hands

$$(4.4) \quad \begin{aligned} \frac{dS}{dt} &= -\rho_{inoc}E_{HS}\pi \\ \frac{dI}{dt} &= \rho_{inoc}E_{HS}\pi - \gamma I \\ \frac{dR}{dt} &= \gamma I \end{aligned}$$

We model pathogens on fomites by considering fomite contamination from droplet-settled pathogens, pathogen loss from either pickup by people or pathogen inactivation, and pathogen gains resulting from deposition by hands to fomites:

$$(4.5) \quad \begin{aligned} \frac{dE_{F1}}{dt} &= I\alpha_1 - E_{F1}(N\rho_1 + \mu_F) + (E_{HS} + E_{HI} + E_{HR})\delta_1 \\ \frac{dE_{F2}}{dt} &= I\alpha_2 - E_{F2}(N\rho_2 + \mu_F) + (E_{HS} + E_{HI} + E_{HR})\delta_2 \end{aligned}$$

We model pathogens on the hands of people by considering direct shedding to the hands of infectious people, pathogen pickup resulting from surface touching, and pathogen loss resulting from either inactivation, self inoculation, or deposition to fomites:

$$(4.6) \quad \begin{aligned} \frac{dE_{HS}}{dt} &= S(E_{F1}\rho_1 + E_{F2}\rho_2) - E_{HS}(\mu_H + \rho_{inoc} + \delta_1 + \delta_2) \\ \frac{dE_{HI}}{dt} &= I\alpha_H + I(E_{F1}\rho_1 + E_{F2}\rho_2) - E_{HI}(\mu_H + \rho_{inoc} + \delta_1 + \delta_2) \\ \frac{dE_{HR}}{dt} &= R(E_{F1}\rho_1 + E_{F2}\rho_2) - E_{HR}(\mu_H + \rho_{inoc} + \delta_1 + \delta_2) \end{aligned}$$

We model two types of interventions: hand hygiene (HH) and surface decontamination (SD). Each intervention is applied at regular intervals to either all hands (HH) or all of the touchable surface area (SD) in a pulse-like fashion. At each intervention application, a proportion of all pathogens residing on hands or surfaces are instantly inactivated. We do not consider any residual effect of the intervention; that is, the μ_H or μ_F remain unchanged immediately after each intervention application. We assess the effectiveness of each intervention by comparing the cumulative incidence (CI) when the intervention is present to when it is not present, summarizing this as the intervention efficacy: $(1 - CI_{intervention}/CI_{nointervention})$. Because these interventions are applied at the population level, we only make comparisons between when the intervention is present versus absent, to summarize the total effects of each intervention.

4.3 Results

4.3.1 Parameterization

Shared parameter values between pathogens

Where possible, use the same values for all shared parameters as listed in table 3.1. We assume that all host behavior is identical between pathogen scenarios. Thus all surface touching and self-inoculation rates are the same. We assume that transmission is occurring in the same type of venue; thus the host density is identical. For simplicity, we also assume that the transfer efficiency, the percent transferred during each touch, is identical across pathogens and symmetric, regardless of whether transfer is occurring from fingertip to fomite or vice versa. To make comparisons across pathogens with regard to the per pathogen transmissibility, as well as to have similar background levels of transmission before any intervention application, we vary the total amount of shedding over the course of infection by varying the shedding rate (α) and recovery rate (γ) simultaneously to achieve desired levels of transmission. In the discussion we comment on what values the literature suggests for these terms, and the implications of these values.

Pathogen specific parameter values

We summarize the differences in contact mediated transmission of each pathogen by considering four pathogen specific parameters: infectivity which we summarize as the per pathogen probability of infection (π), pathogen inactivation rate on hands (μ_H), pathogen inactivation rate on fomites (μ_F), and the proportion of pathogens which enter the transmission system residing on the hands, versus going directly to surfaces in the environment (β_H). The following sections make parameter comparisons across pathogens, as well as describe the rationale used where direct parameter estimates from the literature are not available.

<i>Parameter</i>	<i>Description</i>	<i>Influenza</i>	<i>Rhinovirus</i>	<i>S. Aureus</i>	<i>Norovirus</i>
π	Per pathogen infection probability	0.0014	0.00031	0.0030	0.069
μ_H	Inactivation rate on hands and skin	0.92	0.010	0.0016	0.0048
μ_F	Inactivation rate on fomite surfaces	0.01	0.025	0.0005	0.0016
β_H	Proportion of pathogens excreted directly to shedder's hands	0.15	0.15	0.32	1.0

Table 4.1: Comparison of Contact Mediated Transmission Parameters. All rates are per minute.

Infectivity π

For all infectivity parameters we assume an exponential dose response relationship to calculate the per pathogen probability of infection. The HID_{50} of influenza is 500 $TCID_{50}$ which yields a per $TCID_{50}$ probability of infection of 0.0014 [11, 30]. For rhinovirus, when transmission occurs via touching the tongue, the HID_{50} is 2260 which yields a per pathogen probability of infection of 0.00031. When transmission occurs via touching the external nares, a lower probability of infection results, while touching inside of the nose results in a much higher infectivity [13]. For simplicity, we summarize rhinovirus infectivity between these extremes by using the value from touching the tongue. The per pathogen probability of staphylococcus infection was estimated by Lidwell to be 0.0030 [43]. Norovirus has been called the most infectious agent ever studied. While there is still no definitive dose response study examining its infectivity, we use an HID_{50} of 10 virions, which yields a 6.9% probability of infection per active viral particle. This is plausibly consistent with previous work examining norovirus infectivity [44].

Pathogen inactivation rate on hands μ_H

We assume all inactivation processes to be simple first order decay processes. For influenza, the inactivate rate on hands has been estimated to be 0.92 $TCID_{50}$ per minute [7]. For rhinovirus, this has been estimated to be 0.010 per min [5]. For staphylococcus aureus, this has been estimated to be 0.0016 cfu per minute [59]. For norovirus, we use a value of 0.0048 per minute [45]. This a conservatively slow estimate, because in their research, Liu et al observed a 0.25 log reduction after 2 hours, but all of the die-out occurred in the first 15 minutes. Here we assume that the die-out rate to be constant over the 2 hours. A biphasic decay function may be more appropriate for norovirus, but to hold as much of the model structure constant between pathogens, we do not add such a complexity.

Pathogen inactivation rate on fomites μ_F

For influenza, we use an estimate between what has been observed for porous versus non-porous fomites of 0.01 $TCID_{50}$ per minute [7]. For rhinovirus, we use a similar estimate between what has been observed for porous versus non-porous fomites of 0.025 per minute [32]. For staphylococcus aureus, this has been estimated to be 0.00050 cfu per minute [49]. For norovirus, D'Souza et al observed a 7 log reduction after 7 days in a norovirus surrogate [16]. This yields a rate of 0.0016 per minute. This may be quicker than other observations, which were based on decay while in organic fecal matter. The less fecal matter, the quicker the die-out observed.

Pathogen proportion shed to hands β_H

For influenza, β_H is determined by approximating the proportion of virus on large particles, which deposits to a shedder's hands when a cough is covered with a hand. There is neither any data to inform this nor any precedent in the literature for

what value this would take. We assume that 15% deposits to the hands, but also consider a separate influenza scenario when only 4% deposits to hands, in case the 15% assumption is considered unrealistically large; however, we don't present these results, as they did not alter any inference greatly. For rhinovirus, we assume at least as much virus as for influenza enters the transmission system by being shed directly to the hands. Thus we use a value of 15% here as well. For staphylococcus aureus this proportion is determined by considering the ratios of the cumulative shedding which results from air dispersal, which we assume is constant, and the cumulative excretion which occurs from touching a colonized site and later touching a surface, which we also assume is constant. For details on this estimation, see the supplemental material. The resulting value of β_H was 32%. For norovirus, we assume that all virus which is utilized in the contact route gets into the environment first from the hands, thus assuming a β_H of 100%. We are ignoring norovirus excretion which may enter this system from vomiting, due to the rare nature of these events. A more detailed model could be used to examine how this may alter any inferences here. For all pathogens, we ignore routes besides the contact route, such as aerosolization that occurs during an excretion event so as to focus on the contact route, and interventions specific to the contact route.

Parameter comparison.

Table 4.1 summarizes the pathogen specific parameter values used in this paper while table 4.3 summarizes the shared parameters. Norovirus has the highest infectivity by far, followed by influenza and staphylococcus aureus, while rhinovirus has the lowest per pathogen probability of infection. Staphylococcus aureus has the slowest inactivation rate on hands, followed closely by norovirus, and later rhinovirus; influenza has very rapid inactivation on hands. Staphylococcus aureus also

has the slowest inactivation rate on fomites, followed by norovirus, and later influenza and rhinovirus. For this analysis, we operate under the assumption that norovirus has the highest proportion of pathogens going to the shedder’s hands, followed by staphylococcus aureus, rhinovirus, and influenza.

4.3.2 Contact mediated infection potential via each pathogen

We summarize the per pathogen infection potential of each agent by finding the value of the total shedding which occurs during the course of infection ($\frac{\alpha}{\gamma}$) that yields 50% final fraction infected (FFI). We determine this for each pathogen when touching of surfaces is random, and also when population level surface touching is non-random. When a small fomite is touched at a rate proportional to its own surface area, this may be defined as random touching. When the small fomite is touched at a rate proportional to ten times its surface area, touching is more specified to the small fomite, as this fomite is being touched ten times more than would be expected due to chance alone. When the small fomite is touched at a rate proportional to 100 times its surface area, population surface touching is even more specified (further deviating from random surface touching). Across these three settings, norovirus was much more infectious than any of the other pathogens studied. To compare across pathogens, we compare the shedding required to achieve 50% FFI of each pathogen to the norovirus value at random touching (table 4.2).

	<i>Norovirus</i>	<i>S. Aureus</i>	<i>Rhinovirus</i>	<i>Influenza</i>
At Random Touching	1.0*	14	3700	3400
10-X Random Touching	0.78	13	3500	3400
100-X Random Touching	0.077	5.2	540	2600

Table 4.2: Comparison of total shedding during infection ($\frac{\alpha}{\gamma}$) required to attain 50% final fraction infected.

*Comparison is made between each pathogen’s $\frac{\alpha}{\gamma}$ value to that of norovirus at random touching.

At random touching, staphylococcus aureus required about 14 times more shed-

Parameter	Description	Unit	Value
τ_{S-H-S}	Transfer efficiency (surface to hand to surface)		0.10
ρ_{inoc}^*	Rate of self inoculation transfer	Min^{-1}	0.028
ρ_{touch}	Rate of surface touching	Min^{-1}	0.75
A_{finger}	Fingertip surface area	cm	10
A_{F1}	Fomite-1 surface area	cm	50
A_{F2}	Fomite-2 surface area	cm	99950
$\epsilon_{density}$	Host density	$people/m^2$	1.0

Table 4.3: Shared parameter values between pathogens

* ρ_{inoc} is equal to the product of the self inoculation rate and inoculation transfer proportion here assumed to be 0.08 and 0.35

ding than norovirus to achieve similar transmission levels, while influenza and rhinovirus required more than 3000 times greater shedding. Comparing the random touching scenarios to when touching is more specified we see that each pathogen requires slightly less excretion to achieve similar transmission levels. When touching to the small fomite is done at a rate ten times that which is expected due to chance alone (10-X random touching), norovirus only required 0.78 as many pathogens as required in the pure random touching scenario, while staphylococcus aureus required 13 times more pathogens excreted than norovirus at random touching (compared to its random touching value of 14). When touching to the small fomite is done at a rate 100 times that which is expected due to chance alone (100-X random touching), norovirus required roughly an order of magnitude less pathogen excretion to achieve similar transmission to the random touching scenario, while S. aureus and rhinovirus shedding values were more than halved. Influenza however did not scale similarly, as it still required more than three quarters of its random touching shedding level to achieve similar transmission levels. Thus, for the range considered, touch specification affects norovirus most, staphylococcus aureus, and rhinovirus next most, while affecting influenza the least. Norovirus always remained the most infectious organism followed by staphylococcus aureus. Influenza and rhinovirus, at random touching

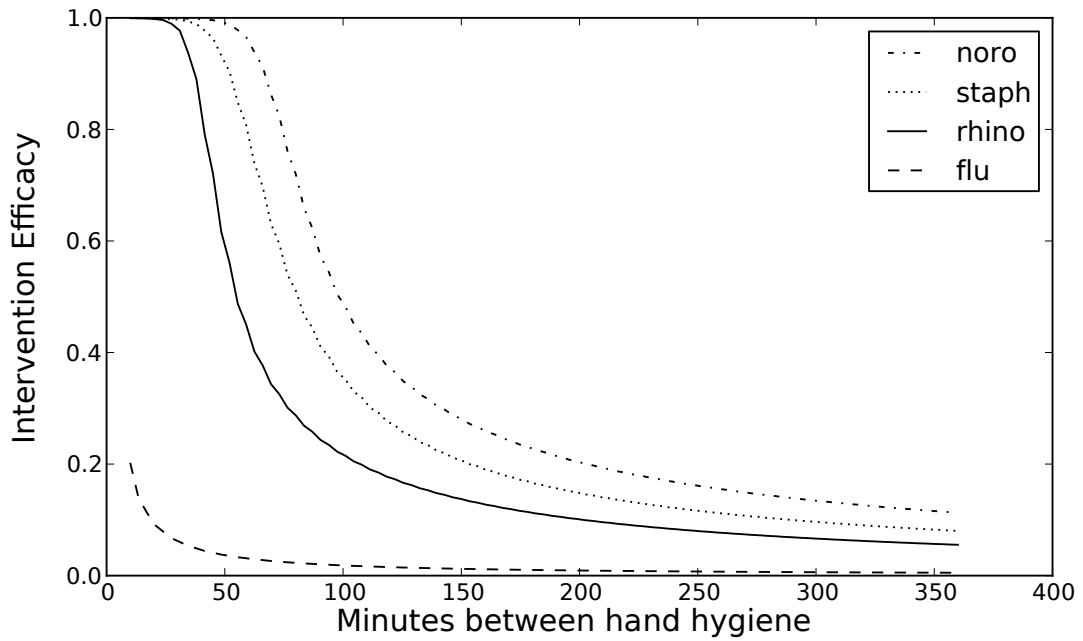
were less infectious at a similar level, although at much higher touch specification, rhinovirus became nearly an order of magnitude more infectious.

4.3.3 Intervention efficacies by pathogen

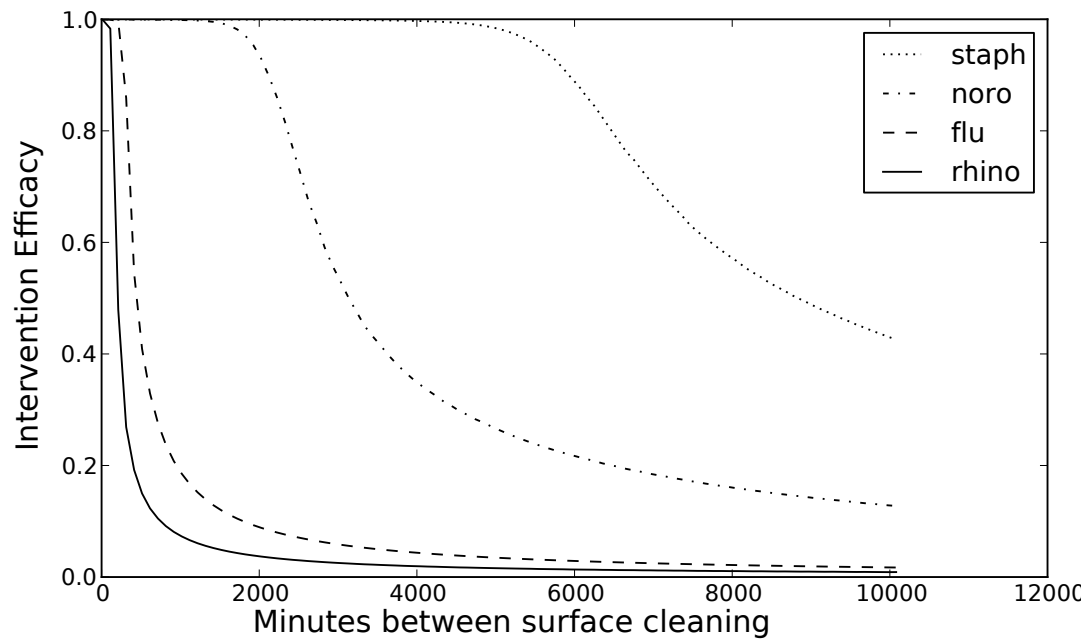
We implemented interventions assuming zero residual effect. That is, all effect conferred was done so at regular intervals. This is meant to mimic regular cleaning of surfaces and regular hand washing practices. At specific intervals in time, each intervention is executed, at which some proportion of pathogens are immediately removed from the system. We examined how intervention efficacy changed as we varied the time interval between intervention applications (Figure 4.1).

For hand hygiene 4.1(a), norovirus transmission was the easiest pathogen to attenuate. HH every 60 minutes was sufficient to have nearly complete (intervention efficacy = 1.0) elimination of norovirus transmission. The other pathogens required the intervention to be applied more often. For *S. aureus* once every 50 minutes was sufficient to nearly eliminate transmission. Rhinovirus required a slightly higher rate of intervention (every 30 minutes) to achieve complete elimination. Influenza did not respond to hand hygiene substantially, as even with it being applied once every 10 minutes to all hands, only 20% intervention efficacy was conveyed; this is likely due to influenza's much higher inactivation rate on hands compared to these other pathogens.

For surface decontamination 4.1(b), *S. aureus* was the most amenable, as cleaning once every 3 days conveyed nearly 100% efficacy. Norovirus was next most amenable, as cleaning once each day conveyed nearly 100% efficacy. Influenza and rhinovirus followed, but required a high frequency of venue cleaning to produce a large intervention effect. Influenza achieved SD efficacy of 76% if SD was applied at least once every five hours. Rhinovirus achieved SD efficacy of 47% if SD was applied at least



(a) Hand hygiene efficacy



(b) Surface decontamination efficacy

Figure 4.1: Hand hygiene and surface decontamination efficacy in norovirus, *S. aureus*, rhinovirus and influenza as a function of rate of intervention application.

once every 3.5 hours. The rate of these SD applications for both rhinovirus and influenza may be prohibitively large and unrealistic to be applied to an entire venue.

Discussion

We have shown that norovirus and *S. aureus* are much more transmissible via the contact route than rhinovirus and influenza. However, we have also shown that they are more susceptible to intervention from hand hygiene and surface decontamination. One of the main reasons for this is that norovirus and *S. aureus* survive longer on surfaces and on human hands than rhinovirus and influenza. This greater persistence in the environment while making them more transmissible, also makes interventions which remove some fraction of total pathogen contamination from the environment or hands at regular increments (as we model hand hygiene and surface decontamination) more successful. Conversely, because rhinovirus and influenza don't remain viable long in the environment, regular pulsing interventions have a much smaller added benefit to their inactivation.

We chose to model these interventions as pulse-like interventions with zero residual effect. Had we modeled them with pure residual effects, each intervention would have modified the pathogen inactivation rate by some factor, say 10%. Thus, using influenza for example, increasing an already high hand inactivation rate could have a much larger effect than say increasing the hand inactivation rate of norovirus, since a slow inactivation rate, when increased by 10% is still a fairly slow rate. However, it is not likely that if hand hygiene were implemented in reality, it would be implemented often enough to change influenza's average hand inactivation rate by 10%. By comparison, using a pulse-like intervention with norovirus, we would be increasing the average pathogen inactivation rate by much more than 10%. Future

more detailed models could model these interventions as a combination of both pulse-like applications as well as some decaying temporary residual effect. By doing so, it is possible that rhinovirus and influenza could become more susceptible to these interventions.

It should be noted that all inferences made in this work are contingent upon values of parameters taken from the literature. If there is considerable error in measurement of these values, our inferences may become questionable. In particular, slowing the extremely rapid inactivation rate of influenza on hands could make these environmental interventions have stronger effects on reducing its transmission. On the other side, if inactivation rates of norovirus and *S. aureus* were found to be quicker, then these interventions would have much weaker effects on reducing their transmission. Clearly better understanding of the survivability of these pathogens would increase the certainty of our inferences and ability to make informed intervention decisions.

From the data in table 4.2, it would appear that norovirus is roughly an order of magnitude more transmissible than *S. aureus*, and more than two orders of magnitude more transmissible than rhinovirus and influenza. However, if total norovirus shedding were much less strong than rhinovirus and influenza, then these agents might actually be transmitted with similar intensities. To examine this, we calculated total pathogen excretion levels for each of these pathogens. Details of this process can be found in the supplemental material. Surprisingly, these four pathogens are all excreted from the body to a contact transmission route at similar levels. When we compare the total excretion levels of all pathogens to norovirus, we find that *S. aureus* only had 14% as much pathogen shedding as norovirus. Rhinovirus excreted roughly 90% as much pathogen shedding as norovirus, while influenza excreted 1.1 times as much as norovirus. These calculations should be taken with a grain of salt,

due to the extreme variability and uncertainty of the parameters which govern the calculation. That said, the total excretion of these pathogens appears to be fairly similar. Thus much of our overall conclusion still holds: that norovirus and to a lesser degree *S. aureus*, are much more transmissible and explosive via the contact route than influenza and rhinovirus. Had total norovirus shedding been much less, this inference would no longer be as valid.

Another interesting result from this paper has to do with how transmission of each pathogen scales with more specified touching. We have already shown that touch specificity affects influenza transmission (Chapter III). However, from this current chapter, touch specificity may be a much stronger factor influencing transmission of these pathogens. Better understanding of contact mediated transmission through understanding concepts such as touch specificity will lead to more informed intervention decision making.

CHAPTER V

Conclusions and Future Directions

5.1 Summary

We have explicitly modeled transmission through the environment for influenza, as well as other pathogens. By doing so we have examined specific features of the host, agent and environment which alter route specific transmission (chapter II); we have examined how population level heterogeneity in surface touching patterns alters contact-mediated influenza transmission and how environmental intervention efficacy is altered by this heterogeneity (chapter III); and finally, we compared contact mediated transmission across influenza, rhinovirus, staphylococcus aureus, and norovirus, to examine how specific parameters differ between these, how transmissible each pathogen is via the contact-mediated route, and how amenable to environmental intervention each pathogen is (chapter IV).

5.1.1 Conclusions from Chapter II

Examining each aim and hypothesis from section 1.1 we make the following conclusions. From chapter II, we conclude that transmission dominance is context-specific. That is, features of the host, pathogen strain, and environment jointly determine which mode or modes of influenza transmission will be operating. We observed i) regions of realistic parameter space where the respiratory, direct-droplet-spray, and

contact-mediated routes each on their own were capable of causing high levels of transmission, ii) regions of parameter space where multiple modes were causing high transmission on their own, as well as iii) regions of parameter space where multiple modes were jointly causing high transmission but no single mode was causing high transmission on its own. Thus, we observed regions where i) there was clear route dominance via only a single route, ii) where multiple modes could be said to be dominating since multiple modes were independently high enough such that eliminating one would not be sufficient to reduce transmission substantially, and iii) regions where no single route was high enough to cause high transmission on its own.

Additionally from chapter II, we conclude that categories of route dominance as explained in the preceding paragraph differ in the distribution of specific parameters which gave rise to them. Certain parameters only affect a single route; for example the lower respiratory HID_{50} is only utilized by the respiratory route, since only particles small enough to remain aerosolized are able to penetrate deep within the lung alveoli. Because this parameter only governs one route, values of this parameter which increase transmission are observed in the respiratory-only category, while in all other categories of route dominance, weaker infectivity was observed. This is in contrast to a parameter which affects all the routes of transmission, such as host density. High values of host density increase transmission by each route. However, the contact-mediated route was affected by this least, compared to the other routes. The other routes of transmission were more likely to require high host density in order to achieve high route-specific transmission.

Thus, under the sufficient-component cause model of causation [56, 38], if we think of each parameter set that yielded high transmission for a given route as one set of sufficient causes, we see that high host density is a *more* necessary causal

component for high respiratory, inspiratory, or direct-droplet-spray transmission, as it is present in nearly all sufficient causal mechanisms compared to the contact-mediated route. For the contact-mediated route, while high host density certainly can be a component cause, as it amplifies contact-mediated transmission, it is much less necessary, as there are many more sufficient causal mechanisms which do not have high host density.

5.1.2 Conclusions from Chapter III

From chapter III we conclude that increasingly non-random surface touching may either increase or decrease contact-mediated influenza transmission. The main feature which determines this relationship is the proportion of pathogens that are initially shed to the hands of the shedder β_H . At high enough levels of β_H , transmission will increase with increasing touch specificity. The proportion of pathogens that are initially shed to the hands of the shedder determines how high transmission from the hand-to-fomite contamination route can be. This sub-route of contact-mediated transmission increases in strength as touch specificity increases. However, if there are not adequate pathogens being directed to this sub-route, meaning if β_H is too low, then this route never causes appreciable transmission. The hand-to-fomite has its highest potential for transmission when β_H is maximized and touching is most specified. Conversely, the droplet-to-fomite contamination route has its highest potential for transmission when β_H is minimized and touching is as close to random as possible.

Because of how these two sub-routes are affected by the degree of non-random touching, both hand hygiene and surface decontamination efficacy are likewise affected. Hand hygiene is inherently better at attenuating the hand-to-fomite contamination route of contact transmission. Because of this, hand hygiene efficacy

is maximized at the most specified levels of surface touching (as well as when β_H is maximized). On the other hand, surface decontamination is better at attenuating the droplet-to-fomite contamination route of contact transmission when surface touching is nearly random. Thus, when droplet-to-fomite contamination is maximized (meaning touching is nearly random) surface decontamination is optimal. As touching becomes more specified, the efficacy of surface decontamination decreases.

5.1.3 Conclusions from Chapter IV

From chapter IV we conclude that norovirus indeed may be the most transmissible of the agents we considered, on the basis of parameter estimation for the particular EITS model we used. This conclusion is in accord with empirical observations noting the highly explosive nature of norovirus. *S. aureus* was the next most transmissible, being roughly an order of magnitude more transmissible than rhinovirus and influenza. However, the weakness of rhinovirus and influenza could be explained in another way; they are fairly weak in the contact mediated transmission route, because they have other routes of transmission that are simultaneously operating. While this does not disprove that the contact route is possible for influenza and rhinovirus, it does show that they may be at a disadvantage compared to other pathogens which are solely transmitted via the contact-mediated route.

Additionally we conclude that rhinovirus and influenza attenuation require the most extreme versions of both hand hygiene and surface decontamination interventions; by this we mean that these pathogens must have interventions implemented at rates which may not be realistically feasible. By contrast, both norovirus and *S. aureus* may be subdued by surface decontamination and hand hygiene, when these interventions are applied at rates that are realistically feasible. The primary explanation for why norovirus and *S. aureus* were more susceptible to these interventions

is that they were much more hearty in the environment at pre-intervention. Thus each intervention was altering average inactivation rates more for these pathogens, compared to influenza and rhinovirus.

5.2 Suggestions for future research

From this work, we can make several suggestions for areas where future research would be helpful. First, from chapter II, we can make recommendations for more empirical influenza studies. Further work examining influenza inactivation on skin and on fomites, to confirm previous work ([7]) would add greater confidence in our work. Additionally, better understanding of influenza infectivity values, to explain the discrepancy of nearly four orders of magnitude disparity between upper and lower respiratory HID_{50} would also add confidence to the inferences in our work. If however, future work yields conflicting parameter values, our inferences may become questionable. A third family of parameters has to do with the proportion of virus which remains aerosolized from cough excretions. The assumption we have made here is that virus is evenly distributed by volume. However, if virus is more likely to exist in very small excretions that are in the aerosolized particle size range, the respiratory route would receive a large bonus to its transmission.

Additionally, behavioral parameters in the form of surface touching rates, self inoculation rates (chapter II), cough-covering behavior, other shedding behaviors, host density measures, and human movement and fomite touching patterns (chapters III and IV) could be observed and specified for different types of venues. Comparing a pre-school environment to a computer lab, it is clear that different types of people with different behaviors are likely to visit different types of venues. We have shown the importance of these behavioral features, but they are largely undocumented

and unreported in the literature. Regular reporting of these to understand realistic boundaries would be beneficial.

We can also make suggestions for future research focusing on additional theory development and understanding. One natural extension involves creating an individual based model which incorporates different degrees of random versus non-random touching. This could be conceptualized by having individuals who each have their own *home* environment, as well as a shared public environment. Then surface touching rates between to one's own home location, someone else's home location, and the public location could be varied. This work could further examine how hand hygiene and surface decontamination efficacy vary with different degrees of random and non-random touching. This model would have the major advantage in that it would be more relate-able to observations from reality. Additionally, it will also be important for future modeling work to examine the effect of more specific targeted hand hygiene and surface decontamination.

5.3 Implications

There are important implications from this dissertation. First, influenza transmission through the environment may occur through one or more transmission routes. At this point it is still unclear if there is a single dominant transmission route in all situations. In fact, from this work we conclude the opposite—that the mode or modes operating will vary from scenario to scenario based on features of the host, pathogen strain, and environment. For example, due to the extremely high host density requirements of the droplet-spray route, a venue such as a packed football stadium or auditorium or subway car at rush hour are potentially high risk venues for this route. For the respiratory route, the rush hour packed subway car, or air-

plane with air-circulation system turned off are also possibilities, since here the host density is fairly high, while also having a less air volume per unit of surface area. The contact route did not have such a requirement for high host density, but rather was more dependent on touching behaviors such as the rate of self-inoculation for high transmission. Because of this, a scenario where people are self inoculating more often such as at a child care center (assuming children self inoculate more often than adults) is a prime example where contact transmission may be likely. Thus, choosing an environmental intervention that reduces transmission via one route exclusively for all situations is unwise, especially when this route may not be present.

Second, hand hygiene efficacy is strongly affected by surface touching patterns. Where surface touching is highly specified, meaning non-random, hand hygiene will have its greatest effects against contact mediated transmission. Broad surface decontamination has its greatest effects when surface touching is most random. Thus, if venues are better understood in terms of how touching is occurring within them, targeted versus untargeted intervention may be better applied. For example, bathrooms, elevators, and subway cars are likely to have some of the more specified touching behaviors. Because of this targeted environmental intervention may be most effective, and in particular, hand hygiene may be more effective at preventing transmission in these scenarios. Better understanding of fomite touching behavior in different venues could lead to better intervention design.

Third, influenza and rhinovirus were much more weakly transmitted via the contact mediated route compared to norovirus and *S. aureus*, while they were also the least amenable to hand hygiene and surface decontamination. From this work it does not appear that these interventions are useful to dampen influenza or rhinovirus transmission if they are applied in an untargeted fashion. However, if they are ap-

plied in a more targeted fashion, perhaps hand hygiene immediately after coughing into one's hands, or cleaning of surfaces immediately after an infectious person was present, they may become useful. Broad untargeted recommendations for these two pathogens does not appear to be useful. However, broad untargeted intervention against norovirus and *S. aureus* does appear quite beneficial.

APPENDICES

APPENDIX A

Preamble and Chapter II Supporting Materials

A.1 Preamble

This thesis was produced using LaTeX. Individual based models were written in Java and were run on a cluster of Linux (Redhat) workstations at the Center for Advanced Computing at the University of Michigan, Ann Arbor. The numerical analysis of deterministic compartmental models was done using Python 3.1.2. Graphics were produced using Python 3.1.2 with Matplotlib v1.0.0, and Inkscape v0.47.

A.2 Chapter II Supporting Materials

A.2.1 Model structure

We explicitly model environmental influenza transmission in a venue by considering contact-mediated, respirable, inspirable, and droplet exposure. Figure 2.2 gives a schematic of the processes resulting from each shedding event that leads to exposure. In our individual based model, we use continuous time to model discrete spatial units, humans, pathogens, and transmission-related events. Specific events related to transmission include shedding, viral inactivation in the environment, touching of surfaces that can contaminate hands, inhalation of air that can carry airborne pathogens, touching of ones eyes, nose or mouth that can self-inoculate pathogens

from the hands, and movement about the venue by humans. We use an event-based modeling scheme, in which we take into account the current state of the system at the current time, and based on the probabilities of all possible events, we determine what the next event will be, and when it will occur. That event is then executed at the specified time, and we then reevaluate the current state of the system to again determine which event to perform next, and when it will occur. By current state of the system, we are concerned with how many susceptible individuals, infected individuals, and influenza virus particles exist in each part of the environment. This modeling strategy is an implementation of the Gillespie algorithm [26]. The process continues until the model terminates when there are no infectious individuals still shedding and there is no remaining pathogen contamination in the environment. The proceeding sections describe specific model components in greater detail.

Vital Dynamics

To avoid issues related to frequency and density dependent transmission, we model a population with a constant size of susceptibles. To do so requires an open system of people in which after each new infection event, the newly infectious individual is instantly replaced with a new susceptible. Thus we are only allowing one infectious person to transmit. This permits us to observe the number of new infections transmitted from one infected person over the course of their infection in the presence of a completely susceptible population of constant size which is one definition of the basic reproductive number, R_0 [4, 15].

The Environment

We model transmission in a single abstract venue. Since appropriate intervention choice may vary from one venue to another, we chose to model only a single venue

at a time, rather than a model of greater complexity which could consider multiple connected venues, to better understand how each transmission mode operates in different types of venues. The venue may be thought of as a lattice grid with discrete cell locations people may visit. Each cell in the lattice has some surface area, given by its length and width (2 meters by 2 meters), and local air volume, which additionally takes into account the surface area to volume ratio $\epsilon_{SA:V}$. These local fomite environments of the cell are independent of the local environments of neighboring cells, meaning that pathogens are not shared between cells unless a human picks pathogens up at one cell, moves to another, and deposits pathogens there. At the beginning of each simulation each cell in the lattice has exactly the same characteristics and infection potential as any other. Within each cell, we assume all pathogens are spread evenly either in air or on surface area. Besides the local-air volume, which we assume contains only non-diffusing medium sized particles (10-100 μm diameter), there is also a global air volume which the entire venue shares. We invoke the well-mixed-room (WMR) assumption in the global air environment which contains only small particles (less than 10 μm diameter), which after being excreted are assumed to have diffused instantaneously, and are evenly distributed throughout. The global-air volume magnitude is calculated by adding together the magnitude of all the local-air volumes. Within a given cell, when people touch a portion of the total surface area or breath a portion of the local and global volume, they are being exposed to a sample of the environment at that location with known pathogen contamination levels.

Infection Progression

After the initiation of infection, we consider eight stages of infection. Each stage has a specific viral concentration [29] associated with each excretion event, such that overall pathogen output starts low, rises to a peak in the second stage, and then tails

off until the final stage, when it is back to the low levels of the first stage. Staged progression occurs with an expected rate of one progression per day.

Shedding

The infectious individual sheds pathogens over the course of their infection. The rate of pathogen excretion varies by stage of infection. Discrete shedding events, analogous to coughs, occur at a constant rate over the course of the infection, although the amount of pathogen released is not constant. Each shedding event puts out some total volume of mucous material. However only part of this volume is the potentially infectious nasal fluid (α_{mag}). This mucous has a viral concentration which varies by stage of infection. As manuscript figure 1 indicates at the left, the shedding volume may be divided into three categories based on particle size. Some proportion of the total volume excreted has a particle size less than $10 \mu\text{m}$ (α_{resp}) which we assume remains aerosolized and may potentially be respired. We assume these $<10 \mu\text{m}$ diameter particles are instantaneously homogeneously distributed throughout the venue the WMR assumption in the global air volume. There is also some proportion which has a particle diameter between 10 and $100 \mu\text{m}$ (α_{insp}). This proportion remains aerosolized temporarily, with the potential for being inspired, until eventually settling to the local fomite environment. This inspirable proportion is only present in the local air volume of the shedder's cell, and is evenly mixed there. The remaining proportion, $>100 \mu\text{m}$ diameter, we assume either settles out from the air instantaneously to local fomite surfaces, or immediately causes droplet exposure by settling on another individual's facial membrane who is collocated with the shedder. The pathogens which settle in the local fomite environment are evenly distributed in the shedder's cell.

Virus Inactivation

We assume a simple first order process to model the loss of viability of the virus. There are separate inactivation events and inactivation rates based on where there is virus: in the air, on hands, or on fomite surfaces (μ_A, μ_H, μ_S). In addition, virus in the air may also leave the venue due to air exchanges. Note that inactivation is not shown in figure 2.2 explicitly.

Virus Settling

Virus on particles with diameter between 10 and 100 μm are initially aerosolized in the cell's local air environment, but may settle to the local fomite environment at a constant rate (ϵ_{settle}) as indicated in figure 2.2. Rather than modeling particles with different sizes and thus different settling rates, we use only one settling rate for medium size particles, although we do vary the settling rate in our parameter sweep. Because the settling rate of virus on particles less than 10 μm in diameter is so low, we assume they all either inactivate, leave the venue due to air exchanges, or are inhaled before settling. Thus, we do not consider any settling of virus on smaller particles.

Human Movement

In this model humans change cell location at a constant rate (ϵ_{move}). We assume the future position to which the human moves is independent of the current position the human occupies. We assume that time spent in transit between two spots is negligible and is ignored. Thus in this model, humans move without respect to space, in essence teleporting to future random locations. In a sensitivity analysis, when we allowed movement to spaces near the current location (the Von-Neumann Neighborhood), all transmission mode strengths were quite similar regardless of movement

type.

Surface Touching

Humans touch surfaces at a constant rate (ρ_{touch}). When a surface touching event occurs, pathogens may transfer to the fomite-surface, to the fingertip, to both, or to neither based on whether there are pathogens on the surface or fingertip prior to the touch event. To determine the quantity of pathogens transferred, we consider four parameters: the surface area of the fingertip doing the touching (A_h), the total surface area in a cell (A_s), the transfer efficiency (the proportion to be transferred) from fingertip to surface (τ_{h-s}), and the transfer efficiency from surface to fingertip (τ_{s-h}). For simplicity we assume (τ_{s-h}), and (τ_{h-s}) are equal and call them by one parameter (τ_{s-h-s}). Where V_s and V_f are the viral numbers present on the surface or hand respectively, the number of pathogens transferred to the hand is: $V_s \tau_{s-h-s} \frac{A_h}{A_s}$. The number of pathogens transferred to the surface is: $V_h \tau_{s-h-s}$.

This formulation assumes that on a single local fomite surface area, all pathogens are evenly distributed. A finger only picks up pathogen from a fraction of the surface proportionate to finger size. But contamination is assumed to cover an entire surface. Thus each pick up is treated as an average pick up.

Self Inoculation

Humans with pathogens on their fingertips touch their eyes, nose or mouth to self-inoculate at some rate (ρ_{inoc}). When this occurs, some proportion of the pathogens present may be transferred (τ_{h-f-f}). Then, some proportion of this may reach a target membrane to potentially initiate infection (τ_{f-t}). This is all performed in one step considering the products of these two transfer parameters.

Breathing

Human breathing events occur at some rate (ρ_{breath}). During inhalation, a specific volume of air is taken in—the tidal volume. Particles less than $10\mu\text{m}$ may be respired to the deep lung alveoli, while particles between 10 and $100\mu\text{m}$ diameter may be inspired and deposit in the upper airway.

To determine if any pathogens are respired (lower airway deposition), we calculate the proportion of the global air volume respired in one breath as the quotient of the tidal volume and total global air volume. If any pathogens are respired, we use a lung deposition fraction (π_L) to determine the proportion that actually deposit on a susceptible location in the lower respiratory tract. If deposition does not occur we assume the virus is exhaled back to the global air volume. To determine if any pathogens are inspired (upper airway deposition), we calculate the proportion of the local air volume inspired in one breath as the quotient of the tidal volume and local air volume. Here no deposition fraction or transfer efficiency is applied; rather, if any are inspired, we assume all deposit on a susceptible tissue in the upper respiratory tract. This over estimates the dose received from inspiratory exposure which is acceptable since we find this to be low despite this overestimate.

Infection

Infection may result from contact-mediated, respiratory, inspiratory, or droplet exposure. In any case, once we have determined the dose which reaches the target susceptible tissue, discussed above, we then use an exponential model of dose response, with site-specific ID_{50} values for the upper and lower respiratory regions (π_U, π_L). We assume the droplet, inspiratory, and contact-mediated modes target the upper respiratory tract, while respiratory exposure has a separate target tissue,

the lower respiratory tract.

A.2.2 Model Parameterization

We next discuss the model parameterization, including literature sources, variability around point estimates, and rationale where needed for deviations from literature values.

Shedding Parameters

When infected individuals shed, they put out some discrete number of pathogens. To determine this we consider: 1) a shedding event rate, 2) a shedding volume, 3) a pathogen concentration within the mucous; and 4) the proportions of virus transported to the respirable air, inspirable air, local fomite environment, or causing droplet exposure.

While the cough fluid volume has been estimated at 0.044 mL [52], and cough rates observed near 0.2 per minute[47] it is highly likely that both of these values vary from person, pathogen strain, and host-strain interactions. In addition, virus may also be excreted in sneezes, which would have different rates and volumes, but similar particle size distributions. We use a constant rate of 0.2 per minute, while modulating the shedding volume to account for this variability. We modify the volume with a parameter we call the shedding magnitude factor (α_{mag}). We let this parameter vary over a wide range (0.005 to 0.075).

To determine the pathogen concentration of the fluid being shed, we consult figure 2 of Hayden [29] to create a shedding function which takes different values by stage of infection. Note the units presented in the referent figure are $TCID_{50}$ per mL of nasal lavage fluid. It is possible to calculate the dilution used of the lavage to calculate the nasal fluid viral concentration. However, it is not apparent how to transform nasal

fluid into cough fluid, as cough fluid is also partially composed of saliva. Thus, the shedding magnitude factor allows for variability in this relationship.

To determine what proportion of the total cough volume stays aerosolized and is potentially respired (α_{resp}) we use a critical post-evaporative particle diameter of $10\mu\text{m}$ [52]. We combine this with the cough particle size distribution data from Loudon [46]. We assume that the pathogen concentration is the same in particles greater and less than $10\mu\text{m}$. This indicates that $1.4\text{E-}6$ of the total volume (and corresponding pathogens residing on this volume) remain aerosolized. We use $1.4\text{E-}7$ and $1.4\text{E-}5$ respectively as lower and upper constraints. Here it should be noted that while coughs and sneezes certainly do not have similar fluid volumes, there is evidence [52, 46, 17] to support that they have similar particle size distributions, indicating that the similar proportions will be going to the different environmental routes regardless of whether a cough or a sneeze is acting. Using the same data [46] and theory [52], we calculate that 0.95% of total volume is between 10 and $100\mu\text{m}$ diameter and has the potential to be inspired (α_{insp}). We use 0.35% and 1.5% as the constraints around this point value.

The remaining viruses all reside on particles with diameter greater than $100\mu\text{m}$. We assume that droplet spray exposure only results from virus on these large particles. As a simplification, we assume the droplet spray is spread evenly over the entire cell surface area, allowing us to use ratio of the facial membrane surface area estimated at 15 cm^2 and the total surface area in a grid cell, 4 m^2 , for each collocated individual to determine the droplet dose received for every person in that cell. The viruses on large particles that are not utilized in droplet spray exposure are assumed to settle immediately and uniformly to the local fomite environment.

Inactivation Parameters

We model inactivation of influenza virus in the environment as a first order decay process with rates informed by empirical literature. We use 0.006 per minute with constraints (0.01, 0.036) for inactivation in the air [31], and 0.92 per minute (0.62, 1.22) for inactivation on hands [7]. For inactivation on fomite surfaces (μ_S), the literature gives values between 0.0297 and 0.12 per minute depending on the surface type [7]. To consider scenarios with different types of surfaces present and thus different surface inactivation rates, we use 0.0005 and 0.2 for lower and upper constraints. In addition to airborne inactivation, the virus may also be removed from the system via airborne ventilation. We use a moderately low air exchange rate of 0.3 per hour.

Movement and Space Parameters

Each cell within the venue is a square with side length equal to 2m. To vary the host density ($\epsilon_{density}$) in the venue, we let the total number of venue grid cells vary from 9 to 900 which yield densities relevant to a rush hour packed subway car, in which there may be roughly 5 people per m^2 , to a more dispersed office setting, in which there may be roughly 0.05 people per m^2 .

To calculate the venue volume we use a surface area to volume ratio of 13m, which, if it is assumed that gravity is the dominant force of particle settling, implicitly indicates there is only one layer of surface area. However, it may be argued that furniture may increase both horizontal surface area for potential settling and touching as well as vertical surface area. While we assume that gravity is still the dominant force affecting $>10\mu\text{m}$ diameter particle settling, to allow for relaxing of the assumption of only a single layer of surface area per unit volume, we allow the surface area to volume ratio vary using constraints of 1/1m and 1/5m. Individuals

change their 2 m by 2 m grid locations at a rate of 0.05 per minute; we consider constraints of 0.00083 and 3 per minute to consider variation around this middle value.

Surface Touching Parameters

When a touch event occurs, we assume five fingertips each 2 cm^2 do the touching. Informed by empirical studies of bacterial transfer between skin and surfaces [58, 65], we use a middle transfer efficiency of 10% with constraints of 1.67% and 60% from fingertip to surface and vice versa. We use plausible surface touching rate (ρ_{touch}) of 0.75 per minute with constraints of 0.1875 and 3 per minute.

Self Inoculation Parameters

When a self inoculation event occurs, we assume that only one of the fingertips does the touching. For the self inoculation rate (ρ_{inoc}) we use 0.08 per minute with constraints of 0.02 and 0.32 per minute, informed by an observation study of hand to face contact [32, 50]. Informed by empirical studies of bacterial transfer from fingertip to mouth [57], we use a transfer efficiency of 35%. The proportion of pathogens which make it from the entry orifice to the target tissue (τ_{f-t}) is completely unknown. We use constraints of 5% to 25% yielding a middle value of 15% for this.

Breathing Parameters

To model discrete breathing events, we consider a breathing rate as well as a tidal volume for each breath, rather than considering the total volume inhaled per day. We use a tidal volume of 0.6 L. We let the breath rate (ρ_{breath}) vary from 10 to 22 breaths per minute. This corresponds to values of adult males resting or performing light activity [24].

Infection Parameters

As a result of self-inoculation, inhalation, or droplet exposure, there is potential for infection to result. To calculate the dose a susceptible tissue receives during respiration, we take the ratio of the tidal volume and total air volume and multiply this by the fraction of pathogen particles which will actually deposit in the lower respiratory tract. For this lung deposition fraction (π_L), we use a value between 15 and 60% [34]. Once the dose is determined we evaluate whether infection results instantaneously by using the HID_{50} of empirical dose response studies of the lower respiratory tract [3]. We convert this HID_{50} as done by others [6] to take into account the deposition fraction to the lungs for the particles sizes administered. This yields a lower HID_{50} (π_L) of 0.671 $TCID_{50}$; we use constraints of 0.0671 and 6.71 $TCID_{50}$. We assume a simple exponential dose response function to consider varying doses for this and all other modes. To determine the dose received from inspiration we use the ratio of the tidal volume and the local cell air volume to determine what proportion of the total amount of virus in the local air. We assume these particles deposit in the upper respiratory tract, and thus we use the upper respiratory HID_{50} (π_U) of 500 $TCID_{50}$ [11, 12] with constraints of 50 and 5000 $TCID_{50}$.

During self inoculation events the dose received is calculated as described previously in the self inoculation parameterization section. This yields the magnitude of virus which eventually gets from entry orifice to target membrane. This dose is evaluated using the upper HID_{50} (π_U) as it is assumed that the site of infection is in the upper respiratory tract.

At each shedding event, collocated individuals may receive droplet exposure. The dose is determined by taking into account the facial surface area of each collocated individual divided by the total surface area of the cell. In addition, we use the same

transfer proportion from entry orifice to target membrane as in the contact mediated mode to diminish the dose received. To evaluate whether infection results we again use upper HID_{50} (π_U), as it is assumed the site of infection is in the upper respiratory tract.

A.2.3 Description of Figure 2.3's Venn Diagram Categories

	Global Mean		Combined Below		Contact Only		Respiratory Only		Droplet Only		Only Combined Above		Multiple Modes Above	
N	10000	4188	3079	121	66	577	1969							
Inactivation in air	0.00976	0.0099	0.00981	0.00573	0.0108	0.0097	0.0096							
Inactivation on surfaces	0.0333	0.04	0.0246	0.0389	0.0544	0.0373	0.0305							
Inactivation on hands	0.92	0.9312	0.8987	0.9605	0.9816	0.9328	0.9210							
Proportion transported to target membrane	0.15008	0.1405	0.1552	0.1318	0.1598	0.1473	0.1641							
Lung deposition fraction	0.4167	0.4115	0.4106	0.4984	0.4081	0.4321	0.4283							
Lower respiratory ID ₅₀	0.4167	0.4115	0.4106	0.4984	0.4081	0.4321	0.4283							
Upper respiratory ID ₅₀	1075.05	1777.89	549.88	2362.3	776.00	1064.55	335.84							
Shedding magnitude respirable	0.02585	0.0189	0.028229	0.0304	0.0205	0.0263	0.0367							
Viral proportion	2.97E-06	2.70E-06	2.88E-06	7.60E-06	1.44E-06	3.80E-06	3.19E-06							
Self inoculation rate	0.1082	0.0857	0.1438	0.067	0.037	0.0765	0.1147							
Surface touch rate	1.0144	0.9842	1.0536	0.9812	0.7813	1.0304	1.0214							
Surface area to volume ratio	3.0009	3.0474	3.0050	2.485	3.1847	2.9866	2.9254							
Host density	0.6314	0.4977	0.5472	2.434	7.904	0.8475	1.8566							

Table A.1: Parametric means in different transmission mode dominance categories.

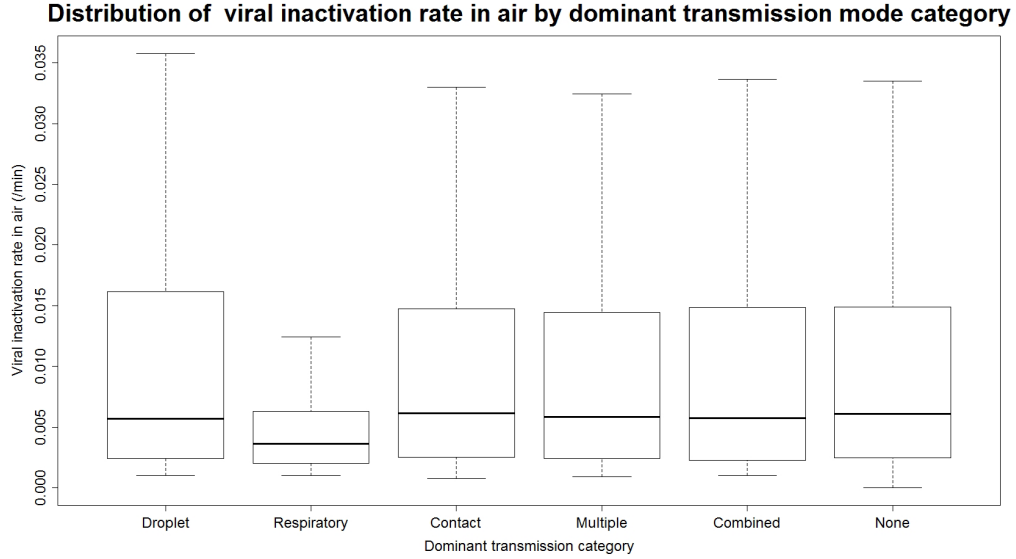


Figure A.1: Distribution of the airborne viral inactivation rate parameter for different categories of transmission mode dominance.

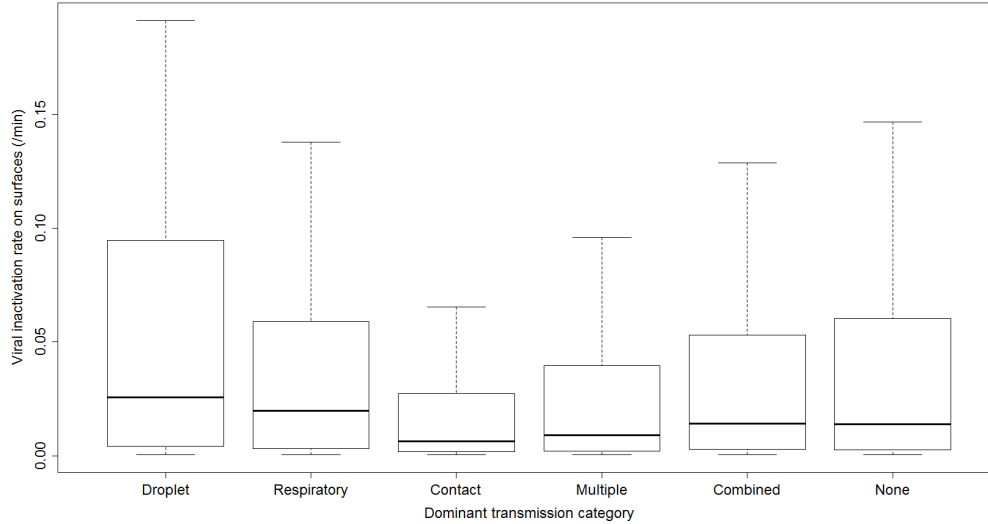
Distribution of the airborne viral inactivation rate parameter for different categories of transmission mode dominance. Droplet, respiratory, and contact refer to parameter sets which only yielded high transmission by these routes alone. Multiple refers to parameter sets where more than one transmission route was causing high transmission. Combined refers to parameter sets which did not contain a single dominant transmission mode, but did cause high transmission by multiple modes combined, and none refers to parameter sets which both had no dominant modes of transmission and also did not combine to cause high transmission.

A.2.4 Description of CART figures

Respiratory CART

As indicated by CART analysis five parameters were important in differentiating between regions of high ($R_0 > 1.7$) and low respiratory transmission ($R_0 < 1.7$): host density ($\epsilon_{density}$), viral proportion respirable (α_{resp}), shedding magnitude (α_{mag}), lower ID_{50} (π_L), and lung deposition fraction (τ_L).

In terminal node ii the respiratory mode was capable of causing pandemic transmission in 90% of the observed scenarios; requirements included at least $4.8E-6$ of all pathogens being excreted to particles less than 10 micrometers in diameter, a host density between 0.78 and 4.7 people per m^2 , a shedding magnitude greater than 0.025, lower ID_{50} less than $1.78 TCID_{50}$, and a lung deposition fraction greater than

Distribution of viral inactivation rate on surfaces by dominant transmission mode category**Figure A.2:** Distribution of the surface viral inactivation rate parameter for different categories of transmission mode dominance.

Distribution of the surface viral inactivation rate parameter for different categories of transmission mode dominance. Droplet, respiratory, and contact refer to parameter sets which only yielded high transmission by these routes alone. Multiple refers to parameter sets where more than one transmission route was causing high transmission. Combined refers to parameter sets which did not contain a single dominant transmission mode, but did cause high transmission by multiple modes combined, and none refers to parameter sets which both had no dominant modes of transmission and also did not combine to cause high transmission.

<i>Terminal Node Number</i>	<i>i</i>	<i>ii</i>	<i>iii</i>	<i>iv</i>	<i>v</i>	<i>vi</i>	<i>vii</i>
Contact R_0	7.55	18.52	12.84	27.28	11.59	6.16	19.69
Respiratory R_0	0.19	5.38	0.47	3.87	1.07	2.49	9.48
Inspiratory R_0	0.02	0.09	0.20	0.37	0.17	0.08	0.29
Droplet-spray R_0	0.85	2.64	8.17	18.65	6.65	3.52	15.99
Total R_0	8.61	26.63	21.68	50.18	19.48	18.54	45.45

Table A.2: Terminal node description of respiratory CART figure.

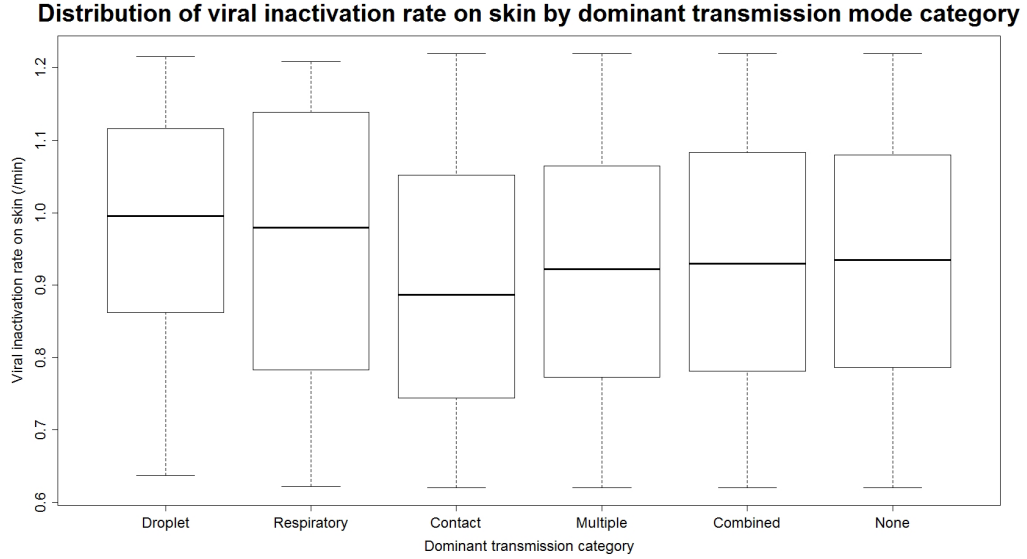


Figure A.3: Distribution of the skin viral inactivation rate parameter for different categories of transmission mode dominance.

Droplet, respiratory, and contact refer to parameter sets which only yielded high transmission by these routes alone. Multiple refers to parameter sets where more than one transmission route was causing high transmission. Combined refers to parameter sets which did not contain a single dominant transmission mode, but did cause high transmission by multiple modes combined, and none refers to parameter sets which both had no dominant modes of transmission and also did not combine to cause high transmission.

41%. When host density was less than 4.7 people per m^2 and at least one of these other conditions was not met, only 2% of scenarios showed pandemic level transmission caused by the respiratory route by itself. In addition to terminal nodes ii, terminal nodes iv and vii also indicated high respiratory transmission. Of the three nodes in which greater than 87% of parameter sets yielded high transmission, note that in two of these it was not necessary to have a very infectious strain (high π_L). In all of these high respiratory transmission terminal nodes, the contact mode was also high in roughly 80% of parameter sets which gave rise to each node. This indicates that these nodes did not pinpoint any high respiratory-only contexts.

We have shown that similar contexts in terms of high respiratory transmission may be achieved as a result of a trade-off between the parameters in figure A.12 :lower values of one which dampen transmission, may be counteracted by higher values of

Distribution of hand-surface transfer efficiency by dominant transmission mode categor

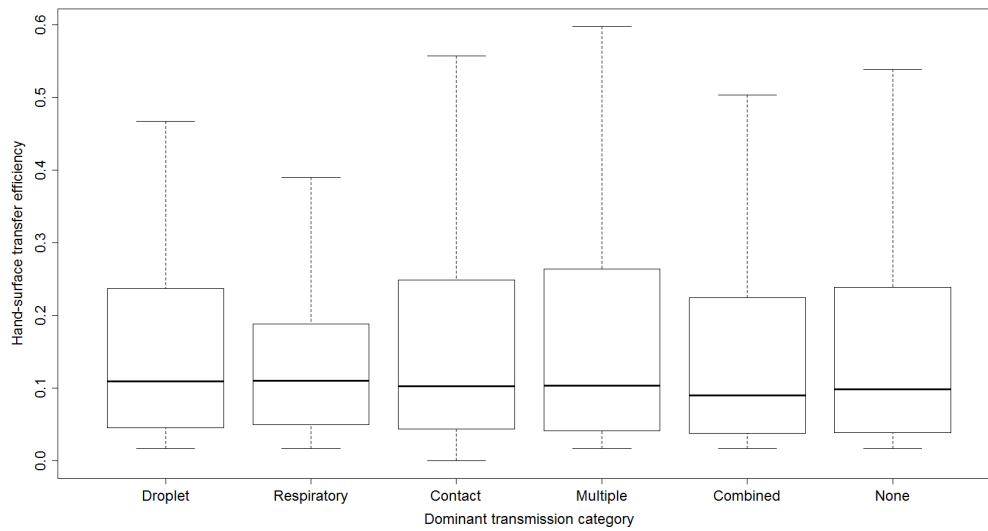


Figure A.4: Distribution of the finger-surface transfer efficiency parameter for different categories of transmission mode dominance.

Distribution of the finger-surface transfer efficiency parameter for different categories of transmission mode dominance. Droplet, respiratory, and contact refer to parameter sets which only yielded high transmission by these routes alone. Multiple refers to parameter sets where more than one transmission route was causing high transmission. Combined refers to parameter sets which did not contain a single dominant transmission mode, but did cause high transmission by multiple modes combined, and none refers to parameter sets which both had no dominant modes of transmission and also did not combine to cause high transmission.

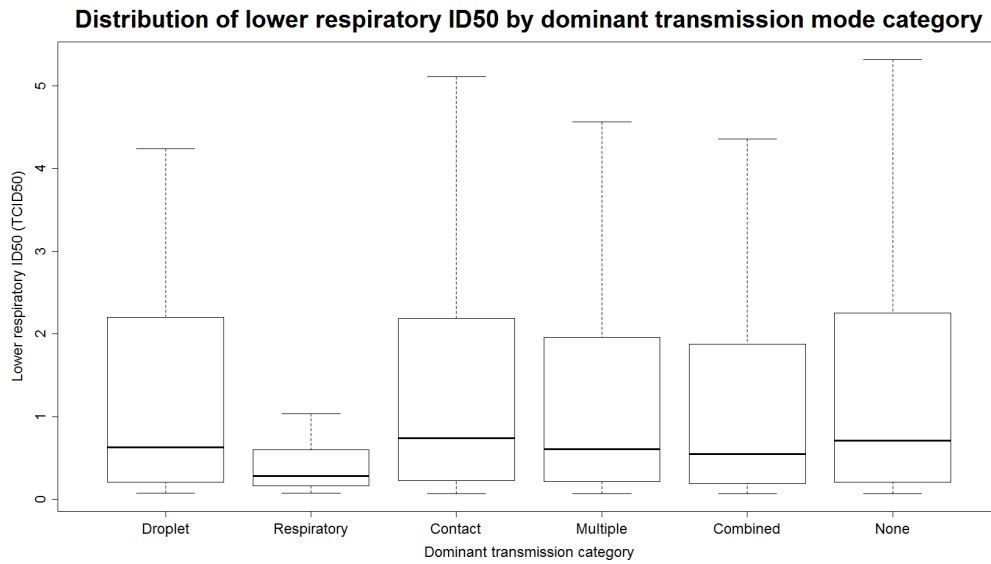


Figure A.5: Distribution of the lower respiratory infectivity parameter for different categories of transmission mode dominance.

Distribution of the lower respiratory infectivity parameter for different categories of transmission mode dominance. Droplet, respiratory, and contact refer to parameter sets which only yielded high transmission by these routes alone. Multiple refers to parameter sets where more than one transmission route was causing high transmission. Combined refers to parameter sets which did not contain a single dominant transmission mode, but did cause high transmission by multiple modes combined, and none refers to parameter sets which both had no dominant modes of transmission and also did not combine to cause high transmission.

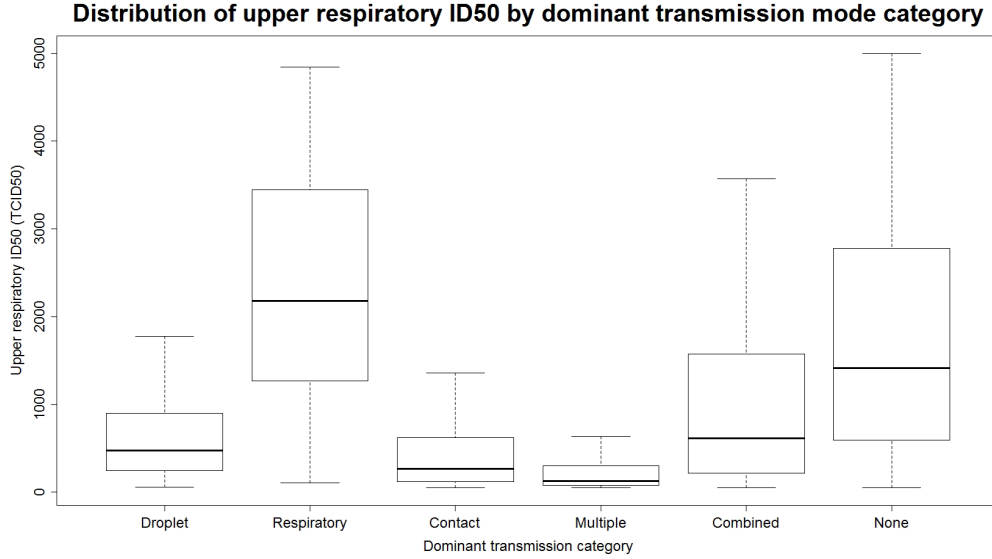


Figure A.6: Distribution of the upper respiratory infectivity parameter for different categories of transmission mode dominance.

Droplet, respiratory, and contact refer to parameter sets which only yielded high transmission by these routes alone. Multiple refers to parameter sets where more than one transmission route was causing high transmission. Combined refers to parameter sets which did not contain a single dominant transmission mode, but did cause high transmission by multiple modes combined, and none refers to parameter sets which both had no dominant modes of transmission and also did not combine to cause high transmission.

others. For example, in terminal node ii, moderate $\epsilon_{density}$ (between 0.78 and 4.7 people per m^2) and weak π_L (<1.78) are counteracted by high α_{resp} ($>4.8E-4$) and high τ_L ($>41\%$). In terminal node iv the situation is reversed with a more moderate α_{resp} (between $1.2E-6$ and $3.7E-6$) and low τ_L ($>24\%$) being counteracted by high $\epsilon_{density}$ (>4.7 people per m^2) and stronger π_L ($<0.64 TCID_{50}$). It is also interesting to consider what respiratory parameters were not present in the CART figure: viral inactivation in the air (μ_A), breath rate (ρ_{breath}), and surface area to volume ratio ($\epsilon_{SA:V}$). These parameters were still influential in causing respiratory transmission, as indicated by correlation analysis, but they do not differentiate between high and low transmission as much as others.

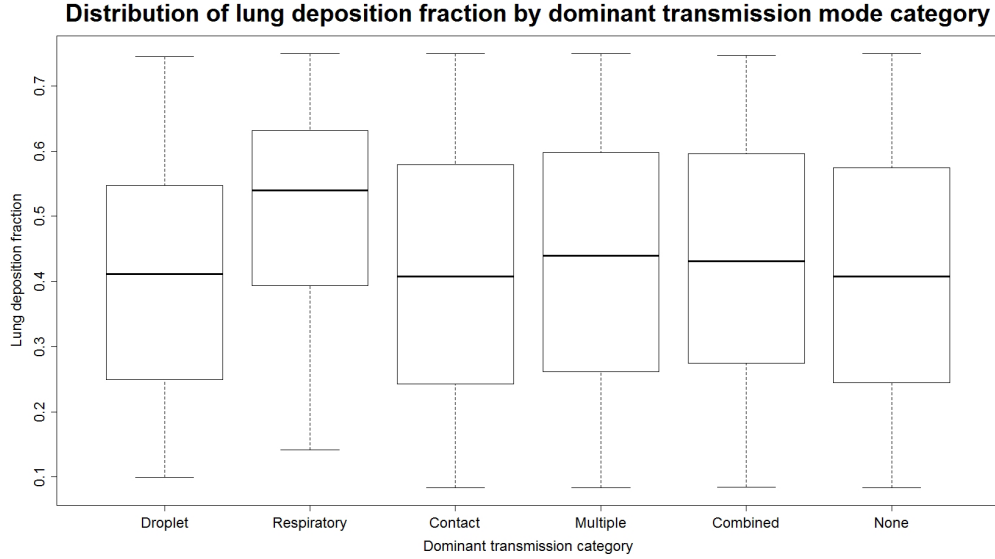


Figure A.7: Distribution of the lung deposition parameter for different categories of transmission mode dominance.

Droplet, respiratory, and contact refer to parameter sets which only yielded high transmission by these routes alone. Multiple refers to parameter sets where more than one transmission route was causing high transmission. Combined refers to parameter sets which did not contain a single dominant transmission mode, but did cause high transmission by multiple modes combined, and none refers to parameter sets which both had no dominant modes of transmission and also did not combine to cause high transmission.

Contact CART

To differentiate between high and low transmission intensity for the contact mediated transmission mode, three parameters were indicated: upper ID_{50} (π_U), self-inoculation rate (ρ_{inoc}), and shedding magnitude (α_{mag}). Terminal nodes iii, v, and vi all show high contact transmission. Terminal node iii was largely contact-only producing high transmission, while the droplet mode was causing high transmission in terminal node v and vi in about 41% and 31% of these parameter sets respectively. As shown by terminal node vi, given a π_U in the more infectious 3/4 of the range considered ($\pi_U < 540.7$) and self inoculations occurring at least once every 19 minutes, 86% of scenarios resulted in high contact transmission. This ρ_{inoc} critical value is lower than self inoculation rates previously observed: 1 touch every 12 minutes [32], and 1 touch every 4 minutes [50]. Thus it is likely a realistic parameter region.

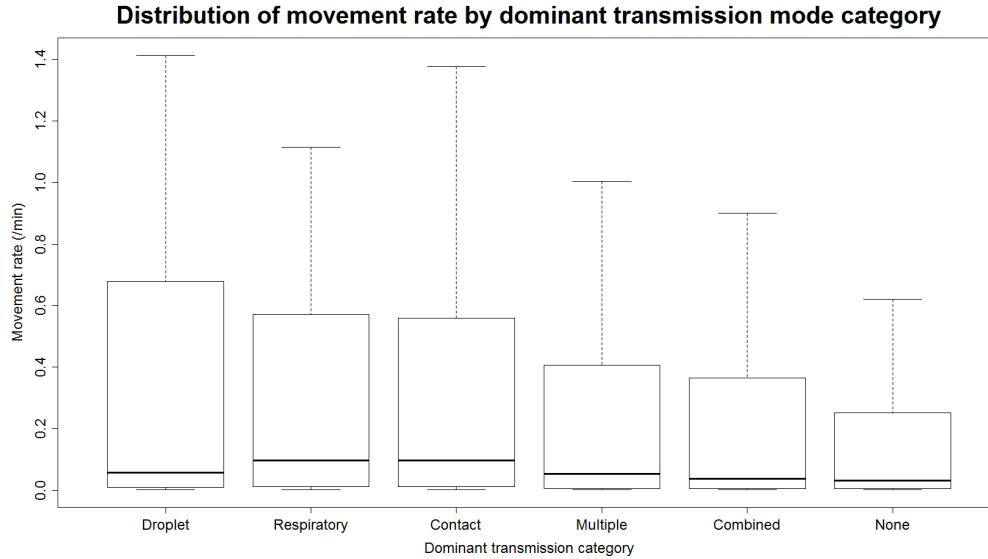


Figure A.8: Distribution of the host movement rate parameter for different categories of transmission mode dominance.

Droplet, respiratory, and contact refer to parameter sets which only yielded high transmission by these routes alone. Multiple refers to parameter sets where more than one transmission route was causing high transmission. Combined refers to parameter sets which did not contain a single dominant transmission mode, but did cause high transmission by multiple modes combined, and none refers to parameter sets which both had no dominant modes of transmission and also did not combine to cause high transmission.

Note that viral inactivation rate on hands (μ_H) and viral inactivation rate on surfaces (μ_S) are not present in figure 2.5. Thus, in the parameter range we considered, these parameters did not greatly differentiate between high and low transmission settings. On hands, the range corresponded to an expected pathogen lifetime between 48 seconds and 96 seconds. On surfaces, the range was larger; the expected lifetime was between 5 minutes and 33 hours with a median expected value of 100 minutes. This helps explain the importance of ρ_{inoc} in figure 2.5 rather than ρ_{touch} . Given an environmental persistence on surfaces of roughly an hour, the bottleneck in the exposure cycle occurs on the fingertip before self-inoculation, rather than in the environment before getting picked up. The self inoculation rate must be high enough to overcome the high inactivation rate on the skin. Given a π_U in the less infectious half of the range considered, and ρ_{inoc} less than 1 touch every 10 minutes,

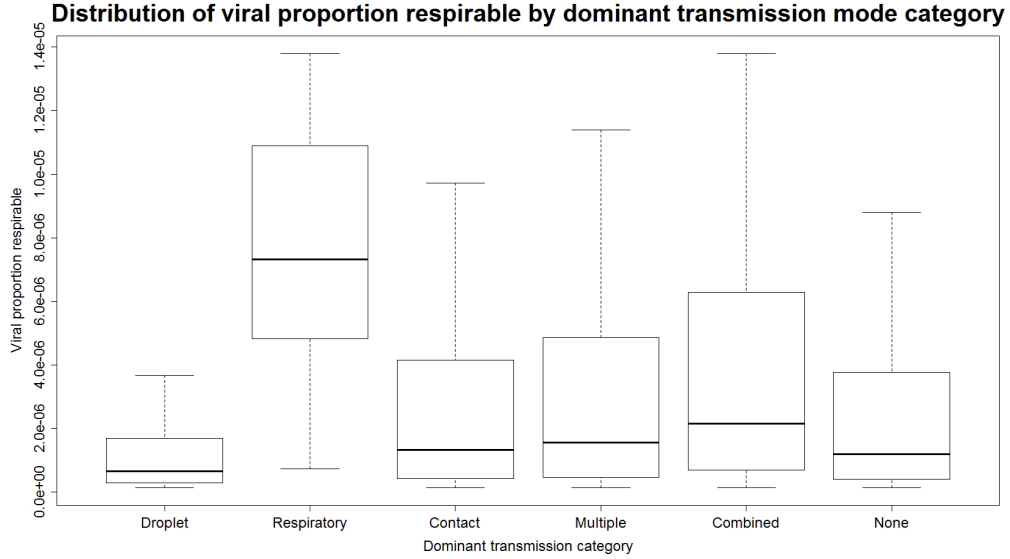


Figure A.9: Distribution of the viral proportion respirable parameter for different categories of transmission mode dominance.

Droplet, respiratory, and contact refer to parameter sets which only yielded high transmission by these routes alone. Multiple refers to parameter sets where more than one transmission route was causing high transmission. Combined refers to parameter sets which did not contain a single dominant transmission mode, but did cause high transmission by multiple modes combined, and none refers to parameter sets which both had no dominant modes of transmission and also did not combine to cause high transmission.

low transmission occurs in 89% of parameter sets.

Droplet CART

The intensity of the droplet mediated transmission mode is differentiated by three parameters: upper ID_{50} (π_U), host density ($\epsilon_{density}$), and shedding magnitude (α_{mag}). Like the respiratory mode, these parameters may compensate for one another to yield high droplet transmission. For example in terminal node ix, under high host density ($\epsilon_{density} > 2.8$ people/ m^2) and $\pi_U < 532.8$, 83% of scenarios resulted in high droplet transmission, but with a less infectious agent ($\pi_U > 532.8$) only 21% of scenarios indicated high droplet transmission. Low host density conditions ($\epsilon_{density} < 2.8$ people/ m^2) may be overcome to achieve high droplet given other compensating parameter values, as in the case of terminal node ii; here 79% of scenarios result in high droplet transmission given a very infectious agent ($\pi_U < 286$), moderate shed-

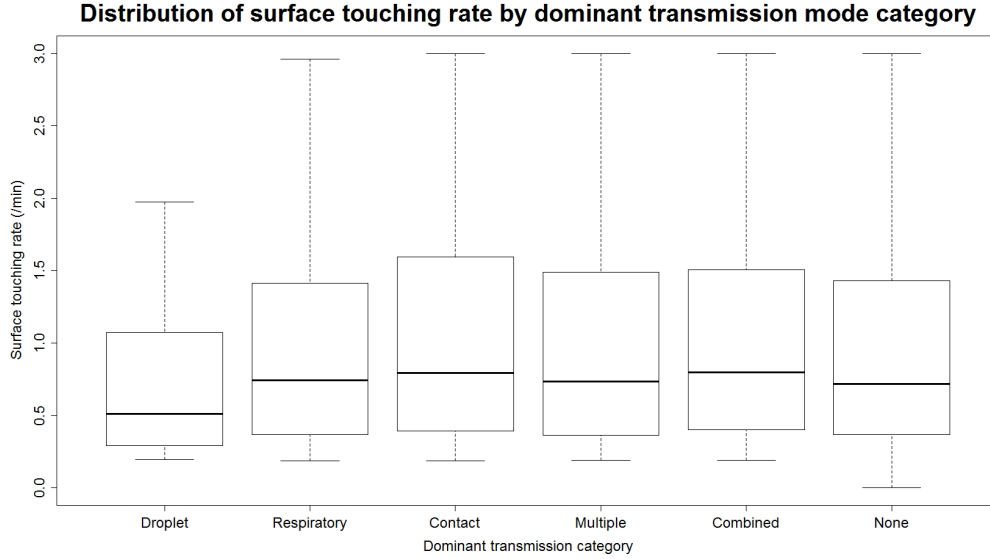


Figure A.10: Distribution of the surface touching rate parameter for different categories of transmission mode dominance.

Droplet, respiratory, and contact refer to parameter sets which only yielded high transmission by these routes alone. Multiple refers to parameter sets where more than one transmission route was causing high transmission. Combined refers to parameter sets which did not contain a single dominant transmission mode, but did cause high transmission by multiple modes combined, and none refers to parameter sets which both had no dominant modes of transmission and also did not combine to cause high transmission.

ding magnitude ($\alpha_{mag} > 0.046$) and excluding very low host densities ($0.65 < \epsilon_{density} < 2.8$). Thus at low host densities, a high infectivity is required for substantial droplet transmission. High droplet transmission is indicated in terminal nodes ii, iv, vi, viii, and ix. In all of these terminal nodes, there was high contact transmission in at least 80% of parameter sets. In terminal node viii, there was high respiratory transmission in about 35% of this node.

<i>Terminal Node Number</i>	<i>i</i>	<i>ii</i>	<i>iii</i>	<i>iv</i>	<i>v</i>	<i>vi</i>	<i>vii</i>	<i>viii</i>	<i>ix</i>
Contact R_0	3.27	32.88	10.35	21.91	25.78	45.25	1.48	6.10	23.81
Respiratory R_0	0.17	0.76	0.08	0.32	0.18	0.50	1.29	2.59	1.64
Inspiratory R_0	0.01	0.07	0.02	0.07	0.04	0.12	0.02	0.08	0.29
Droplet-spray R_0	0.27	3.41	0.76	3.05	1.42	5.24	0.72	3.41	12.79
Total R_0	3.71	37.11	11.20	25.35	27.41	51.11	4.34	12.19	38.53

Table A.3: Terminal node description of droplet CART figure.

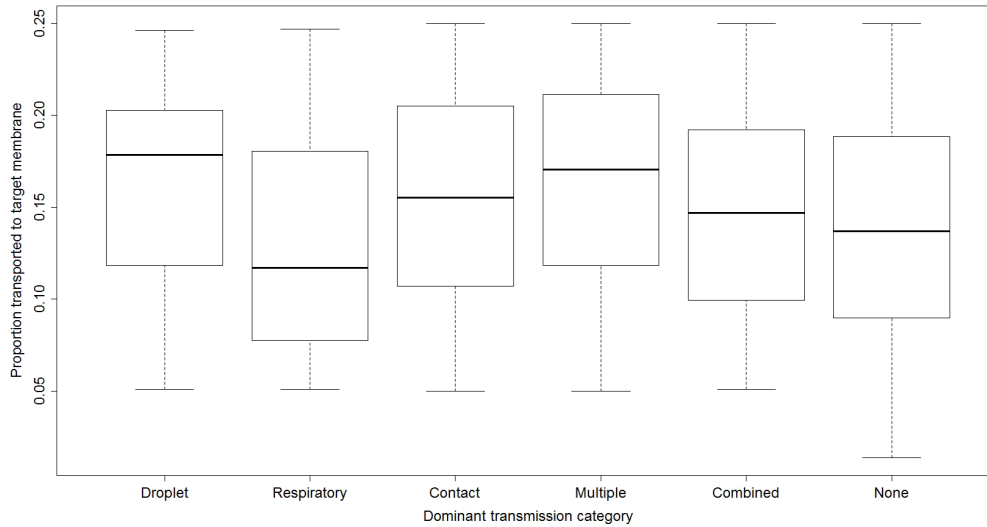
Figure A.11: Distribution of proportion transported to target membrane by dominant transmission mode ca

Figure A.11: Distribution of the transfer proportion from self inoculation site to target site parameter for different categories of transmission mode dominance.

Droplet, respiratory, and contact refer to parameter sets which only yielded high transmission by these routes alone. Multiple refers to parameter sets where more than one transmission route was causing high transmission. Combined refers to parameter sets which did not contain a single dominant transmission mode, but did cause high transmission by multiple modes combined, and none refers to parameter sets which both had no dominant modes of transmission and also did not combine to cause high transmission.

Inspiratory CART

Strength of inspiratory transmission is differentiated by host density ($\epsilon_{density}$), upper ID_{50} (π_U), shedding magnitude (α_{mag}), and surface area to volume ratio ($\epsilon_{SA:V}$). Relatively high host density, infectivity, shedding magnitude, and surface area to volume ratio are all required to cause substantial inspiratory transmission. These conditions are only satisfied by one node in the tree representing 11 parameter sets. Assuming our parameter constraints are reasonable, inspiratory transmission may be the least important influenza mode, as it requires the most extreme (and potentially unlikely) values of these four parameters jointly. This node also had high transmission by the contact and droplet routes.

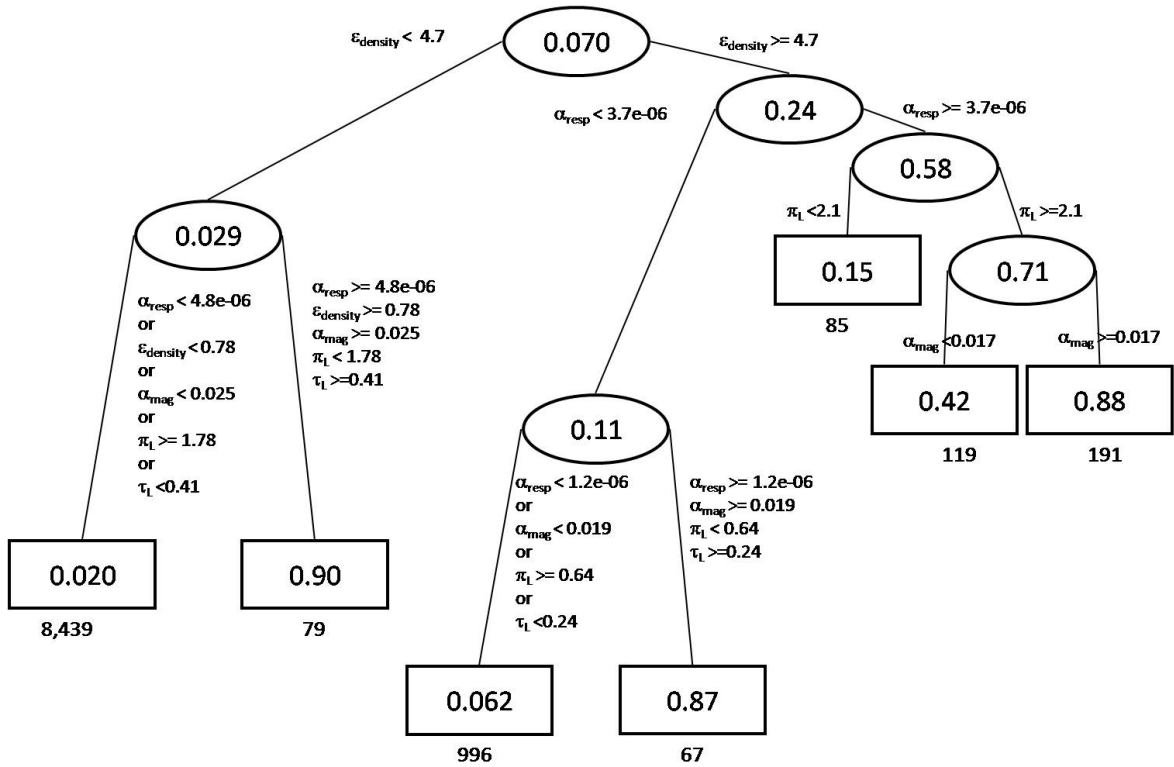


Figure A.12: The respiratory-route CART diagram.

Numbers in ovals and rectangles are the proportions of parameter sets have mode-specific $R_0 > 1.7$ which meet the parameterization criteria shown on edges. Five parameters differentiate between areas of high versus low respiratory transmission: host density ($\epsilon_{density}$), viral proportion respirable (α_{resp}), lower respiratory ID_{50} (π_L), shedding magnitude (α_{mag}), and lung deposition fraction (τ_L).

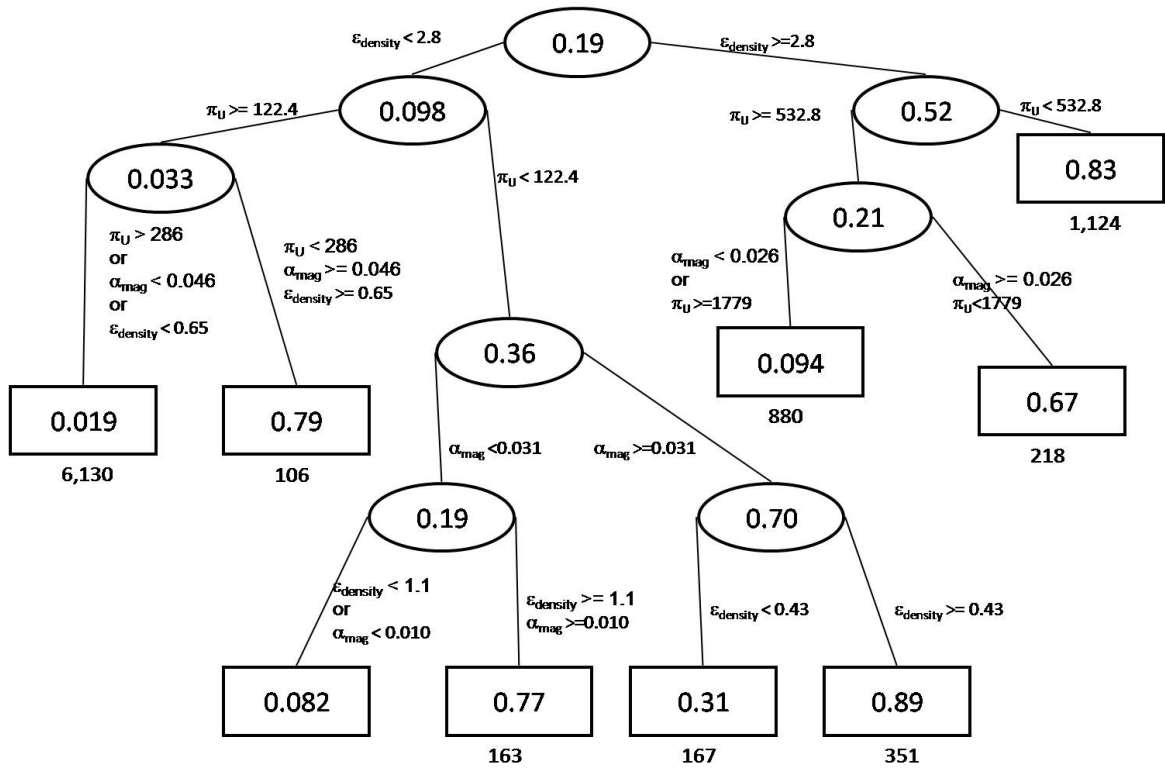


Figure A.13: The droplet-route CART diagram.

The droplet-route CART diagram. Numbers in ovals and rectangles are the proportions of parameter sets have mode-specific $R_0 > 1.7$ which meet the parameterization criteria shown on edges. Three parameters differentiate between areas of high versus low respiratory transmission: host density ($\epsilon_{density}$), upper respiratory ID_{50} (π_L), and shedding magnitude (α_{mag}).

A.2.5 Comparison to Previous Models

To compare our modeling approach and results to previous models, we summarize major differences in model parameterization and model structure. The model of Atkinson and Wein (AW) has only one major parametric difference. They use a surface area to volume ratio of 3:1m. This ratio is generally used to inform particle settling within a given room volume for settling of extremely fine particles in gases. It is unrealistic however for larger particles, where settling is dominated by gravity, making it unlikely that they would settle on non-horizontal surface area. Given a room height of 3m with one layer of horizontal surface area to settle to, the appropriate ratio would be 1:3 m, the inverse of what AW used. It is possible that are multiple surface area layers, or that particles may settle to vertical surfaces; these conditions would result in a ratio closer to AWs value, but would still unlikely reach their value. For these reasons we considered values from 1:1m to 1:5m.

Structurally, important differences in AWs approach relates to assumptions of behavior of individuals in their model. First, the symptomatic shedder does not leave their private room. Second, the symptomatic shedder is only visited by one other person. These two features only allow the possibility of the contact mode infecting the single care-giver, while the airborne routes are allowed to continue to operate on all individuals, as viruses in the air may diffuse from the shedders private room to other areas.

The parametric surface area to volume ratio value and structured human movement in concert greatly magnify the potential of the airborne routes compared to others from AW. Thus, it is not surprising that AWs solution space was not observed in our results. For example, the inspiratory route in AW, accounted for 36% of all transmissions, while the maximum observed in our 10,000 unit set was only 12.5%.

The surface area to volume ratio as well as the strict social isolation imparted in AW can explain this discrepancy. The prior inflates both airborne routes relative to the contact route, while the latter further weakens both the droplet and contact routes, both of which require close proximity. Because of these differences our relative contact, droplet respiratory, and inspiratory transmission vector is different from AW. However, the ratio of respiratory to inspiratory transmissions should not have similar differences resulting from different implementations. In fact 600 parameter sets exist in our results fitting AWs respiratory to inspiratory ratio solution space.

All parameter values used in Nicas and Jones (NJ) fell within the ranges of parameter values included in our sample. However, like AW, NJ was structurally modeling a specific scenario: the transmission resulting from a caregiver visiting a symptomatic individuals room for 15 minutes. The major difference here is that proximity is maintained between the shedder and susceptible for the entire modeled period. This over emphasizes transmissions which require close proximity: the droplet and contact mediated routes.

We were able to find each of the solution spaces NJ summarized. Each space accounted for less than 200 (2%) of our full 10,000 unit space. We summarized the parameter distributions that gave rise to 3 of NJs solution spaces and compared the parameter distributions in each of these to the parameter distribution of the vectors in our sample not part of each subsection. Each parameterization presented in NJ is only a small subset of all possible parameterizations which could produce such relative transmission vectors; conceptually, the same is true of AW there are many parameterizations which could have produced their relative transmission vector we just did not consider any of these to be in a realistic region of parameter space.

As both NJ and AW defined their outcomes in terms of a relative transmission

vector, additionally note that one solution space may cover a broad range of total transmission intensities, from very low to very high total force of infection. For example, a solution space for AW or NJ that suggests dominance in air and droplet may be under the constraint that total- $R_0 < 1$ or total- $R_0 > 3$. Each of these situations has major implications with respect to intervention choices. Decisions on whether to intervene may vary based on total force of infection, and threshold values of each mode-specific absolute intensity may also alter intervention decisions.

There were three key differences between our approach and that of both AW and NJ. First, AW used a surface area to volume ratio of 3:1m, which is suitable for small particles less than 6 μm [66, 54]. These small particles will behave more like a gas, with settling possible on vertical surfaces, while larger particles will be more dominated by gravity, more likely to deposit on horizontal surfaces as indicated by Table 3-5 of Hong [33]. Thus AWs surface area to volume ratio for settling sites for particles greater than 10 μm is not appropriate and will greatly dilute the pathogen surface concentration compared to pathogen air volume concentration, thus artificially diminishing the contact route compared to the respiratory and inspiratory routes. This could be one reason why AW found the contact mode to be negligible as well as why we were not able to observe AWs full solution space in our results.

Second, NJ did not model the transfer which occurs between the pathogen being transferred to the eyes/nose/mouth to the target tissue in the upper airway. NJ acknowledged this, but chose to ignore it as there was no relevant data available. AW on the other hand, while not explicitly modeling this, used a composite contact transmission parameter, which when dissected is consistent with using an additional parameter to decrease the number of pathogens being transferred to the target tissue from the eyes/nose/mouth. Our parameter sweep encompasses the region which AW

pinpointed, while it does not include NJ, as NJ implicitly assumed that 100% was transferred. Third, both AW and NJ assumed a specific contact schedule between the infectious person and at least one susceptible. This further specified a context, as defined by a specific script for interaction. This contrasts with our random movement approach, which while not necessarily modeling any specific interaction, may be the most generalizable to all non-scripted interactions. We allowed close proximity interactions to result from changes in host density and human movement in the venue, rather than scripting specific interactions. NJ required close proximity while AW only allowed one caregiver to have close proximity for a short time period and did not allow proximity otherwise. This may be the most influential factor explaining why similar inferences were not drawn from our work compared to AW and NJ.

A.2.6 Correlation Analysis

This correlation analysis was performed mainly to show that the model was behaving as we would expect; e.g.. features that were programmed to affect only the contact route of transmission were only associated with it.

<i>Parameter</i>	<i>r</i>	<i>p</i>
Viral proportion respirable	0.52096	<.0001
Host density	0.27049	<.0001
Shedding magnitude	0.26541	<.0001
Lower ID_{50}	-0.16025	<.0001
Surface area to volume ratio	-0.10241	<.0001
Viral inactivation in air	-0.08623	<.0001
Lung deposition fraction	0.06828	<.0001
Breathing rate	0.03733	<.0001
Viral proportion inspirable	0.00894	0.1905
Self inoculation rate	-0.00777	0.255
Medium particle settling rate	-0.00716	0.2945
Hand-surface transfer efficiency	-0.00444	0.5155
Upper ID_{50}	-0.0044	0.5198
Viral inactivation on surfaces	-0.00384	0.5738
Proportion of virus transported to target membrane	0.00211	0.7578
Viral inactivation on skin	0.00206	0.7629
Surface touching rate	0.00189	0.7824
Movement rate	-0.00069	0.9192

Table A.4: Univariate correlations of respiratory infection.

<i>Parameter</i>	<i>r</i>	<i>p</i>
Upper ID_{50}	-0.52203	<.0001
Shedding magnitude	0.42527	<.0001
Host density	0.19252	<.0001
Viral proportion inspirable	0.05641	<.0001
Hand-surface transfer efficiency	-0.01146	0.0858
Viral inactivation on surfaces	-0.00799	0.2311
Proportion of virus transported to target membrane	-0.00784	0.2399
Self inoculation rate	-0.00777	0.2441
Medium particle settling rate	-0.00591	0.3753
Viral inactivation in air	0.00564	0.3977
Movement rate	-0.00308	0.6447
Surface area to volume ratio	-0.00274	0.7329
Viral proportion respirable	0.00252	0.706
Viral inactivation on skin	0.0024	0.7185
Lower ID_{50}	-0.00228	0.732
Breathing event rate	0.00218	0.7441
Lung deposition fraction	-0.00195	0.7705
Surface touching rate	-0.00096	0.8859

Table A.5: Univariate correlations of inspiratory infection.

<i>Parameter</i>	<i>r</i>	<i>p</i>
Host density	0.4439	<.0001
Upper ID_{50}	-0.39371	<.0001
Shedding magnitude	0.33395	<.0001
Viral inactivation in air	0.0109	0.1031
Proportion of virus transported to target membrane	-0.01035	0.1217
Viral inactivation on surfaces	-0.00826	0.2169
Hand-surface transfer efficiency	-0.00815	0.2231
Movement rate	-0.00508	0.4477
Breathing event rate	0.00458	0.4935
Surface area to volume ratio	0.00402	0.6175
Self inoculation rate	-0.00381	0.5688
Viral inactivation on skin	0.0037	0.5804
Viral proportion inspirable	0.00256	0.7024
Medium particle settling rate	0.00153	0.8193
Surface touching rate	0.00095	0.8875
Lower ID_{50}	-0.00008	0.9902
Lung deposition fraction	-0.00005	0.9946
Viral proportion respirable	0.00004	0.995

Table A.6: Univariate correlations of droplet-spray infection.

<i>Parameter</i>	<i>r</i>	<i>p</i>
Upper ID_{50}	-0.27871	<.0001
Viral inactivation on skin	-0.2662	<.0001
Shedding magnitude	0.25751	<.0001
Hand-surface transfer efficiency	0.23128	<.0001
Proportion of virus transported to target membrane	0.18915	<.0001
Surface touching rate	0.16394	<.0001
Self inoculation rate	0.15122	<.0001
Host density	0.13211	<.0001
Viral inactivation on surfaces	-0.09667	<.0001
Breathing event rate	-0.01369	0.041
Medium particle settling rate	0.01357	0.0428
Movement rate	0.01295	0.0532
Viral inactivation in air	0.01156	0.0845
Viral proportion inspirable	0.00895	0.1814
Lower ID_{50}	0.00498	0.4569
Viral proportion respirable	-0.00413	0.5373
Lung deposition fraction	-0.00348	0.6031
Surface area to volume ratio	0.00112	0.8896

Table A.7: Univariate correlations of contact mediated infection.

APPENDIX B

Chapter III Supporting Materials

B.1 Sub Route Equations

To keep track of the infections caused by pathogens from either the hand-to-fomite contamination route or the droplet-to-fomite contamination route, we must keep track of these two types of pathogens separately both on people and in the environment. This results in a near doubling of the numbers of compartments to keep track of. In the equations that follow, a final subscript may be added to either determine the type of pathogen being modeled (h for hand-to-fomite and d for droplet-to-fomite) or to keep track of what type of pathogen caused the infection for the *infectious* and *recovered* people. These equations follow. The excretion rate of viruses on large droplets to each fomite(α_1, α_2) as well as to the hands of the shedder(α_H) are given by

$$\begin{aligned}
 \alpha_1 &= \alpha\beta_F\lambda\frac{A_1}{A_{Total}} \\
 \alpha_2 &= \alpha\beta_F\lambda\frac{A_2}{A_{Total}} \\
 \alpha_H &= \alpha\beta_H
 \end{aligned}
 \tag{B.1}$$

The pathogen pickup rate from each fomite to hands is given by

$$(B.2) \quad \begin{aligned} \rho_1 &= \sigma_1 \rho_{tr} \rho_{te} \frac{A_{finger}}{A_1} \\ \rho_2 &= \sigma_2 \rho_{tr} \rho_{te} \frac{A_{finger}}{A_2} \end{aligned}$$

The rate of deposition from hands to each fomite is given by

$$(B.3) \quad \begin{aligned} \delta_1 &= \sigma_1 \rho_{tr} \rho_{te} \\ \delta_2 &= \sigma_2 \rho_{tr} \rho_{te} \end{aligned}$$

We use a standard SIR model of infection progression, where new infections are the result of self inoculations from contaminated susceptible hands

$$(B.4) \quad \begin{aligned} \frac{dS}{dt} &= -\rho_{inoc} E_{HS} \pi \\ \frac{dI_h}{dt} &= \rho_{inoc} E_{HS_h} \pi - \gamma I_h \\ \frac{dI_d}{dt} &= \rho_{inoc} E_{HS_d} \pi - \gamma I_d \\ \frac{dR_h}{dt} &= \gamma I_h \\ \frac{dR_d}{dt} &= \gamma I_d \end{aligned}$$

We model pathogens on fomites by considering fomite contamination via droplet-to-fomite contamination, pathogen loss from either pickup by people or pathogen inactivation, and pathogen gains resulting from deposition by hands to each fomite. Note that only the droplet-to-fomite compartment receives direct shedding in the following equations.

$$(B.5) \quad \begin{aligned} \frac{dE_{F1h}}{dt} &= -E_{F1h}(N\rho_1 + \mu_F) + (E_{HS_h} + E_{HI_h} + E_{HR_h})\delta_1 \\ \frac{dE_{F1d}}{dt} &= -E_{F1d}(N\rho_1 + \mu_F) + (E_{HS_d} + E_{HI_d} + E_{HR_d})\delta_1 + I\alpha_1 \\ \frac{dE_{F2h}}{dt} &= -E_{F2h}(N\rho_2 + \mu_F) + (E_{HS_h} + E_{HI_h} + E_{HR_h})\delta_2 \\ \frac{dE_{F2d}}{dt} &= -E_{F2d}(N\rho_2 + \mu_F) + (E_{HS_d} + E_{HI_d} + E_{HR_d})\delta_2 + I\alpha_2 \end{aligned}$$

We model pathogens on the hands of people by considering direct shedding to the hands of infectious people, pathogen pickup resulting from surface touching, and pathogen loss resulting from either inactivation, self inoculation, or deposition to fomites. The equations for pathogens on susceptibles and recovered people remain largely unchanged:

$$(B.6) \quad \begin{aligned} \frac{dE_{HS h}}{dt} &= S(E_{F1h}\rho_1 + E_{F2h}\rho_2) - E_{HS}(\mu_H + \rho_{inoc} + \delta_1 + \delta_2) \\ \frac{dE_{HS d}}{dt} &= S(E_{F1d}\rho_1 + E_{F2d}\rho_2) - E_{HS}(\mu_H + \rho_{inoc} + \delta_1 + \delta_2) \end{aligned}$$

$$(B.7) \quad \begin{aligned} \frac{dE_{HR h}}{dt} &= (R_h + R_d)(E_{F1h}\rho_1 + E_{F2h}\rho_2) - E_{HR}(\mu_H + \rho_{inoc} + \delta_1 + \delta_2) \\ \frac{dE_{HR d}}{dt} &= (R_h + R_d)(E_{F1d}\rho_1 + E_{F2d}\rho_2) - E_{HR}(\mu_H + \rho_{inoc} + \delta_1 + \delta_2) \end{aligned}$$

The equations for pathogens on the hands of infectious now only have direct shedding to the hand-to-fomite compartment.

$$(B.8) \quad \begin{aligned} \frac{dE_{HI h}}{dt} &= (I_h + I_d)(E_{F1h}\rho_1 + E_{F2h}\rho_2) - E_{HI}(\mu_H + \rho_{inoc} + \delta_1 + \delta_2) + (I_h + I_d)\alpha_H \\ \frac{dE_{HI d}}{dt} &= (I_h + I_d)(E_{F1d}\rho_1 + E_{F2d}\rho_2) - E_{HI}(\mu_H + \rho_{inoc} + \delta_1 + \delta_2) \end{aligned}$$

B.2 Pulsed intervention application

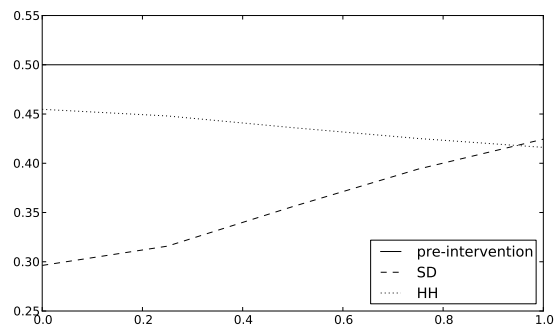


Figure B.1: Pulsed intervention efficacy against contact transmission as a function of surface touching specificity, using fixed pre-intervention total incidence models.

APPENDIX C

Chapter IV Supporting Materials

C.1 Calculation of β_H for S. Aureus

For one minute we would expect this many virus to be excreted to surfaces: Based on steady state assumptions and from a study looking at air dispersal per minute:

$$\text{AirDispersal} = 35.64$$

Also based on steady state assumptions: $\text{Handtouching} = \text{touchrate} * t_{\text{efficiency}} * \text{pathogenOnHand} = 0.75 * .1 * 224.76 = 16.875$

$$\beta_H \text{BetaH} = \text{HandTouch} / (\text{handTouch} + \text{AirDispersal}) = 0.32$$

Note, by steady state assumptions, we are assuming that once someone is infectious, they have constant levels of pathogens either on their fingertips which result in hand-contaminated fomites, or other areas such as the perineum which result in air-dispersal.

C.2 Calculation of $\frac{\alpha}{\gamma}$ for all pathogens

To calculate ballpark estimates of the total expected shedding for each pathogen we take into account the length of shedding and the expected shedding of pathogens per day. For influenza and norovirus, we have estimates of how the viral titer varies by day of infection, so our calculations take this into account. For norovirus, we use

	<i>Norovirus</i>	<i>S. aureus</i>	<i>Rhinovirus</i>	<i>Influenza</i>
<i>Total Shedding</i>	7,600,000	1,100,000	6,900,000	8,500,000

Table C.1: Rough estimate of total shedding over course of infection among pathogens.

assume that 0.01 g of fecal material gets to the shedder's hands per day without be removed. Using estimates of viral concentration in fecal material [64] we estimate 7,593,614 virions are shed over the 28 days of shedding. For *S. aureus*, we assume constant shedding over 14 days. Using the same shedding rate calculations used to estimate β_H for *S. aureus*, 1,058,702 cocci to be shed over 14 days. For influenza, we assume a cough rate of 12 per hour, a cough volume of 0.044mL per cough, and that the proportion of cough volume which settles out rapidly from the cough to be roughly 99%. This yields a daily cough volume excretion which we assume is constant over the course of infection, which we then combine with the viral titer levels by day of infection from Hayden [29]. This yields an estimate of 8,471,735 TCID₅₀ over seven days of shedding. For rhinovirus, we assume rhinovirus excretes 81.3% as much virus as influenza as Atkinson and Wein also assume [6]. Table A.8 summarizes these total shedding values.

BIBLIOGRAPHY

BIBLIOGRAPHY

- [1] Allison E Aiello and Elaine L Larson. What is the evidence for a causal link between hygiene and infections? *The Lancet Infectious Diseases*, 2(2):103–110, February 2002. PMID: 11901641.
- [2] Julia Aledort, Nicole Lurie, Jeffrey Wasserman, and Samuel Bozzette. Non-pharmaceutical public health interventions for pandemic influenza: an evaluation of the evidence base. *BMC Public Health*, 7(1):208, 2007.
- [3] R H Alford, J A Kasel, P J Gerone, and V Knight. Human influenza resulting from aerosol inhalation. *Proceedings of the Society for Experimental Biology and Medicine. Society for Experimental Biology and Medicine (New York, N.Y.)*, 122(3):800–804, July 1966. PMID: 5918954.
- [4] Roy M. Anderson, Robert M. May, and B. Anderson. *Infectious Diseases of Humans: Dynamics and Control*. Oxford University Press, USA, September 1992.
- [5] S A Ansari, V S Springthorpe, S A Sattar, S Rivard, and M Rahman. Potential role of hands in the spread of respiratory viral infections: studies with human parainfluenza virus 3 and rhinovirus 14. *Journal of Clinical Microbiology*, 29(10):2115–2119, October 1991. PMID: 1658033 PMCID: 270283.
- [6] Michael Atkinson and Lawrence Wein. Quantifying the routes of transmission for pandemic influenza. *Bulletin of Mathematical Biology*, 70(3):820–867, April 2008.
- [7] B. Bean, B. M. Moore, B. Sterner, L. R. Peterson, D. N. Gerding, and H. H. Balfour Jr. Survival of influenza viruses on environmental surfaces. *The Journal of Infectious Diseases*, 146(1):47–51, July 1982. ArticleType: primary_article / Full publication date: Jul., 1982 / Copyright 1982 The University of Chicago Press.
- [8] Gabrielle Brankston, Leah Gitterman, Zahir Hirji, Camille Lemieux, and Michael Gardam. Transmission of influenza a in human beings. *The Lancet Infectious Diseases*, 7(4):257–265, 2007.
- [9] Leo Breiman, Jerome Friedman, Charles J. Stone, and R.A. Olshen. *Classification and Regression Trees*. Chapman & Hall/CRC, 1 edition, January 1984.
- [10] John J Cannell, Michael Zasloff, Cedric F Garland, Robert Scragg, and Edward Giovannucci. On the epidemiology of influenza. *Virology Journal*, 5:29, 2008. PMID: 18298852.
- [11] R B Couch, R G Douglas, D S Fedson, and J A Kasel. Correlated studies of a recombinant influenza-virus vaccine. 3. protection against experimental influenza in man. *The Journal of Infectious Diseases*, 124(5):473–480, November 1971. PMID: 5000515.
- [12] R B Couch, J A Kasel, J L Gerin, J L Schulman, and E D Kilbourne. Induction of partial immunity to influenza by a neuraminidase-specific vaccine. *The Journal of Infectious Diseases*, 129(4):411–420, April 1974. PMID: 4593871.

- [13] D. J. D'Alessio, C. K. Meschievitz, J. A. Peterson, C. R. Dick, and E. C. Dick. Short-Duration exposure and the transmission of rhinoviral colds. *The Journal of Infectious Diseases*, 150(2):189–194, August 1984. ArticleType: research-article / Full publication date: Aug., 1984 / Copyright 1984 The University of Chicago Press.
- [14] Markus Dettenkofer, Sibylle Wenzler, Susanne Amthor, Gerd Antes, Edith Motschall, and Franz D. Daschner. Does disinfection of environmental surfaces influence nosocomial infection rates? a systematic review. *American Journal of Infection Control*, 32(2):84–89, April 2004.
- [15] O. Diekmann, J. A. P. Heesterbeek, and J. A. J. Metz. On the definition and the computation of the basic reproduction ratio r_0 in models for infectious diseases in heterogeneous populations. *Journal of Mathematical Biology*, 28(4):365–382, June 1990.
- [16] Doris H. D'Souza, Arnie Sair, Karen Williams, Efstathia Papafragkou, Julie Jean, Christina Moore, and LeeAnn Jaykus. Persistence of caliciviruses on environmental surfaces and their transfer to food. *International Journal of Food Microbiology*, 108(1):84–91, April 2006.
- [17] J. P. Duguid. The size and the duration of Air-Carriage of respiratory droplets and Droplet-Nuclei. *The Journal of Hygiene*, 44(6):471–479, September 1946. ArticleType: primary_article / Full publication date: Sep., 1946 / Copyright 1946 Cambridge University Press.
- [18] J N Eisenberg, E Y Seto, A W Olivieri, and R C Spear. Quantifying water pathogen risk in an epidemiological framework. *Risk Analysis: An Official Publication of the Society for Risk Analysis*, 16(4):549–563, August 1996. PMID: 8819345.
- [19] Joseph N. S. Eisenberg, M. Alan Brookhart, Glenn Rice, Mary Brown, and John M. Colford. Disease transmission models for public health decision making: Analysis of epidemic and endemic conditions caused by waterborne pathogens. *Environmental Health Perspectives*, 110(8):783–790, August 2002. ArticleType: primary_article / Full publication date: Aug., 2002 / Copyright 2002 The National Institute of Environmental Health Sciences (NIEHS).
- [20] Stephen Eubank, Hasan Guclu, V S Anil Kumar, Madhav V Marathe, Aravind Srinivasan, Zoltán Toroczkai, and Nan Wang. Modelling disease outbreaks in realistic urban social networks. *Nature*, 429(6988):180–184, May 2004. PMID: 15141212.
- [21] A R Falsey, M M Criddle, J E Kolassa, R M McCann, C A Brower, and W J Hall. Evaluation of a handwashing intervention to reduce respiratory illness rates in senior day-care centers. *Infection Control and Hospital Epidemiology: The Official Journal of the Society of Hospital Epidemiologists of America*, 20(3):200–202, March 1999. PMID: 10100548.
- [22] Neil M Ferguson, Derek A T Cummings, Simon Cauchemez, Christophe Fraser, Steven Riley, Aronrag Meeyai, Sapon Iamsirithaworn, and Donald S Burke. Strategies for containing an emerging influenza pandemic in southeast asia. *Nature*, 437(7056):209–214, September 2005. PMID: 16079797.
- [23] Neil M Ferguson, Derek A T Cummings, Christophe Fraser, James C Cajka, Philip C Cooley, and Donald S Burke. Strategies for mitigating an influenza pandemic. *Nature*, 442(7101):448–452, July 2006. PMID: 16642006.
- [24] Washington DC US EPA National Center for Environmental Assessment and Jacqueline Moya. Exposure factors handbook (Final report) 1997. <http://cfpub.epa.gov/ncea/cfm/recordisplay.cfm?deid=12464>, March 2000.
- [25] Timothy C Germann, Kai Kadau, Ira M Longini, and Catherine A Macken. Mitigation strategies for pandemic influenza in the united states. *Proceedings of the National Academy of Sciences of the United States of America*, 103(15):5935–5940, April 2006. PMID: 16585506.
- [26] Daniel T. Gillespie. Exact stochastic simulation of coupled chemical reactions. *The Journal of Physical Chemistry*, 81(25):2340–2361, December 1977.

- [27] Robert J Glass, Laura M Glass, Walter E Beyeler, and H Jason Min. Targeted social distancing design for pandemic influenza. *Emerging Infectious Diseases*, 12(11):1671–1681, November 2006. PMID: 17283616.
- [28] M Elizabeth Halloran, Neil M Ferguson, Stephen Eubank, Ira M Longini, Derek A T Cummings, Bryan Lewis, Shufu Xu, Christophe Fraser, Anil Vullikanti, Timothy C Germann, Diane Wagener, Richard Beckman, Kai Kadau, Chris Barrett, Catherine A Macken, Donald S Burke, and Philip Cooley. Modeling targeted layered containment of an influenza pandemic in the united states. *Proceedings of the National Academy of Sciences of the United States of America*, 105(12):4639–4644, March 2008. PMID: 18332436.
- [29] F G Hayden, R Fritz, M C Lobo, W Alvord, W Strober, and S E Straus. Local and systemic cytokine responses during experimental human influenza a virus infection. relation to symptom formation and host defense. *The Journal of Clinical Investigation*, 101(3):643–649, February 1998. PMID: 9449698.
- [30] Frederick G. Hayden, John J. Treanor, Robert F. Betts, Monica Lobo, James D. Esinhart, and Elizabeth K. Hussey. Safety and efficacy of the neuraminidase inhibitor GG167 in experimental human influenza. *JAMA*, 275(4):295–299, January 1996.
- [31] J H Hemmes, K C Winkler, and S M KOOL. Virus survival as a seasonal factor in influenza and polimyelitis. *Nature*, 188:430–431, October 1960. PMID: 13713229.
- [32] J O Hendley, R P Wenzel, and J M Gwaltney. Transmission of rhinovirus colds by self-inoculation. *The New England Journal of Medicine*, 288(26):1361–1364, June 1973. PMID: 4350527.
- [33] Tao Hong. *Estimating Risk of Exposure to Bacillus Anthracis based on Environmental Concentrations*. PhD thesis, Drexel University, May 2009.
- [34] ICRP and ICRP. *ICRP Publication 66: Human Respiratory Tract Model for Radiological Protection*. Elsevier, 1 edition, January 1995.
- [35] P A Jumaa. Hand hygiene: simple and complex. *International Journal of Infectious Diseases: IJID: Official Publication of the International Society for Infectious Diseases*, 9(1):3–14, January 2005. PMID: 15603990.
- [36] Matt J. Keeling and Pejman Rohani. *Modeling Infectious Diseases in Humans and Animals*. Princeton University Press, 1 edition, October 2007.
- [37] Edwin D Kilbourne. *Influenza*. Plenum Medical Book Co, New York, 1987.
- [38] J S Koopman. Interaction between discrete causes. *Am J Epidemiol*, 113(6):716–24, June 1981.
- [39] L R Krilov, S R Barone, F S Mandel, T M Cusack, D J Gaber, and J R Rubino. Impact of an infection control program in a specialized preschool. *American Journal of Infection Control*, 24(3):167–173, June 1996. PMID: 8806992.
- [40] Richard Vaile Lee. Transmission of influenza a in human beings. *The Lancet Infectious Diseases*, 7(12):760–761; author reply 761–763, December 2007. PMID: 18045556.
- [41] Camille Lemieux, Gabrielle Brankston, Leah Gitterman, Zahir Hirji, and Michael Gardam. Questioning aerosol transmission of influenza. *Emerging Infectious Diseases*, 13(1):173–174; author reply 174–175, January 2007. PMID: 17370541.
- [42] Sheng Li, Joseph N. S. Eisenberg, Ian H. Spicknall, and James S. Koopman. Dynamics and control of infections transmitted from person to person through the environment. *Am. J. Epidemiol.*, 170(2):257–265, July 2009.

- [43] O. M. Lidwell. Some aspects of the transfer and acquisition of staphylococcus aureus in hospitals. In *The Staphylococci: Proceedings of the Alexander Ogston Centennial Conference*, pages 175–202. Aberdeen University Press, Aberdeen, 1981.
- [44] Lisa Lindesmith, Christine Moe, Severine Marionneau, Nathalie Ruvoen, Xi Jiang, Lauren Lindblad, Paul Stewart, Jacques LePendu, and Ralph Baric. Human susceptibility and resistance to norwalk virus infection. *Nat Med*, 9(5):548–53, May 2003.
- [45] Pengbo Liu, Yvonne Yuen, Hui-Mien Hsiao, Lee-Ann Jaykus, and Christine Moe. Effectiveness of liquid soap and hand sanitizer against norwalk virus on contaminated hands. *Appl. Environ. Microbiol.*, 76(2):394–399, January 2010.
- [46] R G Loudon and L C Brown. Cough frequency in patients with respiratory disease. *The American Review of Respiratory Disease*, 96(6):1137–1143, December 1967. PMID: 6057616.
- [47] R G Loudon and S K Spohn. Cough frequency and infectivity in patients with pulmonary tuberculosis. *The American Review of Respiratory Disease*, 99(1):109–111, January 1969. PMID: 5762102.
- [48] Stephen P Luby, Mubina Agboatwalla, Daniel R Feikin, John Painter, Ward Billhimer, Arshad Altaf, and Robert M Hoekstra. Effect of handwashing on child health: a randomised controlled trial. *Lancet*, 366(9481):225–233, July 2005. PMID: 16023513.
- [49] Yoshifumi Masago, Tomoyuki Shibata, and Joan B. Rose. Bacteriophage p22 and staphylococcus aureus attenuation on nonporous fomites as determined by plate assay and quantitative PCR. *Applied and Environmental Microbiology*, 74(18):5838–5840, September 2008. PMID: 18621868 PMCID: 2547042.
- [50] Mark Nicas and Daniel Best. A study quantifying the hand-to-face contact rate and its potential application to predicting respiratory tract infection. *Journal of Occupational and Environmental Hygiene*, 5(6):347–352, June 2008. PMID: 18357546.
- [51] Mark Nicas and Rachael M. Jones. Relative contributions of four exposure pathways to influenza infection risk. *Risk Analysis*, 9999(9999), 2009.
- [52] Mark Nicas, William W Nazaroff, and Alan Hubbard. Toward understanding the risk of secondary airborne infection: emission of respirable pathogens. *Journal of Occupational and Environmental Hygiene*, 2(3):143–154, March 2005. PMID: 15764538.
- [53] C. J. NOAKES, C. B. BEGGS, P. A. SLEIGH, and K. G. KERR. Modelling the transmission of airborne infections in enclosed spaces. *Epidemiology and Infection*, 134(05):1082–1091, 2006.
- [54] William J Riley, Thomas E McKone, Alvin C K Lai, and William W Nazaroff. Indoor particulate matter of outdoor origin: importance of size-dependent removal mechanisms. *Environmental Science & Technology*, 36(2):200–207, January 2002. PMID: 11831216.
- [55] L Roberts, W Smith, L Jorm, M Patel, R M Douglas, and C McGilchrist. Effect of infection control measures on the frequency of upper respiratory infection in child care: a randomized, controlled trial. *Pediatrics*, 105(4 Pt 1):738–742, April 2000. PMID: 10742313.
- [56] K J Rothman. Causes. *Am J Epidemiol*, 104(6):587–92, December 1976.
- [57] P. Rusin, S. Maxwell, and C. Gerba. Comparative surface-to-hand and fingertip-to-mouth transfer efficiency of gram-positive bacteria, gram-negative bacteria, and phage. *Journal of Applied Microbiology*, 93(4):585–592, 2002.
- [58] S.A. Sattar, S. Springthorpe, S. Mani, M. Gallant, R. C. Nair, E. Scott, and J. Kain. Transfer of bacteria from fabrics to hands and other fabrics: development and application of a quantitative method using *Staphylococcus aureus* as a model. *Journal of Applied Microbiology*, 90(6):962–970, 2001.

- [59] Elizabeth Scott and Sally F. Bloomfield. The survival and transfer of microbial contamination via cloths, hands and utensils. *Journal of Applied Microbiology*, 68(3):271–278, 1990.
- [60] Lynne Schulster and Raymond Y W Chinn. Guidelines for environmental infection control in health-care facilities. recommendations of CDC and the healthcare infection control practices advisory committee (HICPAC). *MMWR. Recommendations and Reports: Morbidity and Mortality Weekly Report. Recommendations and Reports / Centers for Disease Control*, 52(RR-10):1–42, June 2003. PMID: 12836624.
- [61] Ian H. Spicknall, James S. Koopman, Mark Nicas, Josep M. Pujol, Sheng Li, and Joseph N. S. Eisenberg. Informing optimal environmental influenza interventions: How the host, agent, and environment alter dominant routes of transmission. *PLoS Comput Biol*, 6(10):e1000969, October 2010.
- [62] Julian W Tang and Yuguo Li. Transmission of influenza a in human beings. *The Lancet Infectious Diseases*, 7(12):758; author reply 761–763, December 2007. PMID: 18045554.
- [63] R Tellier. Transmission of influenza a in human beings. *The Lancet Infectious Diseases*, 7(12):759–760, 2007.
- [64] Elise T-V Tu, Rowena A Bull, Mi-Jurung Kim, Christopher J McIver, Leon Heron, William D Rawlinson, and Peter A White. Norovirus excretion in an aged-care setting. *J Clin Microbiol*, 46(6):2119–21, June 2008.
- [65] F. v. Rheinbaben, S. Schünemann, T. Groß, and M. H. Wolff. Transmission of viruses via contact in a household setting: experiments using bacteriophage [phi]X174 as a model virus. *Journal of Hospital Infection*, 46(1):61–66, September 2000.
- [66] L Wallace. Indoor particles: a review. *Journal of the Air & Waste Management Association (1995)*, 46(2):98–126, February 1996. PMID: 8846246.
- [67] Thomas P Weber and Nikolaos I Stilianakis. Inactivation of influenza a viruses in the environment and modes of transmission: a critical review. *The Journal of Infection*, 57(5):361–373, November 2008. PMID: 18848358.
- [68] Lawrence M. Wein and Michael P. Atkinson. Assessing infection control measures for pandemic influenza. *Risk Analysis*, 29(7):949–962, 2009.
- [69] M.H Wilcox, W.N Fawley, N Wigglesworth, P Parnell, P Verity, and J Freeman. Comparison of the effect of detergent versus hypochlorite cleaning on environmental contamination and incidence of clostridium difficile infection. *Journal of Hospital Infection*, 54(2):109–114, June 2003.
- [70] Jijun Zhao et al. Sub-routes of contact mediated transmission (in preparation). 2010.